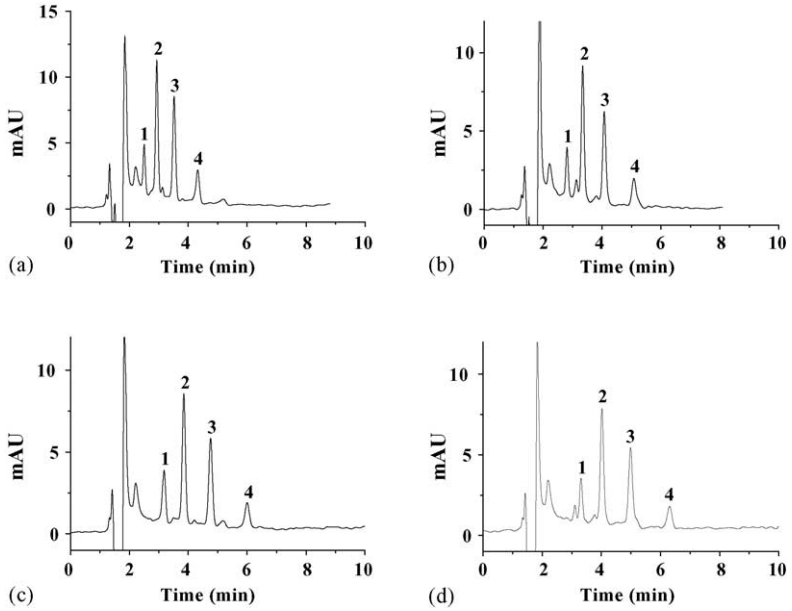

Fig. 5. Chromatograms of mixture of four LAS compounds obtained using 80% (v/v) methanol in water containing various concentrations of sodium acetate: (a) 2 mM; (b) 4 mM; (c) 8 mM; (d) 10 mM. Peak identification: (1) C_{10} LAS; (2) C_{11} LAS; (3) C_{12} LAS; (4) C_{13} LAS.

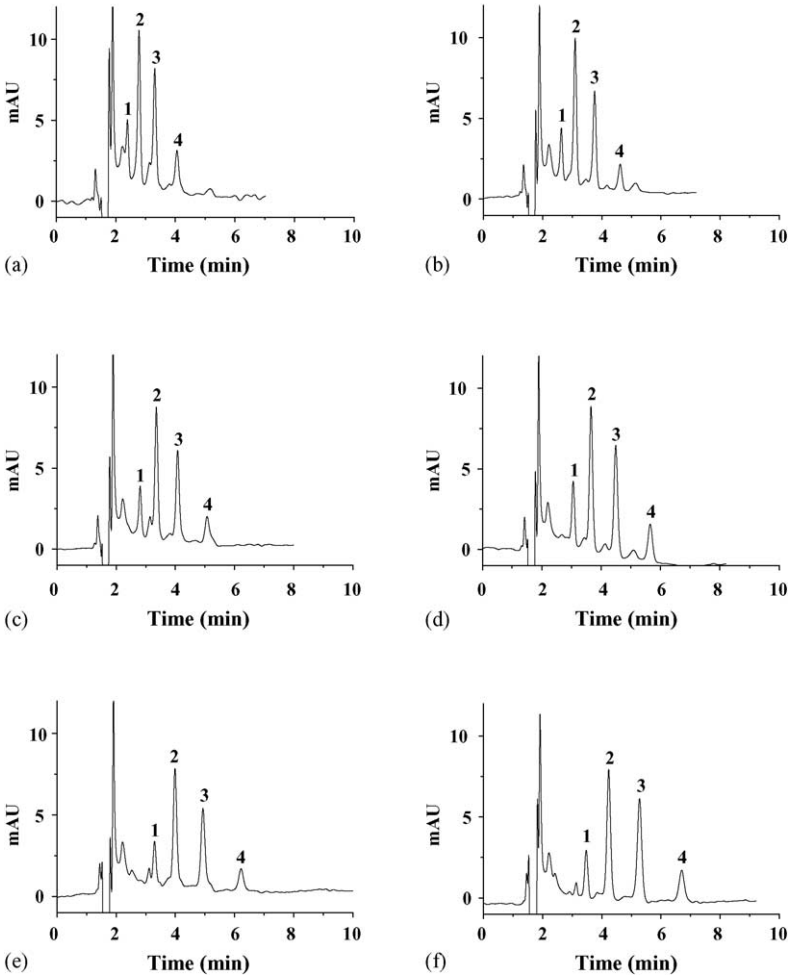

Fig. 6. Chromatograms of mixture of four LAS compounds obtained using 80% (v/v) methanol in water containing various concentrations of ammonium acetate: (a) 1 mM; (b) 1.5 mM; (c) 2 mM; (d) 4 mM; (e) 6 mM; (f) 8 mM. Peak identification: (1) C_{10} LAS; (2) C_{11} LAS; (3) C_{12} LAS; (4) C_{13} LAS.

Table 1
Analytical merits of the proposed method (linearity, accuracy and detection limit)

Compound	Concentration range (ppb)	R^2	Linearity cut-off (ppb) × 10^3	%Recovery	Detection limit[a] (ppb)
C_{10} LAS	6–310	0.9984	41	91–101	1.5
C_{11} LAS	20–1030	0.9997	137	92–99	8.0
C_{12} LAS	20–1070	0.9994	143	95–99	7.0
C_{13} LAS	20–590	0.9979	78	94–102	11.5

[a] Calculation based on three times the background standard deviation.

containing 80% methanol and 1.5 mM ammonium acetate in water were selected for this study due to the results obtained previously in compromising between resolution ($R_s \geq 1.5$) and analysis time (within 5 min). The accuracy expressed in terms of percentage recovery was done by spiking various amounts of LAS standard into the water samples collected from wastewater in Chiang Mai and Utraradit, Thailand. The percentage recoveries of this method for C_{10} LAS, C_{11} LAS, C_{12} LAS and C_{13} LAS were found to be between 91 and 101 ($n=3$), 92 and 99 ($n=3$), 95 and 99 ($n=3$) and 94 and 102 ($n=3$), respectively. Satisfactory recovery was obtained. The limit of detection for each LAS compound was calculated as three times the background standard deviation [29]. The C_{10} LAS had the lowest detection limit of 1.5 ppb. The C_{13} LAS, which is the last compound to elute under the conditions employed, had the highest detection limit value of 11.5 ppb. From the observation, the peak shape of C_{13} LAS is rather broader than that of C_{10} LAS.

3.4. Analysis of LAS surfactant in real water samples using HPLC–UV

Prior to real sample analysis, results obtained with the four LAS standards indicated that an increase of methanol from 75 to 80% is expected to cause C_{10} LAS and C_{11} LAS to elute close to some probable interferences (Fig. 6b). The mobile phase containing 1.5 mM ammonium acetate in methanol/water mixture of 78:22 (v/v), instead of the ratio of 80:20 (v/v) methanol/water, was used in order to avoid matrix effects arising from the water extracts. These effects cause approximately 2 min increase in the separation time of LAS compounds. As for water extracts, the chromatograms in Fig. 7 illustrate the separation of the four compounds for various water samples. Under the condition, the LAS compound concentrations in various water samples determined using a Zorbax Eclipse XDB C_8 column in combination with the methanol/water mixture containing ammonium acetate, are presented in Table 2.

3.5. Identification of LAS surfactants in water extract using LC–ES–MS

It is well known that the identification of LAS compounds using chromatographic techniques is based solely on retention-time matching. As a consequence, errors can result from using this approach, especially in the case of co-eluting compounds. Also of particular interest is the numerous unknown anionic surfactants that have been found in environmental samples when analysing them using HPLC–UV [17–19].

To overcome such problems, the negative-ion electrospray (ES)–mass spectrometry was used for confirmation of LAS compounds in water samples. The mass spectra of water extracts (Fig. 8) show the *m/z* 183 ion common to LAS compounds. In addition, the high intensity of the molecular ions observed at *m/z* 297, 311, 325 and 339 originating from the water extracts are similar to those originating from the LAS

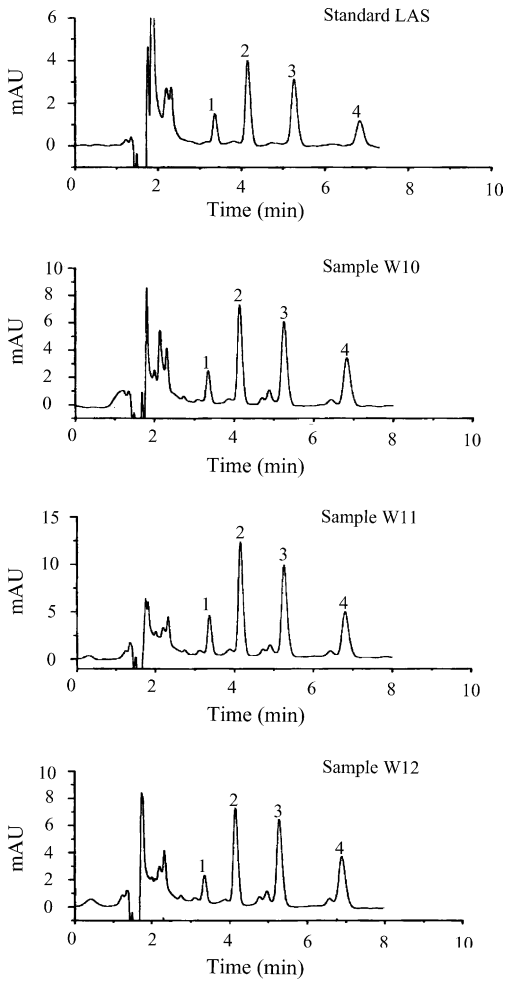

Fig. 7. Chromatograms of mixture of four LAS compounds in standard solution and water extracts obtained using 78% (v/v) methanol in water containing 1.5 mM ammonium acetate. Peak identification: (1) C_{10} LAS; (2) C_{11} LAS; (3) C_{12} LAS; (4) C_{13} LAS.

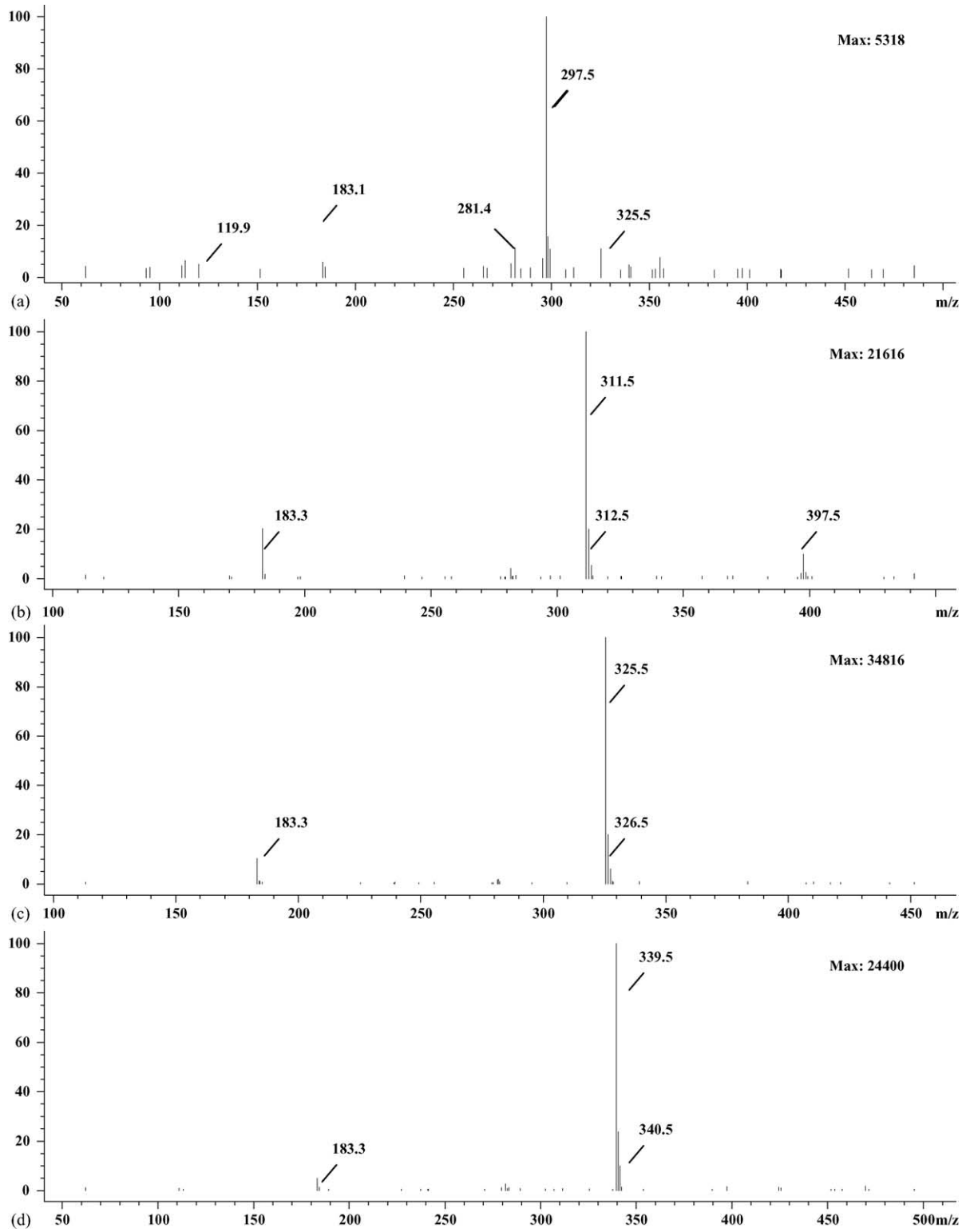

Fig. 8. (a–d) Negative-ion ESI mass spectra of LAS compounds originating from water extract (W10).

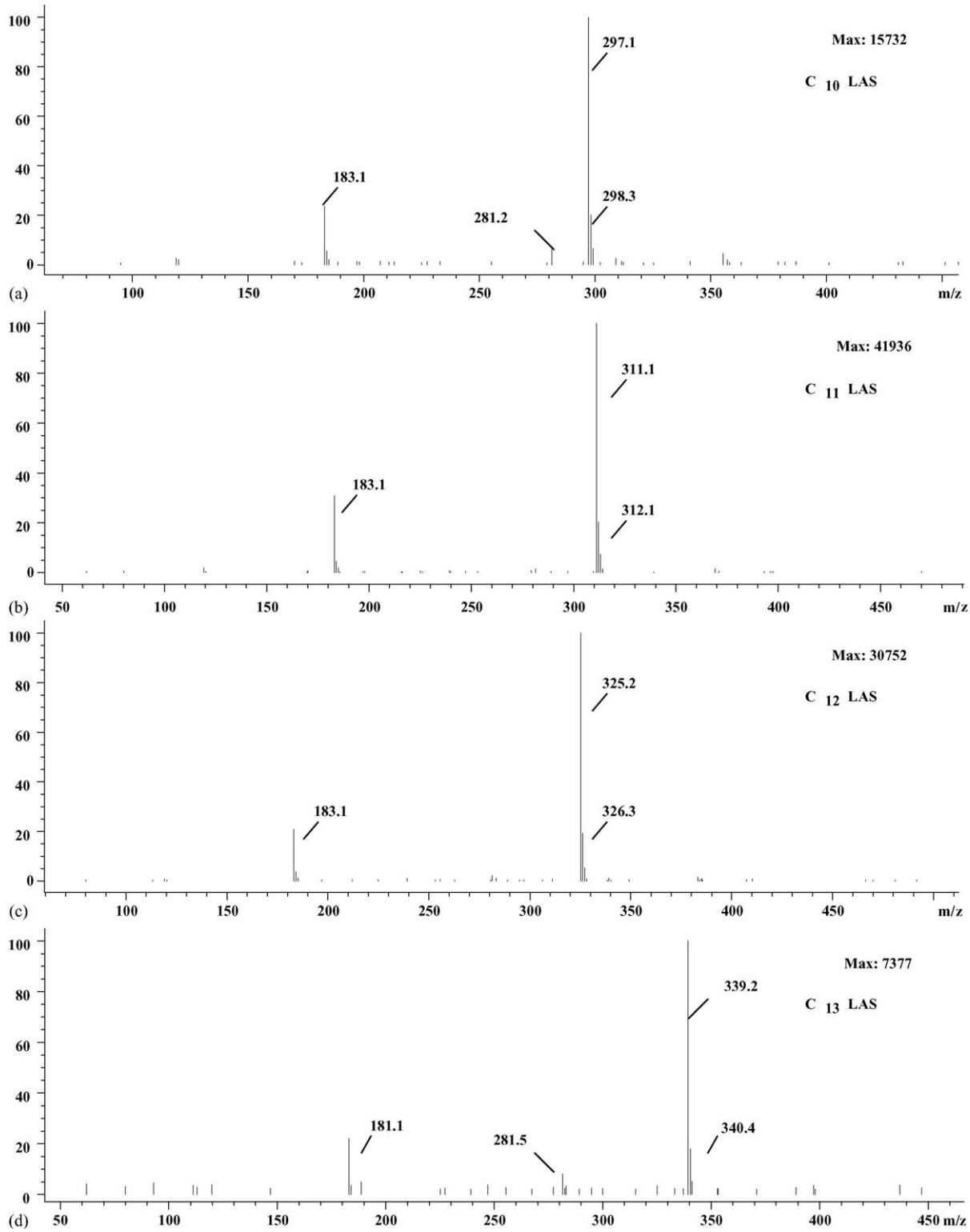

Fig. 9. (a–d) Negative-ion ESI mass spectra of the molecular ion originating from the mixture of LAS standard.

Table 2
Determination of LAS compounds in water samples (mean ± S.D.; $n = 3$)

Type of water	Concentration (ppb)			
	C_{10} LAS	C_{11} LAS	C_{12} LAS	C_{13} LAS
W1	115.3 ± 2.7	303.2 ± 7.9	184.4 ± 8.0	81.9 ± 2.2
W2	310.0 ± 0.3	1173.4 ± 4.6	1145.0 ± 12.9	424.4 ± 5.0
W3	5.0 ± 0.1[a]	23.4 ± 0.5	26.5 ± 1.1	21.1 ± 1.5
W4	n.d.	n.d.	13.0 ± 0.9	14.8 ± 0.5
W5	n.d.	n.d.	n.d.	n.d.
W6	3.4 ± 0.1[a]	12.8 ± 0.9	15.1 ± 1.3	16.7 ± 1.6
W7	54.1 ± 1.9	120.1 ± 5.5	69.1 ± 4.8	36.6 ± 5.2
W8	n.d.	n.d.	n.d.	n.d.
W9	n.d.	n.d.	n.d.	n.d.
W10	8.8 ± 0.3[a]	30.9 ± 0.7	33.5 ± 1.7	25.2 ± 1.7
W11	14.5 ± 0.8[a]	48.0 ± 2.4	46.9 ± 3.5	28.9 ± 2.8
W12	6.5 ± 0.4[a]	27.8 ± 1.9	30.3 ± 2.1	22.6 ± 1.3

n.d., not detected (less than the detection limit value); W1, drainage water from student dormitory, Chiang Mai University; W2, wastewater from Center of Medical Sciences, Ministry of Public Health; W3, wastewater from Khuy Hospital, Utraradit Province; W4, domestic wastewater released into Thorn canal, Utraradit Province; W5, natural water in Mae-Ping River, Chiang Mai Province; W7, wastewater in Mae-Kha canal, Chiang Mai Province; W8, natural water in Ang-Kaew reservoir, Chiang Mai University; W9, water in Chiang Mai Moat, Chiang Mai Province; W6 and W10–W13, natural water from irrigation canal, Chiang Mai Province.

[a] Preconcentration as described in Section 2.3.

standards (Fig. 9). These ions correspond to C_{10} LAS, C_{11} LAS, C_{12} LAS and C_{13} LAS, respectively.

4. Conclusion

The developed method offers superior performance characteristics, i.e. a simple method, significant improvement in resolution, short analysis time and using less amount of common salt (1.5 mM ammonium acetate) under isocratic condition. With this regard, it is easy to use this method with a mass spectrometric detector without any blockage of MS capillary. In addition, the use of low amounts of salt also increases the column's life and only requires very short re-equilibration time between each injection. Overall, these features demonstrate that the method is suitable to be used for routine analysis for both the identification and quantification of individuals of C_{10}–C_{13} LAS surfactants in various water samples.

Acknowledgements

The authors thank the Thailand Research Fund (TRF) for its support, the Development and Promotion for Science and Technology Talents Project of Thailand (DPST) for the scholarship to P.S. and the Postgraduate Education and Research Program in Chemistry Program (PERCH) of Thailand for the partial support.

References

[1] W.H. Ding, C.H. Liu, J. Chromatogr. A 929 (2001) 143.
[2] V.M. León, E. González-Mazo, A. Gómez-Parra, J. Chromatogr. A 899 (2000) 211.
[3] C. Vogt, K. Heining, Fresenius J. Anal. Chem. 363 (1999) 612.
[4] V.M. León, M. Saez, E. González-Mazo, A. Gómez-Parra, Sci. Total Environ. 288 (2002) 215.
[5] S. Terzic, M. Ahel, Mar. Pollut. Bull. 28 (1994) 735.
[6] E. González-Mazo, J.M. Quiroga, D. Sales, A. Gómez-Parra, Toxicol. Environ. Chem. 59 (1997) 77.
[7] J. Blasio, E. González-Mazo, C. Sarasquete, Toxicol. Environ. Chem. 71 (1999) 447.
[8] M.A. Bragadin, G. Perin, S. Raccanelli, S. Manente, Environ. Toxicol. Chem. 15 (1996) 1749.
[9] I. Moreno-Garrido, M. Hampel, L.M. Lubián, J. Blasco, Fresenius J. Anal. Chem. 371 (2001) 474.
[10] A.D. Eaton, L.S. Clesceri, A.E. Greenbreg, Standard Methods for the Examination of Water and Wastewater, Part 5540C, 19th ed., American Public Health Association, Washington, DC, 1995, pp. 42–44.
[11] L.H. Levine, J.E. Judkins, J.L. Garland, J. Chromatogr. A 874 (2000) 207.
[12] J.A. Field, D.J. Miller, T.M. Field, S.B. Hawthorne, W. Giger, Anal. Chem. 64 (1992) 3161.
[13] J.A. Field, Anal. Chem. 67 (1995) 3363.
[14] W.H. Ding, J.H. Lo, S.H. Tzing, J. Chromatogr. A 818 (1998) 270.
[15] W.H. Ding, C.T. Chen, J. Chromatogr. A 857 (1999) 359.
[16] B.L. Moore, L.J. Noertker, C.A. Hensley, J. Chromatogr. 265 (1983) 121.
[17] A. Marcomini, W. Giger, Anal. Chem. 59 (1987) 1709.
[18] K. Heinig, C. Vogt, G. Werner, J. Chromatogr. A 745 (1996) 281.
[19] E. González-Mazo, A. Gómez-Parra, Trends Anal. Chem. 15 (1996) 375.
[20] M. Sáez, V.M. León, A. Gómez-Parra, E. González-Mazo, J. Chromatogr. A 889 (2000) 99.
[21] V.M. León, A. Gómez-Parra, E. González-Mazo, Fresenius J. Anal. Chem. 371 (2001) 479.
[22] E. González-Mazo, M. Honing, D. Barceló, A. Gómez-Parra, Environ. Sci. Technol. 31 (1997) 504.
[23] J. Riu, E. Martínez, D. Barceló, A. Ginebreda, Fresenius J. Anal. Chem. 371 (2001) 448.
[24] P. Eichhorn, M.E. Flavier, M.L. Paje, T.P. Knepper, Sci. Total Environ. 269 (2001) 75.

[25] A. Marcommi, A. Di Corcia, R. Samperi, S. Capri, J. Chromatogr. 644 (1993) 59.
[26] P.W. Taylor, G. Nickless, J. Chromatogr. 178 (1979) 259.
[27] L.M. Nair, R. Saari-Nordhaus, J. Chromatogr. A 804 (1998) 233.
[28] S. Morales-Munoz, J.L. Luque-Garcia, M.D. Luque de Castro, J. Chromatogr. A 1026 (2004) 41.
[29] J.N. Miller, J.C. Miller, Statistics and Chemometrics for Analytical Chemistry, fourth ed., Dorset Press, Dorchester, 2000, pp. 120–123.

Available online at www.sciencedirect.com
SCIENCE DIRECT
Talanta 68 (2005) 459–464
Talanta
www.elsevier.com/locate/talanta

A novel stopped flow injection—amperometric procedure for the determination of chlorate☆

Orawan Tue-Ngeun[a,1], Jaroon Jakmunee[a,b,*], Kate Grudpan[a,b]

[a] *Department of Chemistry, Faculty of Science, Chiang Mai University, Chiang Mai 50200, Thailand*
[b] *Institute for Science and Technology Research and Development, Chiang Mai University, Chiang Mai 50200, Thailand*

Received 13 July 2005; received in revised form 20 September 2005; accepted 20 September 2005
Available online 17 October 2005

Abstract

A novel stopped flow injection—amperometric (sFI-Amp) procedure for determination of chlorate has been developed. The reaction of chlorate with excess potassium iodide and hydrochloric acid, forming iodine/triiodide that is further electrochemically reduced at a glassy carbon electrode at +200 mV versus Ag/AgCl electrode is employed. In order to increase sensitivity without using of too high acid concentration, promoting of the reaction by increasing reaction time and temperature can be carried out. This can be done without increase of dispersion of the product zone by stopping the flow while the injected zone is being in a mixing coil which is immersed in a water bath of $55 \pm 0.5\,^{\circ}C$. In a closed system of FIA, a side reaction of oxygen with iodide is also minimized. Under a set of conditions, linear calibration graphs were in the ranges of 1.2×10^{-6}–6.0×10^{-5} mol l^{-1} and 6.0×10^{-5}–6.0×10^{-4} mol l^{-1}. A sample throughput of 25 h^{-1} was accomplished. Relative standard deviation was 2% ($n = 21$, 1.2×10^{-4} mol l^{-1} chlorate). The proposed sFI-Amp procedure was successfully applied to the determination of chlorate in soil samples from longan plantation area.

Keywords: Stopped flow injection; Chlorate; Amperometry

1. Introduction

One major source of chlorate discharge to the environment is pulp mill effluent where chlorine dioxide is used for bleaching [1]. Minor amounts of chlorate and chlorite are also produced when chlorine dioxide is used to disinfect supply water [2]. Potassium chlorate ($KClO_3$) is used as an oxidant in fireworks and matches [3]. Chlorate compounds have also been widely applied to soil in order to stimulate flowering of longan trees [4], especially at longan plantation in the north of Thailand [5]. Although chlorate is not very toxic to human, it has been shown to cause haemolytic anemia [6]. Chlorate is very toxic to marine brown algae, i.e. Macrocystis and Fucus, which are vital components of the coastal ecosystem [2].

Ion chromatography (IC) has been reported for simultaneous determination of chlorate and other species, such as, IC/mass spectrometry for bromate, chlorate, iodate, and chlorine dioxide determination [7], IC/spectrophotometry using post-column reaction with osmate-catalyzed for chlorate, chlorite, bromate, and nitrite determination by detection the triiodide at 288 nm [8]. A high capacity anion exchange column with suppressed conductivity detection was also used by the U.S. EPA in Method 300.1 for the determination of bromate, bromide, chlorite, and chlorate by direct injection [9]. However, this technique requires relatively expensive instrument and rather long analysis time, so it is not suitable for determination of only one single analyte, when only chlorate is needed.

The iodometric method employing the amplification reaction of chlorate with iodide ion and acidic medium ($ClO_3^- + 6I^- + 6H^+ \rightarrow 3I_2 + Cl^- + 3H_2O$) [10–12] has been commonly used for chlorate determination, but the reaction of chlorate ion with iodide ion is slow under mildly acidic condition. The rate law of the reaction, $-d[ClO_3^-]/dt = k[ClO_3^-][I^-]^{1.5}[H^+]^2$ [10] indicates that the reaction could be accelerated under a high acid concentration. However, under this condition a readily oxidation

☆ Presented at the 13th International Conference on Flow Injection Analysis (ICFIA), 24–29 April 2005, Las Vegas, NV, USA.

* Corresponding author. Tel.: +66 53941910; fax: +66 53222268.
E-mail address: scijjkmn@chiangmai.ac.th (J. Jakmunee).
[1] Permanent address: Department of Chemistry, Faculty of Science, Naresuan University, Phitsanulok 65000, Thailand.

0039-9140/$ – see front matter © 2005 Elsevier B.V. All rights reserved.
doi:10.1016/j.talanta.2005.09.023

of iodide ion by oxygen in air would occur. In a potentiometric titration using sodium thiosulfate as titrant [13], 6 M hydrochloric acid was employed with hexane as oxygen shielding agent. Utilizing a FI system, which prevents direct exposure to air, 12 M hydrochloric acid can be used to accelerate the reaction. This leads to more sensitive methods based on spectrophotometric detection of triiodide at 370 nm [11,12,14]. A similar FI system has been applied to the determination of hypochlorite and chlorate [15]. The former species can react with iodide at room temperature while the latter requires an elevated temperature. A potentiometric flow injection procedure for the determination of oxychlorine species such as chlorate, chlorite and hypochlorite using a redox electrode detection and a Fe(III)–Fe(II) potential buffer solution containing chloride has also been reported [16]. A FI-amperometric method for the determination of chlorate and hypochlorite based on formation of chlorine by the reaction of the analytes with chloride in 8 mol l^{-1} sulfuric acid has also been described [17].

In this work, we developed a sFI-Amp procedure based on the reaction of chlorate with an excess iodide ion in an acidic condition to produce triiodide which is further electrochemically reduced at a glassy carbon electrode. In order to achieve high sensitivity without the use of too high acid concentration, a novel sFI procedure was introduced to promote the reaction by increasing a reaction time and a temperature. This can be done by stopping the flow while the injected zone was being in a mixing coil which was immersed in a water bath. In this way, dispersion of the product zone would be minimized. A simple homemade amperometric analyzer with a lab built flow through electrochemical cell can be used as a detector. A closed system of such a FI also minimizes any side reaction of oxygen with iodide. Moreover, the amperometric detection minimizes interferences from substances usually found in a soil sample which would interfere seriously in a spectrophotometric detection. Application of the proposed sFI-Amp procedure was demonstrated to the determination of chlorate in soil samples from longan plantation area.

2. Experimental

2.1. Apparatus

The sFI-Amp manifold for chlorate determination is illustrated in Fig. 1(a). It was a modified FIAstar system (5010 Analyzer, Tecator, Sweden), consisting of a peristaltic pump (P), a 6-port injection valve (I) and timing controlled unit. A

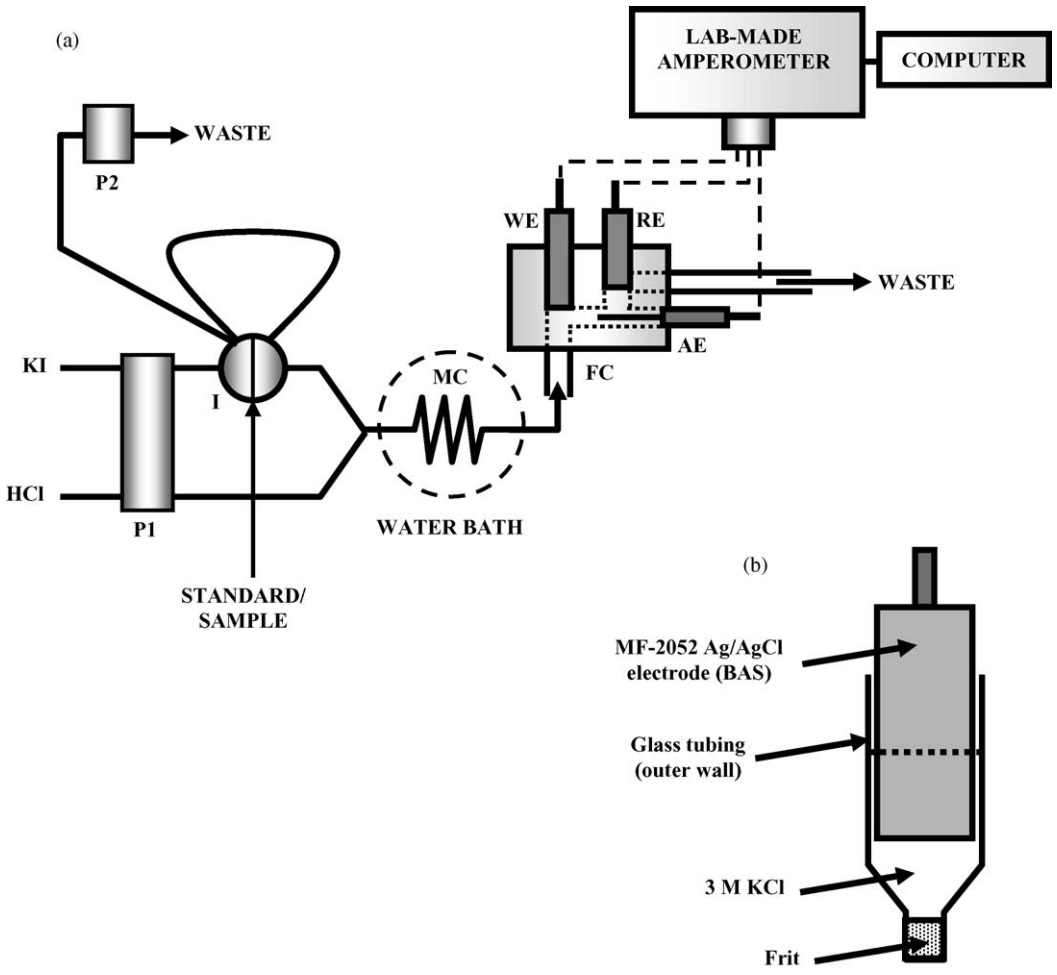

Fig. 1. (a) The sFI-Amp manifold used for determination of chlorate: P1 and P2: peristaltic pump 1 and 2; I: injection valve; MC: mixing coil; AE: auxiliary electrode; WE: working electrode; and RE: reference electrode. (b) A double junction design reference electrode.

lab-made amperometric analyzer with lab built flow through electrochemical cell (FC) was used as a detector. A personal computer with an in-house built software with Basic Stamp 2SX interface unit (Parallex, USA) was employed for recording data. Temperature was controlled by using a water bath (Gallenkamp, England).

A wall jet FC was assembled as shown in Fig. 1(a) (as side view). A Perspex plastic block was drilled to insert electrodes with *o*-ring sealing. Electrolyte carrier solution was entered the cell from the bottom and passed sequentially through a glassy carbon (MF-2012, 3.0 mm diameter, Bioanalytical System (BAS), USA) working electrode (WE), a platinum wire (MW-1032, BAS, USA) auxiliary electrode (AE) and an Ag/AgCl (MF-2052, BAS, USA) reference electrode (RE), respectively. A double junction design of RE (Fig. 1(b)) was used in order to prolong the lifetime of the MF-2052 RE.

All tubings for assembling the FI system were Teflon tube of 0.8 mm i.d., except pump tubes.

2.2. Reagents

Potassium iodide (AnalaR, BDH) and hydrochloric acid (Reagenti, CARLO ERBA) were used to prepare reagent solutions of concentration 0.07 mol l^{-1} and 7.0 mol l^{-1}, respectively. The potassium iodide solution was freshly prepared by dissolving 2.92 g KI in 250 ml water and kept in a dark bottle.

Potassium chlorate (99.5 %, w/w, AJAK), after standardization by standard iodometric procedures [18], was used to prepare stock standard solution of 12×10^{-3} mol l^{-1} chlorate. A stock solution was stored in a cool and dark place. Working standard solutions were daily prepared by appropriate dilution of the stock solution with water.

All solutions were prepared using Ultrapure water (Milli-Q, Millipore).

2.3. Collection and preparation of soil sample

Soil samples were collected from the longan plantation field in Chiang Mai, northern of Thailand. A soil sample was taken from 15 points at around the rim of the longan tree, at the depth of 15 cm. The sample was dried and ground before a portion of about 100 g was taken for further treatment.

A 25 g of dried-soil sample was extracted by shaking for 2 h with 50 ml of water. It was filtered with filter paper (Whatman, No. 42) and rinsed with water. The filtrate was made up to 100 ml in a volumetric flask with water.

2.4. sFI-Amp manifold and procedure

The sFI-Amp manifold (Fig. 1(a)) was designed to inject a standard or sample (100 μl) into a 0.07 mol l^{-1} potassium iodide stream before merging with 7.0 mol l^{-1} hydrochloric acid stream. This would prevent high concentration of hydrochloric acid entering/destroying the injection valve. The closed FI system also helps to reduce an oxidation of iodide ion by oxygen in air which is an extremely fast reaction in high concentration of hydrochloric acid ($4I^- + 4H^+ + O_2 \rightarrow 3I_2 + 2H_2O$) [10]. A period (called "travelling time") after injection was made until the pump was stopped was set to be 12 s. By doing this, the sample zone was being inside a mixing coil (MC), which was immersed into a water bath of 55 ± 0.5 °C. This temperature would promote the reaction of chlorate with iodide and acid to form triiodide. After a period of stopping (called "stopping time") of 90–120 s, the sample zone was flowed further through a FC and the reduction current of the triiodide was monitored by applying a constant potential of +200 mV at a glassy carbon working electrode versus Ag/AgCl reference electrode. The current was converted to potential by the amperometric analyzer and then recorded by the computer as a FI peak. A calibration graph was plotted between the peak height (mV) and chlorate concentration. Chlorate concentrations in sample was calculated using the calibration equation.

3. Results and discussion

3.1. Optimization of the FI-Amp system for the determination of chlorate

3.1.1. Amperometric instrument parameters

The sFI-Amp procedure for determination of chlorate is based on the conversion of chlorate to triiodide by reacting with an excess iodide and hydrochloric acid. A previous report on the detection of triiodide by amperometry based on the reduction of triiodide at a glassy carbon working electrode with an applied potential of +200 mV versus Ag/AgCl reference electrode was followed [19]. The home-made FC was designed to allow the solution passing to WE, AE and RE, respectively, in order to prevent the reaction product at AE to pass over the WE, so this kind of interference could be avoided.

3.1.2. Effect of concentration of potassium iodide

Concentrations of potassium iodide were studied. From the preliminary study, it was found that HCl concentration of at least 7 mol $l^{-1}$and a temperature of 45 °C should be used in order obtained a signal of chlorate in concentration range of 6.0×10^{-5}–6.0×10^{-4} mol l^{-1}. The concentrations of KI in range of 0.01–0.3 mol l^{-1} was investigated, while the following conditions were selected and kept constant: injection volume, 100 μl; MC length, 300 cm; flow rate of both of potassium iodide and hydrochloric acid streams, 2.9 ml min^{-1}; water bath temperature, 45 °C; travelling time, 12 s; and stopping time, 120 s. A series of chlorate standard solutions (6.0×10^{-5}–6.0×10^{-4} mol l^{-1}) was injected into the system. The obtained peak heights (mV) were plotted versus chlorate concentration (mol l^{-1}) yielding a calibration graph. Linear calibration graph was obtained for each concentration of KI used. A plot of the slopes of the calibration graphs versus KI concentrations is depicted in Fig. 2. It should be noted that at a higher concentration of KI, higher baseline signals were obtained which might be due to air oxidation of iodide or some iodate impurity presented in KI and this may lead to decrease of sensitivity (slope). Too low concentration of KI is not sufficient

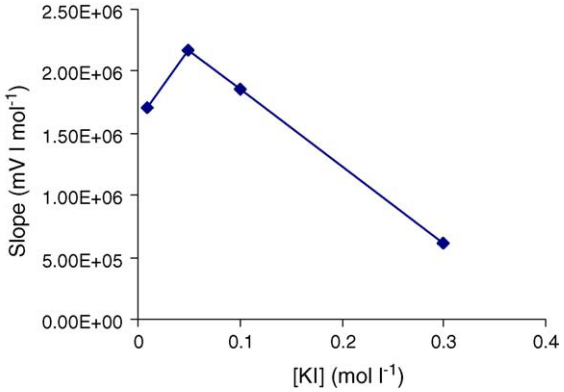

Fig. 2. Effect of concentration of potassium iodide (stopping time = 120 s, temperature = 45 °C, HCl concentration = 7 mol l^{-1}, other conditions see text).

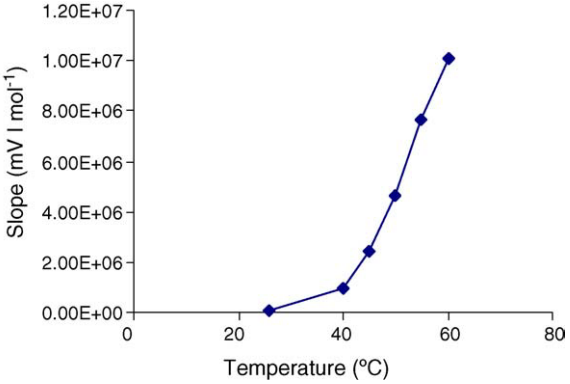

Fig. 4. Effect of temperature (stopping time = 120 s, HCl concentration = 7 M, KI concentration = 0.07 mol l^{-1}, other conditions see text).

in the reaction with the selected concentration range of chlorate and lead to a less sensitivity as well. KI of concentration 0.07 mol l^{-1} was chosen for further study.

3.1.3. Effect of stopping time and temperature

The stopping time in a range of 0–300 s was studied while the above selected condition, with 0.07 mol l^{-1} KI and temperature of 45 °C was used. The results in Fig. 3 show that the slope of calibration graph increased linearly with the increasing of the stopping time. The stopping time of 90–120 s was chosen in order to compromise between sensitivity and rapidity of the analysis.

With a 120 s stopping time, the effect of temperature was then studied. A plot of slope of calibration graph versus temperature is shown in Fig. 4. It can be noticed that sensitivity increased linearly with the increase of temperature in a range of 40–60 °C. The temperature of 55 °C was selected in order to avoid the evolution of bubble in the line when using a higher temperature. It should be noted that although the longer stopping time or higher temperature lead to high sensitivity, the higher peak height of blank solution was also observed. This may be due to the air oxidation of iodide which can be minimized by purging the reagent and sample solutions with oxygen-free nitrogen gas.

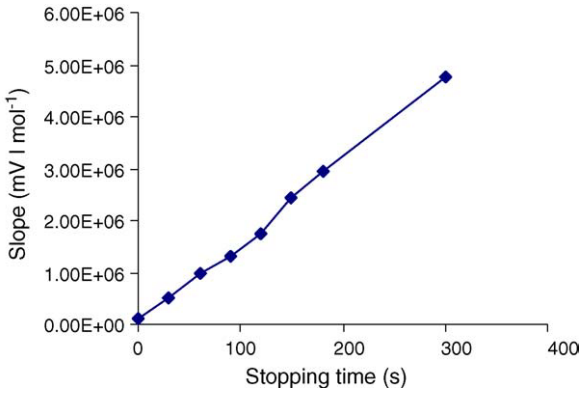

Fig. 3. Effect of stopped time (temperature = 45 °C, HCl concentration = 7 mol l^{-1}, KI concentration = 0.07 mol l^{-1}, other conditions see text).

3.1.4. Effect of HCl concentration

Attempts have been made to reduce concentration of the HCl used. Under the above selected conditions, it was found that sensitivity rapidly decreased when a concentration of HCl was reduced less than 7 mol l^{-1}. So 7 mol l^{-1} HCl should be recommended. However, a lower acid concentration may be employed but a longer stopping time should be applied so that a desired sensitivity would be obtained. This would then affect the sample throughput.

3.2. Analytical characteristics

Employing the above selected conditions as shown in Table 1, a series of concentration of chlorate standard solution was injected into the system. FI peaks similar to those of normal FI were obtained as shown in Fig. 5. A calibration graph was constructed by plotting peak height (mV) versus chlorate concentration (mol l^{-1}). Calibration graphs were linear in the ranges of 1.2×10^{-6}–6.0×10^{-5} mol l^{-1} ($y = (1.217 \times 10^{7})x + 14.3$, $r^2 = 0.9977$) and 6.0×10^{-5}–6.0×10^{-4} mol l^{-1} chlorate ($y = (6.421 \times 10^{6})x + 451.5$, $r^2 = 0.9964$). With a 120 s stopping time, a detection limit of 1.2×10^{-6} mol l^{-1} chlorate was

Table 1
Selected conditions of the proposed sFI-Amp procedure

Parameter	Analytical characteristics
Injection volume (μl)	100
Mixing coil length (cm)	300
Reagent concentration (mol l^{-1})	
KI	0.07
HCl	7
Flow rate (ml min^{-1})	
KI	2.9
HCl	2.9
Travelling time (s)[a]	12
Stopping time (s)[b]	90–120
Temperture of water bath (°C)	55 ± 0.5

[a] Travelling time: the period between the point of injection to the point at which the flow is stopped.
[b] Stopping time: the period during the flow is stopped.

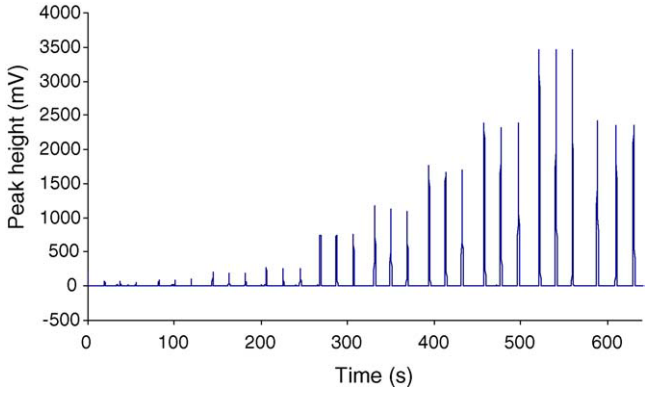

Fig. 5. FIgram obtained from sFI-Amp system for chlorate determination: peaks from left to right were blank, 1.2, 6.0, 12, 60, 120, 240, 360 and 600 μmol l^{-1} of chlorate standard and sample 1, respectively. Conditions as in Table 1 were employed, with stopping time 120 s. Signal was recorded only at the period after the flow was restarted to push the reaction product into the detector.

obtained. A sample throughput was 25 h^{-1}. Relative standard deviation was 2% (1.2×10^{-4} mol l^{-1} chlorate, $n = 21$).

Another merit of sFI is the less consumption of reagent, especially when a high concentration of reagent solution is concerned. In this procedure, the consumption of about 1.5 ml each of 7 mol l^{-1} HCl and 0.07 mol l^{-1} KI per injection should be noted.

3.3. Interference study

The species that can react easily with iodide ion to produce triiodide, e.g. iodate, hypochlorite, chlorite, could be seriously interfere in this system. These ions could be determined first by employing low acid concentration and room temperature and chlorate concentration could be obtained later using elevated conditions [15]. However, these ions are expected to present in some selected soil samples with concentrations of much lower than that of chlorate.

The common ions (CO_3^{2-}, NO_3^-, SiO_3^{2-}, Ca^{2+}, Cu^{2+}, Fe^{3+}, Mn^{2+} and Zn^{2+}), which may be found in soil sample, were studied. The effects of these ions were investigated, by adding the ions to the 1.2×10^{-4} mol l^{-1} chlorate standard solution. The relative error in concentration of the standard chlorate solution of less than 5% was obtained for the interfering ion/chlorate mole ratios of 3 for Cu^{2+}, 4 for Fe^{3+}, and 50 for CO_3^{2-}, NO_3^-, SiO_3^{2-}, Ca^{2+}, Mn^{2+} and Zn^{2+}. Cu^{2+} and Fe^{3+} exhibited positive interference because the Cu^{2+} and Fe^{3+} can reduce the iodide ion. Fortunately, copper and iron in soil-extracted solution (using water) were at very low concentrations (less than 2.4×10^{-5} mol l^{-1} of both ions, determined by flame-atomic absorption spectrophotometry) and did not interfere in this system.

3.4. Analysis of soil samples

The developed sFI-Amp procedure was applied to the determination of chlorate in soil samples from longan orchards in Chiang Mai, Thailand. Potassium/sodium chlorates are applied to the soil to stimulate flowering of the fruit. Due to a good solubility of the chlorate compounds in water, the soil was extracted with deionized water to have a chlorate concentration in the extract in a suitable range of the calibration graphs (1.2×10^{-6}–6.0×10^{-5} and 6.0×10^{-5}–6.0×10^{-4} mol l^{-1} chlorate). The extracted solution was injected into the system and chlorate content was obtained from the calibration graphs as presented in Table 2. The iodometric titration [18] was performed for comparison. The results of the batch titration method were slightly different from the sFI-Amp method, which may come from interfering of oxygen in air and slow reaction of chlorate with iodide and hydrochloric acid, which was difficult to control in batch titration method. However, the results obtained from both methods are in agreement (*t*-test, 95% confidence).

Table 2
Chlorate contents in soil samples from longan orchards determined by the proposed sFI-Amp procedure and the iodometric titration method [18] (triplicate results)

Sample number[a]	Chlorate (μg/g) of dried soil	
	sFI-Amp	Iodometric titration
1	335 ± 3	341 ± 6
2	108 ± 6	118 ± 5
3	88 ± 5	100 ± 4
4	20 ± 4	16 ± 5
5	27 ± 1	34 ± 7
6	15.1 ± 0.4	11 ± 5
7	3.9 ± 0.4	ND[b]
8	28 ± 1	21 ± 4
9	15 ± 2	10 ± 4
10	5.9 ± 0.4	ND
11	140 ± 1	147 ± 6

[a] Dried soil samples were obtained from Assoc. Prof. Dr. Somchai Ongprasert, Department of Soil Resource and Environment, Faculty of Agricultural Production, Maejo University, Chiang Mai, Thailand.
[b] ND: not detected.

4. Conclusion

A novel stopped flow injection amperometric procedure was developed for the determination of chlorate in soil sample. Chlorate in micro-molar concentration can be easily determined with this simple procedure even using a home-made amperometric analyzer and a home-made flow through electrochemical cell. High sensitivity can be obtained without conditions employing too high acid concentration, by promoting the reaction using longer reaction time and higher temperature by stopping the flow while the reaction zone being in a mixing coil which is immersed in a water bath. In a closed FI system, air oxidation of iodide reagent is also minimized. The amperometric detection also reduced the interferences from the substances (e.g. colored species) usually found in soil sample which may interfere very much in spectrophotometric detection. The proposed system provided a sample throughput of 25–35 h^{-1} with less reagent consumption and successfully demonstrated for application to soil samples.

Acknowledgements

We thank the Thailand Research Fund (TRF) and the Postgraduate Education and Research Program in Chemistry (PERCH) for financial support. O.T. thanks the Commission on higher Education (CHE) of Thailand and Naresurn University for providing her scholarship. Assoc. Prof. Somchai Ongprasert is gratefully acknowledged for providing of soil samples. Thanks also to Dr. Ponlayuth Sooksamiti for AAS determination of copper and iron contents in the samples.

References

[1] A. Rosemarin, K. Lehtinen, M. Notini, J. Mattson, Environ. Pollut. 85 (1994) 3.
[2] http://wlapwww.gov.bc.ca/wat/wq/BCguidelines/chlorate/chlorateoverview1-04.html.
[3] See http://www.bartleby.com/65/ch/chlorate.html, Chlorate (25/07/2004).
[4] M.A. Nagao, E.B. Ho-a, J. Haw. Pac. Agric. 11 (2000) 23.
[5] http://www.mju.ac.th/fac-agr/HORT/pomo/research/e-daw.html.
[6] http://www.rse.uquebec.ca/ang/vol12/v12n3a7.htm.
[7] L. Charies, D. Pepin, Anal. Chem. 70 (1998) 353.
[8] B. Nowack, U.v Gunten, J. Chromatogr. A 849 (1) (1999) 209.
[9] U.S. EPA, Method 300.1, U.S. Environmental Protection Agency, Cincinnati OH, 1997.
[10] Y. Ikeda, T.F. Tang, G. Gordon, Anal. Chem. 56 (1984) 71.
[11] K.G. Miller, G.E. Pacey, G. Gordon, Anal. Chem. 57 (1985) 734.
[12] G. Gordon, K. Yoshino, D.G. Themelis, D. Wood, G.E. Pacey, Anal. Chim. Acta 224 (2) (1989) 383.
[13] Y. Ikeda, T.F. Tang, G. Gordon, Anal. Chem. 56 (1984) 71.
[14] D.G. Themelis, D.W. Wood, G. Gordon, Anal. Chim. Acta 225 (2) (1989) 437.
[15] K. Tian, P.K. Dasgupta, Talanta 52 (2000) 623.
[16] H. Ohura, T. Imato, S. Yamasaki, Talanta 49 (5) (1999) 1003.
[17] A.A. Alwartan, M.A. Abdalla, Intern. J. Chem. 3 (3) (1992) 105.
[18] J. Bassett, R.C. Denney, G.H. Jeffery, J. Mendham, Vogel's Textbook of Quantitative Inorganic Analysis Including Elementary Instrumental Analysis, Longman, New York, 1978, 901.
[19] J. Jakmunee, K. Grudpan, Anal. Chim. Acta 438 (2001) 299.

Available online at www.sciencedirect.com
SCIENCE DIRECT
Talanta 68 (2005) 416–421
Talanta
www.elsevier.com/locate/talanta

Exploiting sequential injection analysis with lab-at-valve (LAV) approach for on-line liquid–liquid micro-extraction spectrophotometry☆

Rodjana Burakham[a], Somchai Lapanantnoppakhun[b,c], Jaroon Jakmunee[b,c], Kate Grudpan[b,c,*]

[a] Department of Chemistry, Faculty of Science, Khon Kaen University, Khon Kaen 40002, Thailand
[b] Department of Chemistry, Faculty of Science, Chiang Mai University, Chiang Mai 50200, Thailand
[c] Institute for Science and Technology Research and Development, Chiang Mai University, Chiang Mai 50200, Thailand

Available online 10 October 2005

Abstract

Sequential injection analysis (SIA) with lab-at-valve (LAV) approach for on-line liquid–liquid micro-extraction has been exploited. Sample, reagent and organic solvent were sequentially aspirated into a coil attached to a central port of a conventional multiposition selection valve, where the extraction process was performed. The aqueous and organic phases were separated in a conical separating chamber LAV unit attached at one port of the valve. The organic phase containing extracted product was then monitored spectrophotometrically. The system offers a novel alternative on-line automated extraction in a micro-scale and has been successfully demonstrated for the assays of diphenhydramine hydrochloride (DPHH) in pharmaceutical preparations and anionic surfactant in water samples.

Keywords: Sequential injection analysis; Lab-at-valve; On-line liquid–liquid micro-extraction

1. Introduction

Liquid–liquid extraction is one of the most versatile techniques for sample matrix separation and/or analyte preconcentration. It has been applied to various analytical fields. For pharmaceutical applications, liquid–liquid extraction involves in the analytical processes for determination of active ingredient compounds such as cinnarizine [1], diphenhydramine hydrochloride (DPHH) [2,3] and paracetamol [4]. For environmental applications, it also exists in the determination of various compounds such as iron(II) and iron(III) [5], phenolic compounds [6] and surfactant [7]. However, manual extractions present a series of drawbacks such as high consumption of sample and toxic organic solvent, low sampling frequency, loss of analyte through manipulation and contamination of atmosphere by organic vapor. Many efforts have been made to overcome these inherent drawbacks. Among them, the successful techniques are probably the on-line liquid–liquid extraction using flow systems [8–10].

A variety of flow-based systems have been reported for the on-line liquid–liquid extraction. Flow injection liquid–liquid extraction was proposed in 1978 by Karlberg and Thelander [11] and Bergamin et al. [12]. Consumption of reagents and organic solvent are lower than those in manual procedures, consequently reducing the waste generated.

Based on this feature, different flow injection systems for liquid–liquid extraction were developed for a large number of analytical applications [7,13–18].

As another generation, the technique called sequential injection analysis (SIA) [19–22] has also been employed for on-line liquid–liquid extraction by sequential aspiration of a small volume of organic solvent and aqueous sample into contact before either resolve them using phase separator [23] or performing back extraction [24].

In the recent years, SIA has been modified into miniaturization with different concepts. Ruzicka proposed SIA with lab-on-valve (LOV) format in which a very precisely specific LOV module was mounted atop a selection valve to perform chemical reaction and monitor for a change in a conduit on such a modified multiposition valve [25]. SIA with a simple approach called lab-at-valve (LAV), firstly introduced by our group [26], is another approach of SIA which becomes an alternative cost effective micro total analysis system. SIA-LAV uses a designed LAV unit that can be fabricated using an ordinary less precise

☆ Paper presented at the 13th International Conference on Flow Injection Analysis (ICFIA), Las Vegas, USA, 24–29 April 2005.

* Corresponding author. Tel.: +66 5394 1910.
E-mail address: kate@chiangmai.ac.th (K. Grudpan).

0039-9140/$ – see front matter © 2005 Published by Elsevier B.V.
doi:10.1016/j.talanta.2005.09.002

machine tool, to have a suitable function for chemistry of interest and can be easily attached at a port of the conventional selection valve in a usual way. This simpler approach was successfully demonstrated for potentiometric determination of chloride [27].

In the present work, SIA-LAV approach was investigated as a novel alternative for simple on-line liquid–liquid microextraction. A desired component, a separating chamber, was attached at one port of a conventional multiposition selection valve. Sample, reagents, and organic solvent were sequentially aspirated into an extraction coil (EC). By flow reversal, good extraction efficiency can be achieved. After that, the aqueous and organic phases were separated in a conical separating chamber attached at one port of a conventional multiposition selection valve ("Lab-at-Valve" concept). The organic phase containing extracted product was then monitored spectrophotometrically. Applications to the assays of diphenhydramine hydrochloride in pharmaceutical preparations and anionic surfactant in water samples were selected as models.

2. Experimental

2.1. Chemicals and reagents

All of reagents used were analytical reagent grade. Deionized water was used throughout the experiments. Diphenhydramine hydrochloride reference standard of 100% purity (Ministry of Public Health, Thailand) was used. Stock solution (1000 mg/l) of diphenhydramine standard was prepared by dissolving 0.1000 g of the reference standard in water and diluting to the mark of 100 ml volumetric flask. Working standards were freshly prepared by diluting the stock solution with water to obtain appropriate concentrations. A bromocresol green (BCG) solution (5×10^{-4} mol/l) was prepared by dissolving 0.0349 g BCG powder in water with addition of 0.2 ml of 0.1 mol/l sodium hydroxide and diluting to 100 ml with water. The solution was filtered before use. A phthalate buffer (pH 3) was prepared using 100 ml of 0.1 mol/l potassium hydrogenphthalate, 40.6 ml of 0.1 mol/l hydrochloric acid and diluting to 200 ml with water.

Stock solution (1000 mg/l) of sodium dodecylsulphate (SDS) was prepared by dissolving 0.1087 g of the standard in water and made up to a volume of 100.00 ml.

Stock solution (0.10%, w/v) of methylene blue was prepared by dissolving 0.10 g of the methylene blue in 100 ml of water.

2.2. Apparatus

The SI system used is schematically depicted in Fig. 1. It consisted of a modified autoburette Dosimat 765 (Metrohm, Switzerland) equipped with a 10 ml exchange unit, for a pumping system, and connected to a personal computer via RS232C interface, a 10-position selection valve VICI with a microelectric actuator (Valco Instruments, USA) and a Spectronic21 (Bausch & Lomb, USA) detector with a flow through cell (Hellma, Germany) of 1 cm light path. The autoburette was connected to the center of the selection valve via the EC (0.79 mm i.d. × 400 cm PTFE tubing) and a separating chamber was placed at port-1 of the selection valve. Both instrumental control and data acquisition were manipulated via a software using LabVIEW, developed in house and using a CYDAS ULV interfacing board (CyberResearch, USA). This software provided control of the volume to be dispensed or aspirated by the autoburette, flow rate, selection of the different valve positions and performed data acquisition. The data processing was computed by using Microcal Origin 6.0.

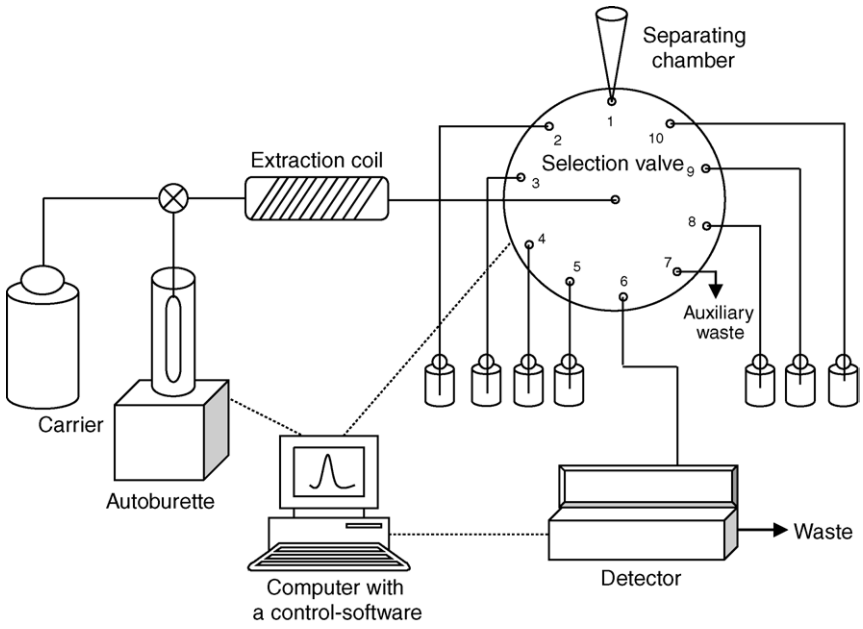

Fig. 1. Schematic diagram of SIA system.

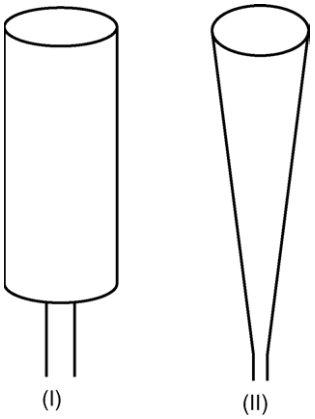

Fig. 2. Two types of separating chamber; I: cylindrical shape (8 mm i.d. × 5 cm long) and (II): conical shape (8 mm i.d. of the wider end × 7 cm long, modified from a 1 ml pipette tip (Eppendoft, Germany)).

3. Results and discussion

3.1. The assay of diphenhydramine hydrochloride

3.1.1. Optimization of the operational sequence

By using the separating chamber type I, as shown in Fig. 2, a sequence order of aspiration was firstly optimized. Three sequence orders (Fig. 3) were examined and a suitable one, as demonstrated in Fig. 3(c), which provided better sensitivity, was selected. BCG solution was firstly aspirated into the EC, then the standard/sample solution was introduced, an ion-association formed. A phthalate buffer (pH 3) and chloroform were then aspirated. At pH 3, a high extraction efficiency of ion-pair compound was obtained [2]. The extraction step was performed in the EC by programming the autoburette to aspiration and dispensed modes. This process determines the time and efficiency that the two phases are in contact and is a key parameter for better extraction efficiency. The solution was then dispensed into the separating chamber where the aqueous and organic phases were separated. The organic phase containing ion-association product was transported into the EC and transported into a flow through cell of the spectrophotometer. An absorbance at 415 nm was followed.

It should be noted that although the exchange unit of the autoburette was made from glass and furnished with PTFE plunger, manipulation of the organic extractant was accomplished by filling the syringe of the exchange unit with water. Before the detection step, the organic solvent was aspirated and stored in EC for use. It is necessary to avoid the introducing of aqueous into the flow cell of detector to prevent the change of baseline signal due to aqueous droplet.

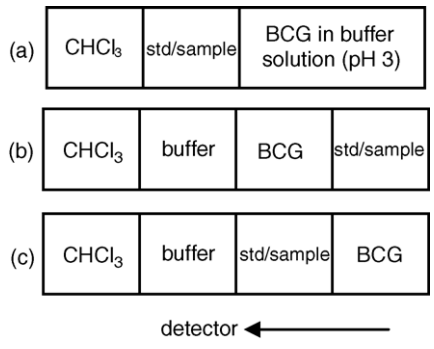

Fig. 3. Sequence orders of the SIA system for the determination of diphenhydramine hydrochloride.

3.1.2. Influence of the separating chamber shape

Two types of the separating chambers, as shown in Fig. 2, were examined to reach the best separation between the organic and aqueous phases. The results show that the better separation between two phases was obtained by using the conical shaped separating chamber. Therefore, the separating chamber type II was adopted.

3.1.3. Optimization of the chemical parameters

The concentration and volume of the reagents concerning in the reaction were optimized. According to the preliminary study, the concentration of BCG of 5×10^{-4} mol/l was excess to form the ion-association with diphenhydramine hydrochloride in the working range of 10–40 mg/l [2].

The selected conditions and operational sequence of the proposed system were summarized in Table 1. By fixing the aque-

Table 1
Selected conditions and operational sequence of the SIA system for the determination of diphenhydramine hydrochloride

Sequence	Valve position	Mode[a]	Volume (μl)	Description
1	5	PIP	170	Aspirate 5×10^{-4} mol/l BCG into EC
2	3–4, 8–9	PIP	170	Aspirate standard/sample into EC
3	2	PIP	150	Aspirate 5×10^{-4} mol/l buffer (pH 3) into EC
4	10	PIP	400	Aspirate chloroform into EC
5	1	PIP	1300	Extract
6	1	DIS C	2000	Extract
7	1	PIP	1100	Extract
8	1	DIS C	2000	Extract and propel to the separating chamber[b]
9	7	DIS C	3000	Clean EC
10	10	PIP	400	Aspirate chloroform into EC
11	1	PIP	250	Aspirate chloroform phase containing ion-association compound into EC
12	6	DIS C	40	Dispense chloroform phase containing ion-association compound through the selection valve
13	7	DIS C	3000	Clean EC
14	10	PIP	2900	Aspirate chloroform into EC
15	6	DIS C	2000	Dispense to detector with flow rate of 10 ml/min

[a] PIP = pipetting/aspiration, DIS C = cumulative dispensing.
[b] No standing time for phase separation.

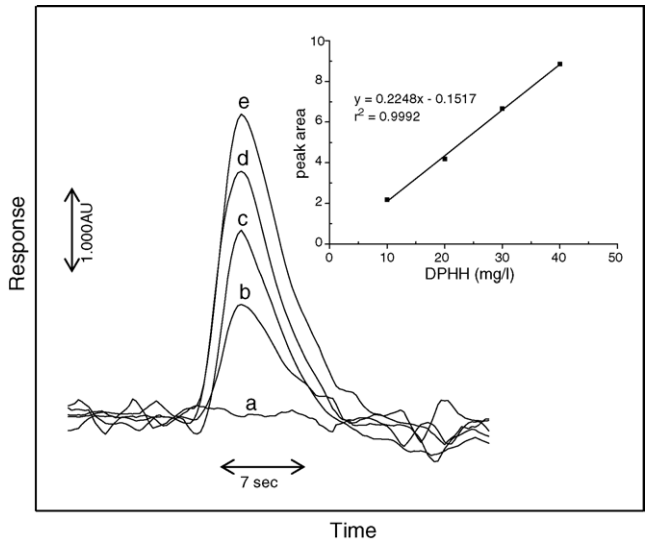

Fig. 4. Typical SI-grams and calibration graph of diphenhydramine hydrochloride; a = blank, b = 10, c = 20, d = 30, e = 40 mg/l.

ous volume (see Table 1), the volume ratio between aqueous to organic phases is of great importance in solvent extraction because it determines enrichment factor in the preconcentration of the analyte. The volume of chloroform used for the extraction was varied. The slopes of the calibration equation indicated that the sensitivity increased with decreasing the volume of chloroform: $y = 0.2248x - 0.1517$, $y = 0.1922x - 1.7877$ and $y = 0.0833x + 1.0726$ for 400, 450 and 470 μl, respectively. Using chloroform less than 400 μl, it was difficult to reach the complete separation between the two phases, i.e. aqueous droplets being entrapped within the organic phase. Better enrichment factor may be obtained by increasing the volume of the standard/sample solutions for a fixed volume of chloroform, but a larger separating chamber must be used.

3.1.4. Analytical characteristics

Fig. 4 shows the calibration graph and typical SI-grams of diphenhydramine hydrochloride. Calibration graph of diphenhydramine hydrochloride versus peak area was found to be linear in the range of 10–40 mg/l with the linear equation and correlation coefficient (r^2) of $y = 0.2248x - 0.1517$ and 0.9992, respectively. The limit of detection (LOD) calculated as three times the standard deviation was 1.90 mg/l. The relative standard deviation (%RSD) was less than 3.6 (n = 11, 20 mg/l diphenhydramine hydrochloride). The recovery was found to be 102%. Sample throughput of 5 h^{-1} can be achieved. A higher throughput may be possible if the modified autoburette would be replaced by another type of syringe pump, although it could be more expensive.

According to our previous study [2], using this reaction, the amount of the foreign compounds commonly presented together with diphenhydramine hydrochloride in preparations containing single tertiary alkylamine drug would not interfere in the determination.

3.1.5. Application to samples

The proposed SI method was applied to the determination of diphenhydramine hydrochloride in some pharmaceutical preparations (containing single tertiary alkylamine). Some locally commercial pharmaceutical preparations were taken as samples to be assayed. A weighed quantity of a sample was dissolved with deionized water, shaken for 15 min and adjusted to a volume with water to obtain a solution having a concentration in the range of a calibration graph. The solution was then filtered before analysis. The results were compared to those obtained by the standard method using high performance liquid chromatography [28], as summarized in Table 2. Evaluation by t-test at 95% confidence level indicates that there is no significant difference in the results obtained by the proposed SIA and the standard methods.

3.2. The assay of anionic surfactant

3.2.1. Optimization of the experimental parameters

The same SIA setup was used for the determination of anionic surfactant in water samples. The anionic surfactant reacts with methylene blue to form ion-association compound, which can be extracted into chloroform. The concentration of anionic surfactant can be determined by measuring the absorbance of the chloroform phase at 650 nm [29]. Some experimental parameters, i.e. operational sequence, volume and concentration of reagents were optimized. Zone sequence was chosen: standard/sample-methylene blue-chloroform. The aqueous sample containing anionic surfactant was firstly aspirated into the EC. Next, the methylene blue solution was introduced, the ion-association compound formed. Then, chloroform was aspirated and the extraction was done by programming the autoburette to aspiration and dispensed modes. After extraction in the EC, the solution was propelled to the separating chamber, where the separation between aqueous and chloroform phases occurred. The chloroform phase containing ion-association compound was re-aspirated into the EC for transportation to a detector.

The concentration of methylene blue solution was varied from 0.0038 to 0.02%. The sensitivity increased with increasing the methylene blue concentration and reached the maximum at

Table 2
Determination of diphenhydramine hydrochloride in pharmaceutical preparations by the proposed and standard methods

Sample	Label	Proposed method		Standard method [28]	
	(mg/5 ml)	Amount found (mg/5 ml)	% label	Amount found (mg/5 ml)	% label
1	12.50	12.57 ± 0.27	101	13.55 ± 0.49	108
2	12.50	12.81 ± 0.55	102	13.91 ± 0.12	111

Table 3
Selected conditions and operational sequence of the SIA system for the determination of anionic surfactant in water samples

Sequence	Valve position	Mode[a]	Volume (μl)	Description
1	2–4, 8–9	PIP	250	Aspirate standard/sample into EC
2	5	PIP	250	Aspirate methylene blue into EC
3	10	PIP	400	Aspirate chloroform into EC
4	1	PIP	1300	Extract
5	1	DIS C	2000	Extract
6	1	PIP	1100	Extract
7	1	DIS C	2000	Extract and propel to the separating chamber[b]
8	7	DIS C	3000	Clean EC
9	10	PIP	400	Aspirate chloroform into EC
10	1	PIP	250	Aspirate chloroform phase containing ion-association compound into EC
11	6	DIS C	40	Dispense chloroform phase containing ion-association compound through the selection valve
12	7	DIS C	3000	Clean EC
13	10	PIP	2900	Aspirate chloroform into EC
14	6	DIS C	2000	Dispense to detector with flow rate of 10 ml/min

[a] PIP = pipetting/aspiration, DIS C = cumulative dispensing.
[b] No standing time for phase separation.

0.01%. Using a methylene blue solution of higher concentration than 0.01% can cause higher background level due to methylene blue partition into chloroform phase. Therefore, methylene blue concentration of 0.01% was selected. The selected conditions and operational sequence of the SIA system for the determination of anionic surfactant are summarized in Table 3.

3.2.2. Analytical characteristics

Using the SIA setup shown in Fig. 1 and under the above-mentioned selected conditions, the linear calibration graph was obtained for SDS in the concentration range of 1–10 mg/l with the regression equation of $y = 1.0711x - 0.1356$ and the correlation coefficient of 0.9995, as shown in Fig. 5. The LOD of 0.48 mg/l was obtained. The RSD was less than 5% ($n = 11$, 5.0 mg/l SDS). A five samples per hour assay can be obtained. Increase of the throughput may be obtained by employing another type of pump.

3.2.3. Application to samples

The applicability of the proposed procedure was demonstrated for the determination of anionic surfactant in drainage water samples. The results were compared to those obtained by the methylene blue standard method [29], as summarized in Table 4. There is no significant difference in the results obtained from the proposed and the standard procedures.

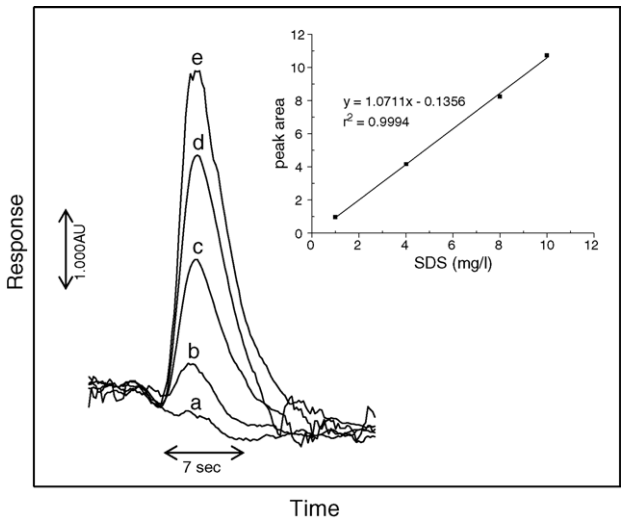

Fig. 5. Typical SI-grams and calibration graph of standard SDS; a = blank, b = 1, c = 4, d = 8, e = 10 mg/l.

Table 4
Determination of anionic surfactant in drainage water samples by the proposed and standard methods

Sample	Found (mg/l)	
	Proposed method	Standard method [29]
1	3.38 ± 0.01	3.42
2	2.76 ± 0.02	2.77

4. Conclusion

Sequential injection analysis with lab-at-valve approach for alternative simple on-line liquid–liquid micro-extraction was exploited. A simple fabricated LAV unit, a separating chamber, attached at a port of a conventional multiposition selection valve offers an on-line automated extraction in a micro-scale. Therefore, consumption of sample, reagent and organic solvent, also waste generation, is tremendously reduced. A cost effective LAV apparatus can be easily fabricated using a less precise machine tools. Applications for the assays of diphenhydramine hydrochloride in pharmaceutical preparations and anionic surfactant in water samples have been successfully demonstrated. Instead of using Spectronic 21 detector, investigation to plug a fiber optic spectrophotometric detection system to the conical separation chamber has been in progress to make such a system become a real SIA-LAV liquid–liquid extraction.

Acknowledgements

The Staff Development Project of the Ministry University Affairs, the Commission on Higher Education, is gratefully acknowledged for the scholarship to R.B. during the Ph.D. study at Chiang Mai University. This work was supported by the Thailand Research Fund (TRF), the Postgraduate Education and Research Program in Chemistry (PERCH) and the Graduate School, Chiang Mai University. Metrohm Siam and Metrohm AG are acknowledged for the on-loan autoburette.

References

[1] H. Abdine, F. Belal, N. Zoman, Farmaco 57 (2002) 267.
[2] P. Tipparat, S. Lapanantnoppakhun, J. Jakmunee, K. Grudpan, J. Pharm. Biomed. Anal. 30 (2002) 105.
[3] R.H. Maghssoudi, A.B. Fawzi, M.A.N.M. Meerkalaiee, J. Assoc. Off. Anal. Chem. 60 (1977) 926.
[4] F. Priego-Capote, M.D. Luque de Castro, Anal. Chim. Acta 489 (2003) 223.
[5] T. Kyaw, T. Fujiwara, H. Inoue, Y. Okamoto, T. Kumamaru, Anal. Sci. 14 (1998) 203.
[6] A. Cladera, M. Miro, J.M. Estela, V. Cerda, Anal. Chim. Acta 421 (2000) 155.
[7] W. Praditwiengkum, K. Grudpan, J. Flow Inject. Anal. 17 (2002) 202.
[8] A.N. Anthemidis, G.A. Zachariadis, C.G. Farastelis, J.A. Stratis, Talanta 62 (2004) 437.
[9] J. Liu, X. Liang, G. Jiang, Y. Cai, Q. Zhou, G. Liu, Talanta 60 (2003) 1155.
[10] S.C. Nielsen, S. Sturup, H. Spliid, E.H. Hansen, Talanta 49 (1999) 1027.
[11] B. Karlberg, S. Thelander, Anal. Chim. Acta 98 (1978) 1.
[12] H.F. Bergamin, J.X. Medeiros, B.F. Reis, E.A.G. Zagatto, Anal. Chim. Acta 101 (1978) 9.
[13] T. Sakai, H. Harada, X. Liu, N. Ura, K. Takeyoshi, K. Sugimoto, Talanta 45 (1998) 543.
[14] K. Backstrom, L.G. Danielsson, Anal. Chim. Acta 232 (1990) 301.
[15] T. Sakai, H. Harada, X.Q. Liu, N. Ura, K. Takeyoshi, K. Sugimoto, Talanta 45 (1998) 543.
[16] T. Sakai, S. Piao, N. Teshima, T. Kuroishi, K. Grudpan, Talanta 63 (2004) 893.
[17] S. Motomizu, M. Kobayashi, Anal. Chim. Acta 261 (1992) 471.
[18] S. Motomizu, M. Oshima, N. Goto, J. Flow Inject. Anal. 10 (1993) 255.
[19] J. Ruzicka, G.D. Marshall, Anal. Chim. Acta 237 (1990) 329.
[20] S. Nakano, Y. Luo, D. Holman, J. Ruzicka, G.D. Christian, Microchem. J. 55 (1997) 392.
[21] K.L. Peterson, B.K. Logan, G.D. Christian, J. Ruzicka, Anal. Chim. Acta 337 (1997) 99.
[22] Y. Luo, S. Nakano, D.A. Holman, J. Ruzicka, G.D. Christian, Talanta 44 (1997) 1563.
[23] J. Wang, E.H. Hansen, Anal. Chim. Acta 456 (2002) 283.
[24] A. Cladera, M. Miro, J.M. Estela, V. Cerda, Anal. Chim. Acta 421 (2000) 155.
[25] J. Ruzicka, Analyst 125 (2000) 1053.
[26] K. Grudpan, Talanta 64 (2004) 1084.
[27] J. Jakmunee, L. Patimapornlert, S. Suteerapataranon, N. Lenghor, K. Grudpan, Talanta 65 (2004) 789.
[28] The United States Pharmacopoeia, 24th ed., United States Pharmacopoeia Convention Inc., Rockville, 2000, pp. 583–584.
[29] Standard Method for the Examination of Water and Waste Water, 17th ed., American Public Health Association, Washington, 1989, pp. 59–63.

Available online at www.sciencedirect.com
SCIENCE DIRECT®
Talanta 68 (2005) 262–267
Talanta
www.elsevier.com/locate/talanta

Exploiting guava leaf extract as an alternative natural reagent for flow injection determination of iron

Thapanon Settheeworrarit [a], Supaporn Kradtap Hartwell [a,*], Somchai Lapanatnoppakhun [a], Jaroon Jakmunee [a], Gary D. Christian [b], Kate Grudpan [a]

[a] *Department of Chemistry, Faculty of Science, Chiang Mai University, 239 Huay Kaew Road, Suthep, Chiang Mai 50200, Thailand*
[b] *Department of Chemistry, University of Washington, Box 351700, Seattle, WA 98195-1700, USA*

Received 26 May 2005; received in revised form 16 July 2005; accepted 16 July 2005
Available online 29 August 2005

Abstract

Guava leaf extract is utilized as an alternative natural reagent for quantification of iron. The flow injection technique enables the use of the extract in acetate buffer solution without the need of further purification. Some properties of the extract such as its stability and ability to form a colored complex with iron were studied. The proposed system is an environmentally friendly method for determination of iron with less toxic chemical wastes.

Keywords: Guava leaf extract; Natural reagent; Flow injection; Iron

1. Introduction

Many scientific studies involve the use of chemicals that cause contamination in the environment. For example, water studies to determine the amount of different ions in natural water may need chemical reagents that are not normally present in the environment. If wastes from such studies are not properly stored or treated, these foreign substances could contaminate soil or water sources. Gaining popularity, the research area known as green chemistry aims to explore the use of alternative reagents or alternative synthetic methods that minimize the use of toxic chemicals.

In this study, a natural guava (*Psidium guajava* L., Myrtaceae family) leaf extract has been investigated as an alternative natural indicator for iron quantification by the flow injection technique. Reports have indicated that guava leaves contain chemicals that are useful for whitening [1], anti-pigmentation [2], anti-bacterial treatment [3], leather tanning [4], and diet food and beverage components [5], and in the prevention of diabetes. [6] In Thailand, there has been some local usage of guava leaves as an indicator of the presence of iron in ground water. A change in color of water to a darker color helps local villagers in making pre-treatment decisions such as adding alum to precipitate the iron. This use has never been published and no scientific explanation is available.

To determine the concentration of iron by a FI system, a water sample is introduced into a closed flow system and mixed with reagent that can form a colored complex, which can be detected by a colorimeter. Examples of some reagents [7] that have been used in determination of iron include 1,10-phenanthroline, 2,4,6-tri(2′-pyridyl)-1,3,5-triazine, azo-dye derivatives, mercaptoquinoline, thiocyanate and salicylate. [8] In this study, we investigate the use of guava leaf extract as an alternative reagent for quantification of iron using a FI system. Although the active chemical species in the extract is unknown and the extract may not be pure, the use of this guava leaf extract to determine the amount of iron in solution is made possible by the FI system. One of the features of FI systems is that they can be employed with reagents, which are not necessarily pure. This is because in the flow injection technique, an analyte to be determined goes through the

* Corresponding author. Tel.: +66 53 941909; fax: +66 53 941910.
E-mail address: kradtas@yahoo.com (S.K. Hartwell).

0039-9140/$ – see front matter © 2005 Elsevier B.V. All rights reserved.
doi:10.1016/j.talanta.2005.07.039

system in exactly the same condition as that of the standard. [9]

The use of a natural and easily available material in place of a toxic and expensive reagent should be beneficial from both environmental and economic aspects. In this report, the authors conduct preliminary studies of the potential use of guava leaf extract as an alternative reagent to quantify iron using a simple FI system. Some properties of the extract, including its stability, ability to form a complex with iron (II) and (III), spectral properties, suitable extraction medium, and its potential to be used for quantification of iron in water samples have been investigated.

2. Experimental

2.1. Reagents

A 100 mL volume of 1000 ppm stock standard Fe (II) solution was prepared by dissolving 0.7022 g of $(NH_4)_2Fe(SO_4)_2{\cdot}6H_2O$ (Carlo Erba) in water containing 1% (v/v) concentrated H_2SO_4 (BDH). A 1000 ppm stock standard Fe (III) solution was prepared similarly but with 0.7240 g of $Fe(NO_3)_3{\cdot}9H_2O$ (Carlo Erba). A 250 mL volume of 0.2 M sodium acetate buffer pH 4.8 solution was prepared by dissolving 6.87 g $CH_3COONa{\cdot}3H_2O$ (Merck) in water containing 1.16% (v/v) acetic acid (Carlo Erba). HCl solution of the same pH 4.8 was prepared by diluting concentrated HCl (Merck) with deionized water to the desired pH. Ascorbic acid (Merck) was prepared at the concentration of 2% (w/v). Interference studies were done by spiking some cations, Ca^{2+} ($CaCl_2$, Merck), Mg^{2+} ($Mg(NO_3)$, Merck), Co^{2+} ($CoCl_2$, BDH), Ni^{2+} ($NiCl_2$, BDH) and Cr^{3+} ($CrCl_3$, BDH) into Fe (III) 10 ppm solutions at the final concentration of 1, 5 and 10 ppm (10:1, 2:1 and 1:1 concentration ratios of Fe (III):interference ion).

2.2. Guava leaf extraction

Fresh guava leaves of 10.0 g were ground in 150 mL water (pH 7.0), diluted HCl (pH 4.8) or acetate buffer (pH 4.8) with a blending machine for 5 min. Then the suspension was filtered through filter paper no. 1 (Whatman) and the filtrate was kept at room temperature for further use. The extract was prepared daily.

2.3. Study of the conditions for guava leaf extract–iron complex formation

Both Fe (II) and Fe (III) solutions were prepared in three sets; in water, in HCl solution and in acetate buffer. Two iron concentrations of 10 and 100 ppm were used. Guava leaf extracts in the three media were mixed with iron solutions prepared in the matching medium at the ratio of 1:1 (v/v) (10 mL extract:10 mL Fe solution). Guava leaf extract without iron solution was used as a blank solution. Mixtures of guava leaf extract and iron solution were scanned for absorption spectra, measured against each medium, in the visible region 400–700 nm using a UV–vis spectrophotometer (Lambda 25, Perkin-Elmer).

2.4. Study of stability of guava leaf extract

After selection of the suitable medium for the extract from the previous experiment, guava leaf extract was prepared in that medium and allowed to stand in an uncovered beaker for 1, 2, 3, and 4 h. Mixtures of the extract and Fe (II and III) 10 and 100 ppm solutions were prepared as previously described. Mixtures were then scanned for absorption spectra to investigate absorption characteristics.

2.5. Apparatus

Peristaltic pumps (Ismatec) were used for reagent drawing. Pump tubing was Tygon and all the other tubing was PTFE (1/16 in. i.d.). Samples were introduced via a six-port injection valve (FIAlab). A Spectronic 21 spectrophotometer (Spectronic Instruments) with a flow through cell (80 μL, Hellma, Germany) was set at 570 nm and connected to a computer to record the FIA-grams using Stamp (Parallax, USA) and Microsoft Excel (Microsoft Corp., USA) software programs.

2.6. Manifold designs

2.6.1. Normal FI system

The simple one line normal FI manifold, where a sample is injected into the stream of reagent, is shown in Fig. 1(a).

2.6.2. Reverse FI system

In order to save reagent, the reverse FI manifold with two lines was tried where the reagent was injected into the stream of buffer that was later mixed with the stream of sample solution (Fig. 1(b)).

2.6.3. Column FI system

To shorten the extraction process, a column packed with ground guava leaves was connected in-line with the FI system, see Fig. 1(c). This column is made from a small Perspex glass tube with 3 mm i.d. and 2.5 cm length. Both ends were plugged with Teflon wool.

All three types of manifolds have an injection loop of 60 μL.

3. Results and discussion

3.1. Optimum condition of guava leaf extract-iron complex formation

The aim of this study was to find a suitable acidic solution for guava leaf extract–iron complex formation. Buffers

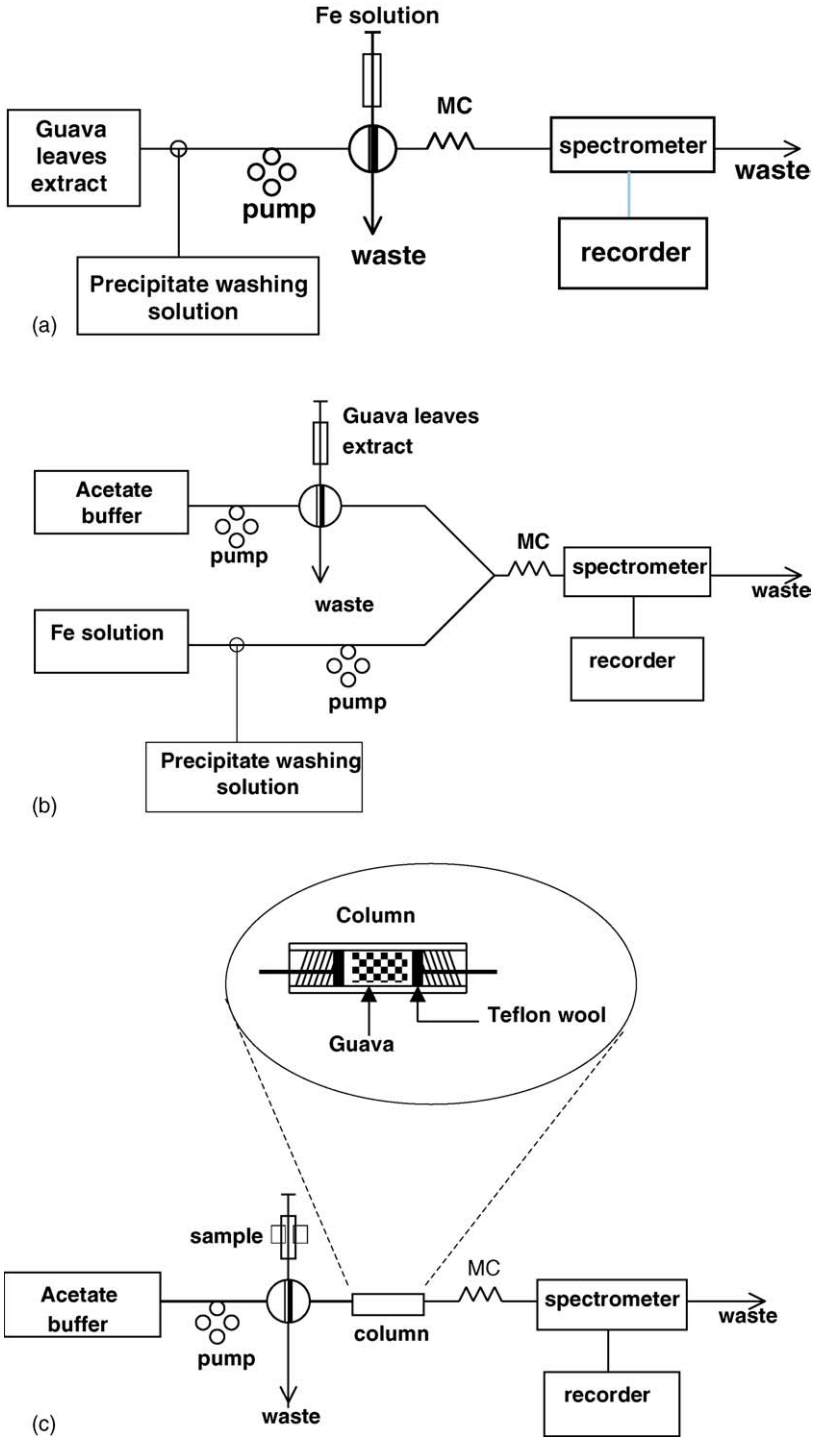

Fig. 1. (a) A normal FI manifold, (b) a reverse FI manifold and (c) a FI manifold with packed column.

of acidic pHs that can be prepared with easily available chemicals that would not interfere with the iron determination are rare. A suitable solution was sodium acetate buffer pH 4.8. Ammonium acetate was avoided because ammonium may form a complex with the metal ion of interest. To ensure the necessity of buffer solution in this study, water pH 7.0 and HCl diluted to pH 4.8 were also used as media for extraction to compare the results.

Fig. 2(a) and (b) represents the absorption spectra of guava leaf extract-iron complexes in water and buffer solution, respectively. In water (Fig. 2 (a)), no significant iron complex absorption is shown in the region of 450–700 nm, and except for high Fe (III) concentration, it is suppressed. This is likely because water cannot extract active species from the guava leaf. It could also be possible that there was no formation of iron complex with the active species or the

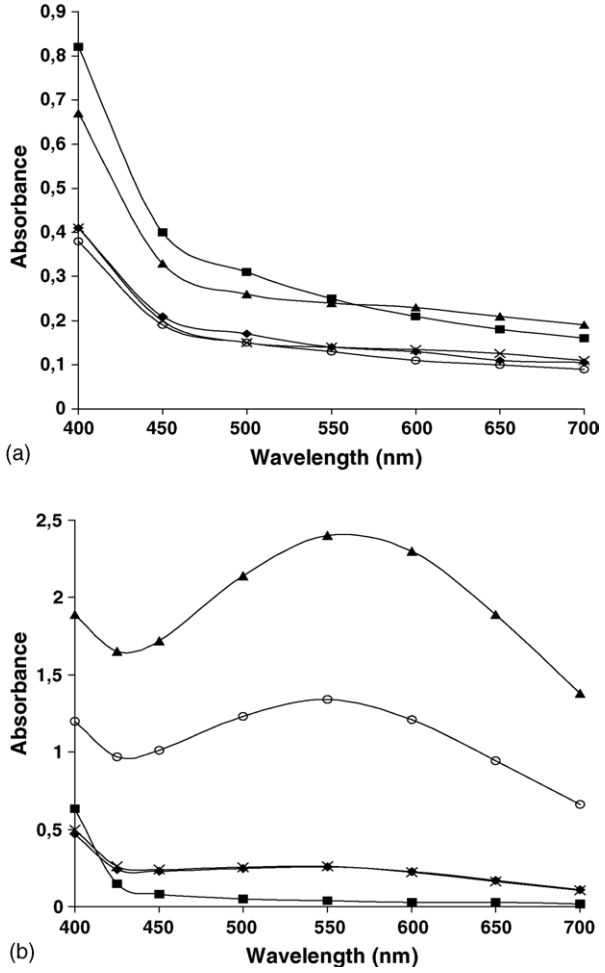

Fig. 2. (a) The absorbance spectra of guava leaf extract–iron complex in water, measured against water. (b) The absorbance spectra of guava leaf extract–iron complex in acetate buffer solution, measured against acetate buffer: (■) guava leaf extract; (▲) guava leaf extract with Fe (III) 100 ppm; (♦) guava leaf extract with Fe (III) 10 ppm; (◯) guava leaf extract with Fe (II) 100 ppm and (×) guava leaf extract with Fe (II) 10 ppm.

complex may not be stable in water. The exact cause of the results still needs further investigation, and the reason for the decreased absorbance is unknown. In acetate buffer solution pH 4.8 (Fig. 2 (b), both Fe (II) and (III) can form complexes with a chemical or chemicals in the guava leaf extract. Both Fe (II) and (III) complexes show maximum absorption at 570 ± 20 nm. The blank solution, guava leaf extract, did not show any significant absorption in the visible region. In a medium of diluted HCl pH 4.8, maximum absorption at 570 ± 20 nm was observed (not shown) only at high Fe (III) concentration but at much lower value as compared to the one in acetate buffer of the same pH. This indicates that guava leaf extract–iron complexes can only be formed at a suitable pH and that the use of buffer solution to control pH is necessary.

It has been observed that at low concentration of iron (10 ppm), the absorbances of Fe (II) and Fe (III) complexes were about the same while at high concentration of iron (100 ppm), the absorbance of the Fe (III) complex was higher

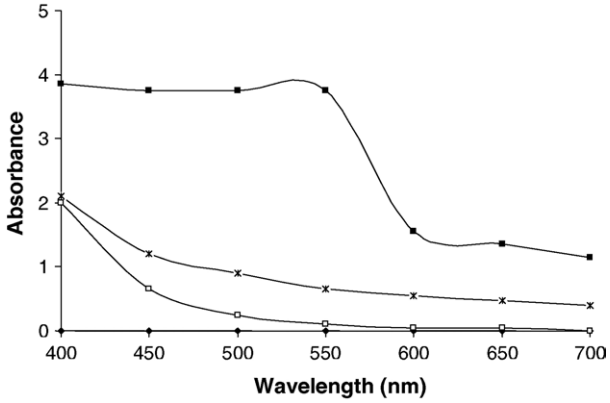

Fig. 3. The absorbance spectra studies for the reducing effect of ascorbic acid in. guava leaf extract: (♦) acetate buffer; (×) guava leaf extract and phenanthroline mixture; (□) Fe (III) 100 ppm with 0.3% (w/v) phenanthroline and (■) mixture of Fe (III) 100 ppm with 0.3% w/v phenanthroline and guava leaf extract.

than that of the Fe (II) complex. This might be explained as follows; at low concentration of iron, some chemicals (e.g., tannin) naturally present in guava leaves may reduce Fe (III) to Fe (II) and form guava leaf extract–Fe (II) complex. At high concentration of iron, there may be insufficient amount of reducing agents naturally present in the guava leaf extract to reduce all Fe (III). Therefore complexes formed were both Fe (II) and Fe (III) complexes. To test this hypothesis that guava leaf has a natural reducing effect, an additional experiment was carried out. Phenanthroline does not form a reddish complex with Fe (III) but does so with Fe (II). [10] Therefore, no significant absorbance should be observed at about 500 ± 20 nm when Fe (III) solution was mixed with phenanthroline. However, if some natural occurring substances in the guava leaf can reduce Fe (III) to Fe (II), the Fe (II)–phenanthroline complex should be formed when adding guava leaf extract into the mixture of Fe (III)–phenanthroline and the reddish colored complex with the absorption maxima at 500 ± 20 nm should appear. The absorbance at 570 ± 20 nm from the guava leaf extract–Fe (III) complex from excess Fe (III) that has not been reduced should also be observed.

In this experiment 3% (w/v) 1,10-phenanthroline, 100 ppm Fe (III) solution and guava leaf extract were mixed 1:1:1 by volume. The results shown in Fig. 3, comparing absorption spectra of 100 ppm Fe (III)–phenanthroline solution and 100 ppm Fe (III)–phenanthroline–guava leaf extract solution, confirm that guava leaf has a natural reducing effect. The mixture of Fe (III)–phenanthroline shows only slight absorbance at 500 nm and lower wavelengths. Guava leaf extract–phenanthroline mixture in the absence of Fe (III) was slightly turbid with white precipitate and might block the light, showing the result as if the solution had absorbed the light at 500 nm and lower wavelengths. The increase of absorbance at that region, when adding guava leaf extract into the Fe (III)–phenanthroline solution, was due to the reducing effect of guava leaf extract that changed Fe (III) to Fe

(II) which formed a reddish complex with phenanthroline that was observed with bare eyes. The comparable graph for 100 ppm Fe (III) with guava extract in acetate buffer is shown in Fig. 2(b) with the absorbance being about one half that when phenanthroline is added.

The results from both experiments in this study also indicate that the guava leaf extract–Fe (III) complex has higher absorbance (higher molar absorptivity) than that of the Fe (II) complex at 570 nm.

3.2. Stability of the guava leaf extract indicator

Guava leaf extract in acetate buffer was set-aside for 1, 2, 3, and 4 h before mixing with Fe (II) and Fe (III) solutions. Absorbances at 570 nm were recorded every hour. It was found that there were no significant changes in absorbance with time. This indicates that guava leaf extract is stable for at least 4 h, which is sufficient for a continuous experiment using FI.

3.3. Comparison of different manifold designs

In order to reduce the consumption of guava leaf extract, a reverse two line FI manifold was developed. Guava leaf extract was injected into the acetate buffer stream before merging with Fe solution.

In both the normal and reverse FI systems, purple precipitate adhering to the tubing and the detection cell was observed. Such a precipitate can cause unreliable and faulty results. Therefore, the procedure was modified by having a precipitate washing step with ascorbic acid. Fig. 4 shows the characteristics of the signals obtained from the reverse FI system which are similar to those obtained from the normal FI system. Signals from the Spectronic 21 are recorded as transmittance. Peaks between each run, which are constant throughout the experiment, are due to the Schlieren effect that occurs from injection of ascorbic acid for line washing.

Apart from minimizing the consumption of guava leaf extract, the reverse FI also showed better sensitivity than the normal FI system. This is possibly due to higher amount and less dilution of the Fe solution introduced by pumping as compared to injection. In terms of precision, the results obtained from the reverse FI system showed a slightly higher relative standard deviation (3–10%) as compared to the normal FI system (1–7%), for the Fe (III) concentration range of 1–10 ppm, which could be due to the high diffusion of reagent into the Fe solution stream thereby causing inconsistency of the complex formation.

Another attempt was to reduce the process of guava leaf extraction by packing the ground guava leaves in a column and placing it in the FI manifold. It was found that the guava leaves packed column-FI system could not be used effectively. The chemical from the leaves only came out at the edge of each piece, yielding a very small amount of color reagent in the flow stream. In addition, the active chemical was used up quickly, resulting in the need to change the column for every analysis, which is not practical.

3.4. Standard calibration graph and figures of merit

Calibration graphs for Fe (III) were prepared using both normal and reverse FI systems. Only calibration graphs of Fe (III) were constructed because species found in real samples such as water samples should be in the form of Fe (III).

Calibration graphs were obtained from standard Fe (III) solutions of 1, 2, 4, 6, 8 and 10 ppm. Both the normal FI and the reverse FI systems offer linear calibration graphs, represented as $Y = 11.09X + 4.06$, $R^2 = 0.9982$ and $Y = 24.93X - 20.05$, $R^2 = 0.9997$, respectively (where Y is peak height in mV and X is concentration of iron in ppm). The normal FI system showed higher blank signal due to the color of the guava leaf extract in the carrier line. In the reverse FI system, guava leaf extract was injected into the stream of colorless Fe solution and, therefore, the blank signal was low.

Even though the relative standard deviation is higher (3–10% R.S.D. in the Fe (III) working range of 1–10 ppm), the reverse FI system offers much better sensitivity than the normal FI system does. The practical lowest detectable concentration of Fe (III) obtained from the reverse FI system (estimated based on 3σ of blank signals [11]) was 1 ppm. Sample throughput was 20 injections/h. A sample with simple matrices, tap water, was spiked with Fe (III) standard solution at 2, 5, 7 and 30 ppm. Percent recoveries were found to be 95–97%.

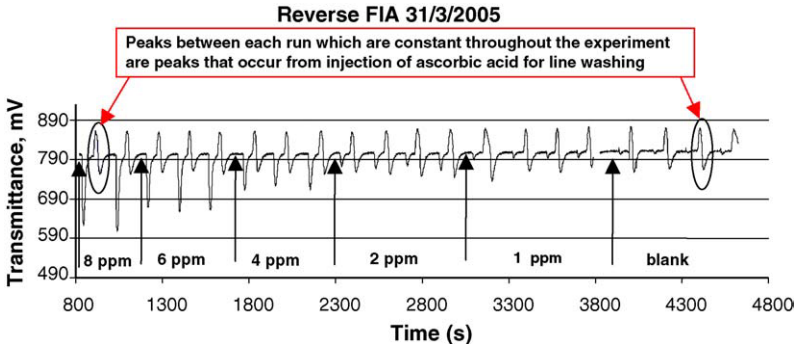

Fig. 4. Characteristics of the signals obtained from the reverse FIA system.

3.5. Interferences

It was found that the proposed system for iron (III) determination could tolerate Ca^{2+}, Mg^{2+}, Co^{2+}, Ni^{2+} and Cr^{3+} at least up to 1:1 concentration ratio (10 ppm Fe:10 ppm interference ion). Additional studies are required for general applicability.

4. Conclusion and future works

The results obtained from these preliminary studies indicate the potential use of guava leaf extract as an alternative reagent for quantification of iron in samples with simple matrices. The detection limit may possibly be improved by increasing the concentration of the guava leaf extract. No sample treatment is needed for iron concentrations at or below 30 ppm since Fe (III) and Fe (II) absorbances are similar, probably due to complete reduction of the Fe (III) by some chemicals naturally present in the guava leaves. Higher concentrations might be measured by adding a reducing agent such as hydroxylamine to convert the Fe (III) to Fe (II). Further studies are needed. Prior to applying the guava leaf extract in studies of samples containing complicated matrices, further studies should be made. Extensive interference studies, especially from other cations, should be evaluated. Even if the extract proves non-selective, it would serve for post-column detection of iron in separation or speciation studies. Although impure reagents can be used in a FI system, it would be interesting to find out what the exact chemical in guava leaf is that forms complexes with iron so that leaves of other plant species with similar chemical contents can be explored. Comparison of extracts from young and old leaves together with an additional separation technique such as HPLC or GC and NMR may help to identify the active chemical species. The use of dry leaves rather than fresh ones and the method of stabilizing the extract to be kept for future use should also be investigated. This will extend the use of the extract when guava leaf is not in season.

Acknowledgements

The Junior Student Talent Project, Thailand Research Fund (TRF) and the Post Graduate Education and Research in Chemistry (PERCH) are acknowledged for the support.

References

[1] T. Takashita, Y. Inoue, T. Ishihara, T. Ishihara, Patent No. JP 2,000,069,938 (2000).
[2] T. Kouge, Fragrance J. (Abstract) 28 (2000) 86–90.
[3] H. El Khaden, Y.S. Mohammed, J. Chem. Soc. (1958) 3320–3323.
[4] G.D. Pande, M. Kumar, J. Indian Leather Tech. Assoc. 8 (1960) 139–142.
[5] T. Makino, R. Aiyama, Y. Deguchi, M. Watanuki, M. Nakazawa, H. Mizukoshi, M. Nagaoka, K. Harada, K. Osada Patent No. WO 2,001,066,714, AU 2,001,041,078, EP 1,262,543, BR 2,001,008,957, US 2,003,124,208 (2001).
[6] Y. Deguchi, K. Osada, K. Uchida, H. Kimura, M. Yoshikawa, T. Kudo, H. Yasui, M. Watanuki, Nippon Nogei Kagaku Kaishi (Abstract) 72 (1998) 923–931.
[7] Z. Marczenko, Separation and Spectrophotometric Determination of Elements, 2nd ed., Ellis Horwood Ltd., 1986.
[8] Y. Udnan, J. Jakmunee, S. Jayasvati, G.D. Christian, R.E. Synovec, K. Grudpan, Talanta 64 (2004) 1237–1240.
[9] K. Grudpan, Talanta 64 (2004) 1084–1090.
[10] K. Jitmanee, S. Kradtap Hartwell, J. Jakmunee, S. Jayasvasti, J. Ruzicka, K. Grudpan, Talanta 57 (2002) 187–192.
[11] G.D. Christian, Analytical Chemistry, 6th ed., John Willey and Sons, New York, 2004.

A Simple Flow Injection Assay of Ca(II) in Mineral Supplement Using Mg(II)-EDTA

Kwuanjit Manee-on[1], Somchai Lapanantnoppakhun[1,2], Jaroon Jakmunee[1,2] and Kate Grudpan[1,2]*

[1] Department of Chemistry, Faculty of Science, Chiang Mai University, Chiang Mai 50200, Thailand.
[2] Institute for Science and Technology Research and Development, Chiang Mai University, Chiang Mai 50200, Thailand.

Abstract

A new concept for a simple FI assay of Ca(II) employing a replacement reaction of Mg(II)-EDTA by Ca(II) in the present of Eriochrome Black T (EBT) is proposed. The released magnesium reacts with EBT. FI peak due to absorbance change of Mg(II)-EBT is proportional to Ca(II) concentration. Even with such a very simple FI set up, a through-put of 200 injections/h can be achieved. The procedure was applied to assay Ca(II) in mineral supplement samples. The results obtained agreed well with that of the British Pharmacopoeia titration method.

Key words Calcium, Magnesium, EDTA, Eriochrome Black T, mineral supplement

1. Introduction

Calcium is an important mineral for human body especially women. It reduces the risk of osteoporosis, the increased porosity or softening of bone, which usually occur in mature and postmenopausal women. However, too much of calcium consumption can cause problems. The effects of calcium overdose include renal damage and deposition of calcium in other areas of the body besides the bones. It can contribute to stone formation for people who are at risk of developing kidney stones.

Various analytical procedures have recently been developed for the determination of Ca(II) such as spectrophotometry [1], atomic spectroscopic techniques[2], electrochemical techniques [3] and complexometric titration [4-6]. The last ones are also employed as a standard method [4-6]. Flow based procedures [3, 7, 8] have also been reported for Ca(II) determination.

In this work, a new concept for a simple FI set-up with procedure employing a replacement reaction of Mg(II)-EDTA by Ca(II) in a present of Eriochrome Black T (EBT) is proposed. The released Mg (II) reacts with EBT in ammonia – ammonium chloride buffer of pH 9.5. Absorbance change due to Mg-EBT (at 530 nm) is followed. Peak height is proportional to the concentration of Ca(II). The procedure is demonstrated to be an alternative high sample through-put assay for Ca(II) in mineral supplement.

2. Experimental

2.1 Flow Manifold

FI manifold is schematically depicted in Fig. 1. It consists of simple components including a filter colorimeter.

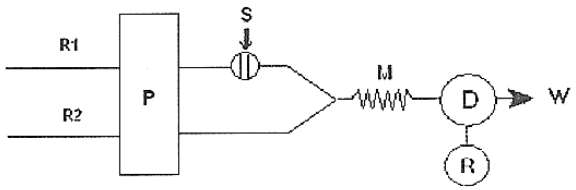

Fig. 1 Flow injection system for the determination of Ca(II) : R1= Mg(II)-EDTA reagent, R2 = EBT , P = peristaltic pump (Ismatec), S = injection valve (Rheodyne 6- Port valve), M = mixing coil, D = colorimeter (Cole Parmer 5564-15 with a green filter), R = recorder (Philips PM 8251) and W = waste.

2.2 Chemicals and Reagents

Stock standard Ca(II) solution (0.10 M) was prepared by dissolving 1.0010 g $CaCO_3$ (Fluka) in 1 ml of 1 M HCl. The solution was boiled to remove carbon dioxide before making the volume up to 100 ml with deionized water. Standard Ca(II) solutions of appropriate concentrations were obtained by further dilutions.

A solution containing Mg(II)-EDTA was prepared by dissolving 20.3300 g Na_2EDTA ($Na_2C_{10}H_{14}N_2O_8.H_2O$, Merck) and 37.2240 g $MgCl_2.6H_20$ (Fluka) in ammonia-ammonium chloride buffer (pH 9.5, 0.1 M) in a total volume of 1000 ml. The solution should have a Mg(II) : EDTA mole ratio of 1:1.5. A portion (0.01 g) of Eriochrome Black T (Aldrich) was dissolved in 100 ml of the ammonia-ammonium chloride buffer to become 0.01 % (w/v) solution.

2.3 Sample preparation

To prepare sample solutions from calcium carbonate tablets, the standard procedure was followed [6]. Not less than 20 tablets were weighed and finely powdered. A portion of the powder was weighed to obtain calcium equivalent to 100 mg and dissolved with 10 ml of 1 M HCl. The solution was boiled until clear solution was observed. After that it was diluted to 250 ml with deionized water. The treated sample was analyzed by the

*Corresponding author
E-mail: kate@chiangmai.ac.th

proposed method and the British Pharmacopoeia titration method [6].

For the capsule sample, 20 capsules were weighed. The accurate sample powder weight was obtained by the difference of the full and empty capsule.

3. Results and discussion

A set of conditions as summarized in Table 1 was selected. Fig. 2 illustrates the FI-gram.

Table 1 The conditions of the FI procedure for the determination of Ca(II).

R1	$[Mg^{2+}]$ in 0.1 M NH_3/NH_4Cl buffer	0.008 M
	[EDTA] in 0.1 M NH_3/NH_4Cl buffer	0.012 M
	Flow rate	5.1 ml/min
R2	Eriochrome Black T (EBT) in 0.1 M NH_3/NH_4Cl buffer	0.006 % w/v
	Flow rate	2.7 ml/min
S	Injection volume	50 µl
M	Mixing coil	75 cm
D	Detection wavelength	green filter (530 nm)

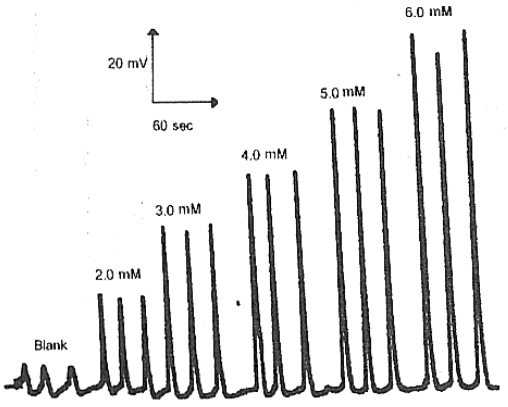

Fig. 2 FI-gram of Ca(II) 2.0-6.0 mM.

A linear calibration graph was obtained for 2.0-6.0 mM Ca(II) : y = 22.094x- 14, r^2 = 0.9972 with a detection limit (3σ) [9] of 0.6 mM, and 2% RSD (5 mM, n=11). A through-put of 200 injections per hour was achieved.

Effect of pH of solution injected was studied. According to the preliminary study, the standard solutions were chosen to be prepared in 0.01 M HCl (pH 2). Solutions adjusted to various pH values (2, 3 and 5) containing 5 mM Ca(II), were prepared. The solutions were injected into the FI system and evaluated for their analysis results by using a calibration graph prepared by employing standard solutions of pH 2. The analysis results were found to be the same as those of the standard Ca(II) prepared in pH 2 solution. This indicates that pH of the injected solution could be in the range of 2-5.

Although the procedure is not specific for Ca(II) but with its instrument simplicity and a high sample through-put, it should be useful to some certain types of samples which contain no interferents.

The results of the assay for Ca(II) in mineral supplement samples by the proposed procedure are summarized in Table 2 and agree well with the values obtained by the British Pharmacopoeia titration method [6]. This also indicates that no interference found in such assay of the samples.

Table 2 The determination results of Ca(II) mineral supplement samples by the proposed FI procedure and the British Pharmacopoeia titration method (average of triplicate results).

Sample[a]	Label	This work		BP Titration	
	mg/unit	mg/unit	%Label	mg/unit	%Label
No.1	600	573	96	610	102
No.2	250	243	97	246	99

[a] carbonate form, No.1 : tablet, No.2 : capsule

4. Conclusion

A simple FI determination of Ca(II) is proposed. It is based on the replacement of Mg(II)-EDTA by Ca(II). The released Mg(II) forms colored Mg(II)-Eriochrome Black T complex. The FI peak due to absorbance (at 530 nm) of the complex is proportional to Ca(II) concentration. The proposed procedure with very simple detection and high sample through-put is an alternative cost-effective assay of Ca(II) in mineral supplement.

5. Acknowledgements

We thank the Thailand Research Fund (TRF), the Postgraduate Education and Research Program in Chemistry (PERCH) and the Commission in higher Education including the University Development Committee (UDC) for supports and Dr. Yuthsak Vaneesorn for useful discussion.

6. References

[1] S.C. McCleskey, P.N. Floriano, S.L. Wiskur, E.V. Anslyn and J.T. McDevitt, *Tetrahedron*, **59**, 10089 (2003).

[2] A. Moreno-Cid and M.C. Yebra, *Anal. Bioanal. Chem.*, **379**, 77 (2004).

[3] A. Bratov, N. Abramova, C. Dominquez and A. Baldi , *Anal. Chim. Acta,* **408**, 57 (2000).

[4] *The United State Pharmacopeia USP 25: the National Formulary*, USP Convention, Inc., Rockville, 2002, p. 280.

[5] *Official Methods of Analysis of the Association of Official Analytical Chemists*, AOAC, Inc., Virginia, **1**, 1990, p. 502.

[6] *British Pharmacopoeia*, the Stationery Office, London, **1,** 1998, p. 220.

[7] K. Grudpan, J. Jakmunee, Y. Vaneesorn, S. Watanesk, A. U. Maung and P. Sooksamiti, *Talanta*, **46,** 1245 (1998).

[8] N. Sanchez-Rosado, A. Morales-Rubio and M. de la Guardia, *J. Flow Injection Anal.,* **19**, 121 (2002).

[9] J.C. Miller and J.N. Miller, *Statistics for Analytical Chemistry*, **3rd ed.,** Ellis Horwood, Sussex, 1993.

(Received March 18, 2005)
(Accepted March 30, 2005)

WATER RESEARCH 40 (2006) 2044–2054

Available at www.sciencedirect.com

SCIENCE DIRECT®

journal homepage: www.elsevier.com/locate/watres

Interaction of trace elements in acid mine drainage solution with humic acid

Siripat Suteerapataranon[a,b,1], Muriel Bouby[a], Horst Geckeis[a,*], Thomas Fanghänel[a,c], Kate Grudpan[b]

[a]Forschungszentrum Karlsruhe, Institut für Nukleare Entsorgung, Postfach 3640, D-76021 Karlsruhe, Germany
[b]Department of Chemistry, Faculty of Science, Chiang Mai University, Chiang Mai 50200, Thailand
[c]Universität Heidelberg, Physikalisch-Chemisches Institut, Im Neuenheimer Feld 253, D-69120, Heidelberg, Germany

ARTICLE INFO

Article history:
Received 5 July 2005
Received in revised form
24 February 2006
Accepted 7 March 2006

Keywords:
Acid mine drainage
Trace metal ions
Humic acid
Flow field-flow fractionation

ABSTRACT

The release of metal ions from a coal mining tailing area, Lamphun, Northern Thailand, is studied by leaching tests. Considerable amounts of Mn, Fe, Al, Ni and Co are dissolved in both simulated rain water (pH 4) and 10 mg L^{-1} humic acid (HA) solution (Aldrich humic acid, pH 7). Due to the presence of oxidizing pyrite and sulfide minerals, the pH in both leachates decreases down to ~3 combined with high sulfate concentrations typical to acid mine drainage (AMD) water composition. Interaction of the acidic leachates upon mixing with ground- and surface water containing natural organic matter is simulated by subsequent dilution (1:100; 1:200; 1:300; 1:500) with a 10 mg L^{-1} HA solution (ionic strength: 10^{-3} mol L^{-1}). Combining asymmetric flow field-flow fractionation (AsFlFFF) with UV/Vis and ICP-MS detection allows for the investigation of metal ion interaction with HA colloid and colloid size evolution. Formation of colloid aggregates is observed by filtration and AsFlFFF depending on the degree of the dilution. While the average HA size is initially found to be $\leqslant 2$ nm, metal–HA complexes are always found to be larger. Such observation is attributed to a metal induced HA agglomeration, which is found even at low coverage of HA functional groups with metal ions. Increasing the metal ion to HA ratio, the HA bound metal ions and the HA entities are growing in size from <3 to >450 nm. At high metal ion to HA ratios, precipitation of FeOOH phases and HA agglomeration due to colloid charge neutralization by complete saturation of HA complexing sites are responsible for the fact that most of Fe and Al precipitate and are found in a size fraction >450 nm. In the more diluted solutions, HA is more relevant as a carrier for metal ion mobilization.

1. Introduction

Approximately 20% of the total electricity in Thailand is generated by coal burning (Arbhabhirama et al., 1987). Most of the coal mines are the open-pit mines, where the tailings are placed around the mining area exposed to weathering and leaching by rain. It is well known that the tailings in mining areas are composed of various kinds of minerals containing high amounts of heavy metals (Kucukonder et al., 2003; Matlock et al., 2002; Lee et al., 2002; Dang et al., 2002). Residual waste crushed rock from mining activities represents a major source for metal rich acid mine drainage (AMD) water. The tailing minerals can release metal ions over long time scales due to oxidation of sulfide minerals leading to the production

*Corresponding author. Tel.: +49 7247 82 4992; fax: +49 7247 82 4308.
E-mail address: geckeis@ine.fzk.de (H. Geckeis).
[1] Presently at School of Science, Mae Fah Luang University, 333 T.Tasud, Muang, Chiang Rai 57100 Thailand.
0043-1354/$ - see front matter © 2006 Elsevier Ltd. All rights reserved.
doi:10.1016/j.watres.2006.03.009

of sulfuric acid (e.g. Bunce et al., 2001) according to the overall equations:

$$FeS_2(s) + \tfrac{7}{2}O_2(g) + H_2O \rightarrow Fe^{2+}(aq) + 2H^+(aq) + 2SO_4^{2-}(aq),$$
$$2Fe^{2+}(aq) + \tfrac{1}{2}O_2(g) + 5H_2O(l) \rightarrow 2Fe(OH)_3(s) + 4H^+(aq).$$

Metals in the waste rock can be released by the low pH AMD (Kucukonder et al., 2003; Matlock et al., 2002; Lee et al., 2002; Dang et al., 2002; Bunce et al., 2001; Vigneault et al., 2001) and possibly be transported by rainwater and surface water away from the source. Quite a number of studies in many countries have been performed to study the release of metals from coal mine spoils, but only a few in Thailand. Those reports concerned the weathering process of the tailings using leaching experiment and sequential extraction (Yukselen and Alpaslan, 2001; Sun et al., 2001; Sahuquillo et al., 2002; Badulis, 1998). They focused on only how the metals are leached out. However, the mechanisms leading to the possible migration of heavy metals further away downstream from the mining site is still not clear. The geochemical behavior of metals released from the acidic tailing minerals depends on a number of different parameters. As soon as the AMD is diluted and pH increases, a number of precipitating phases have been observed: jarosite, schwertmannite, ferrihydrite (Hochella et al., 1999; Dinelli et al., 2001) and mixed amorphous gel like phases with more or less variable composition (Featherstone and O'Grady, 1997; Munka et al., 2002). Precipitation of those phases going along with metal adsorption and co-precipitation leads to the retention of released metal ions. The mobility of metal ions then is often determined by potentially forming particulate and colloidal species being stabilized and dispersed in the water. Particulate and colloidal species of metals such as Fe, As, Cd, Cu, Mn, Pb and Zn derived from tailing minerals have indeed been observed to migrate over long distances (Featherstone and O'Grady, 1997; Kimball et al., 1995; Zänker et al., 2002; Schemel et al., 2000). Purely inorganic colloidal species composed of high AlOOH and FeOOH amounts have their isoelectric point close to the pH of natural water and thus exhibit only low colloidal stability. Surface sorption or coating with silicate or natural organic matter as humic or fulvic acid is known to shift the isoelectrical point of colloidal particles to lower pH (e.g. Kretzschmar et al. 1998), and to increase inter-particle charge repulsion and thus colloidal stability. Humic and fulvic acids being present in natural water in concentrations ranging from 0.5 to 100 mg/L (Frimmel, 1998) can on the other hand form metal-complexes in certain pH ranges (Gundersen and Steinnes, 2003) and by this way enhance the metal mobility.

The aim of the present work is to study the colloid formation upon AMD dilution in presence of humic acid to simulate the interaction of acidic leachates upon mixing with ground- and surface water containing natural organic matter. Humic and fulvic acids are known to be major constituents of organic matter in most soils and groundwater (see e.g. Stevensen, 1994). Humic acid is thus taken to simulate the influence of natural organic matter on metal ion colloid formation. AMD is prepared by leaching of a tailing sample taken from a disposal of the Lamphun area with simulated rain water (RW) or humic acid containing solution. The solution compositions of the two leachates are compared with water samples taken from a pond fed by draining water from the mine. The leachate obtained with the humic acid solution (10 mg L^{-1}, pH 7) is then subsequently diluted with 10 mg L^{-1} humic acid solution to final pH values ranging from 4.6 to 7.6 and the colloidal species formed are characterized by using the asymmetric flow field-flow fractionation (AsFlFFF) combined with UV/VIS absorbance and ICP-mass spectrometric detection. Humic acid concentration and pH values lie in the range of natural conditions.

2. Materials and methods

2.1. Analysis of the tailings and water samples

AMD water samples from a coal mine disposal area in northern Thailand (Lamphun area) were collected from two sites of a pond during summer season (September: BP-S; LN-S) and rainy season (October: BP-O; LN-O). Tailing samples were taken from the same site. Grain particles with a size < 1 mm were separated by sieving and used for characterization by X-ray diffraction (XRD-3000, Seifert, Germany), scanning electron microscopy (SEM-EDX, CamScan CS44 FE, England), X-ray fluorescence (XRF, Siemens, SRS 3000, Germany), Organic carbon analysis (TOC-5000, Shimadzu, Japan) and trace element analysis by ICP-mass spectrometry (ELAN6000, Perkin-Elmer, USA) after total digestion (HNO_3/HF) in a microwave oven.

2.2. Leaching of the tailing sample

Batch leaching tests with two leachants were performed to follow the leaching behavior of some metals in the tailings: (1) simulated RW (2×10^{-5} mol L^{-1} HNO_3 (Merck, Germany), 3×10^{-5} mol L^{-1} H_2SO_4 (Merck, Germany), 1×10^{-5} mol L^{-1} HCl (Merck, Germany) and 2×10^{-5} mol L^{-1} NH_3 (Merck, Germany) (recipe: Sigg and Stumm, 1989) and (2) 10 mg L^{-1} Aldrich humic acid (pH 7, in 10^{-3} mol L^{-1} $NaClO_4$). Fifty mL aliquots of each leachant were added to 2.5 g of ground tailings material. Each mixture was rotated vertically at a rate of 1 rpm for 10 days. After the leaching period, the mixture was centrifuged and the leachate was separated and collected into a container. Metal ions and anions in the leachates were analyzed by ICP-MS and IC, respectively. Fe(II)/Fe(III) speciation was done by application of the classical spectrophotometric procedure described in American Water Works Association and Water Pollution Control Federation (1989).

2.3. Sequential dilution of the leachate

In order to simulate the interaction of metal ions released from the tailings to the surface- or groundwater, a sequential dilution of the humic acid solution leachates was performed. In experiment 1, aliquots of the leachate were diluted with a 10 mg L^{-1} humic acid solution of an initial pH 6.7 and containing 10^{-3} mol L^{-1} $NaClO_4$. In parallel, an analogous test was made with a 10 mg L^{-1} humic acid solution of higher initial pH (pH 9; ionic strength: 10^{-3} mol L^{-1} $NaClO_4$) (experiment 2). The dilution ratios studied in the present work were

1:100, 1:200, 1:300, and 1:500. The diluted leachate solutions were stored up to a week until the final pH established. The colloid particles <450 nm in the filtered solutions (syringe filter with pore size: 450 nm) were characterized by the AsFlFFF-ICP-MS system. The solutions before and after filtration were analyzed by ICP-MS in order to determine the particulate metal ion fraction. The particulate fraction in this case is defined as particles $>450\,nm$.

2.4. Analysis of colloidal species

Characterization of the colloidal species in the leachates was performed by AsFlFFF (HRFFF 10.000 Series, Postnova Analytics, Germany). The carrier was degassed by a 1100 series vacuum degasser model G1322A (Hewlett–Packard, Waldbronn, Germany). Buffer solutions were used as carriers for the AsFlFFF experiments: MES (pH 5, 10^{-3} mol L^{-1}) (Sigma, USA) and TRIS (pH 7, 10^{-3} mol L^{-1}). Samples generated in experiment 1 (pH ranging from 4.6 to 6.1) were fractionated in the MES buffer (pH 5), experiment 2 samples (pH ranging from 6.0 to 7.6) in the TRIS buffer (pH 7). The pH of sample solutions and the respective carrier solution, therefore, did not vary by more than 1 unit. We do not expect a major influence of these pH differences in sample and carrier solutions on the HA colloids. In-line filters (teflon membrane; pore size: 0.1 μm) were placed in the carrier tubings before entering the channel in order to retain particulate impurities coming from the internal constituents of the FFF-equipment e.g. abraded material from pumps. Thickness of the channel was 350 μm. The ultrafiltration membrane used as accumulation wall consists of regenerated cellulose with 5 kDa cutoff (Postnova Analytics, Germany). Previous experiments proved that more than 85% humic acid passed the channel under the fractionation conditions used here even though the average molecular weight was clearly lower than 5 kDa (Ngo Manh et al., 2001). Major reasons for this finding are the molecular structure of humic acid being more extended than that of globular proteins for which the membrane cutoffs are usually defined and the negative charge of the humic colloids leading to repulsion from the membrane surface (Guo et al., 2000). For each experiment, sample aliquots of 500 μL were injected into the channel via a 6-port Rheodyne injection valve. A focusing time of 180 s was selected. Elution was carried out by applying an axial channel flow rate of 1 mL min^{-1} and a cross flow rate of 0.7 mL min^{-1}.

From the channel the carrier solution was directed through an UV–Vis detector (LambdaCmax 481, Waters, USA) recording the signal at $\lambda = 225\,nm$. The ICP-MS (ELAN6000, Perkin Elmer, USA) was connected to the AsFlFFF -UV–Vis flow-through cell via a T-junction (UpChurch, USA) to analyze metal ions continuously in a simultaneous mode. The stream eluted from the AsFlFFF system was in-line mixed with a 6% HNO_3 solution containing Rh as an internal standard (100 μg L^{-1}). The size calibration using latex standards (20, 50 and 100 nm in diameter, Duke Scientific Corporation, California) is made by plotting $\log V_R$ against $\log d_h$ ($\log V_R = 0.34 + 0.5 \log d_h$, $R = 0.9968$), where V_R is the retention volume and d_h is the hydrodynamic diameter and R is the correlation coefficient.

3. Results and discussion

3.1. Characterization of solids and solutions

The elemental composition of the tailing sample used for leaching experiments is given in Table 1. Main mineral components as derived by XRD inspection are quartz (SiO_2), jarosite ($KFe_3(SO_4)_2(OH)_6$) (an oxidation product of pyrite (FeS_2)), gypsum ($CaSO_4 \cdot 2H_2O$), and additionally muscovite ($KAl_3Si_3O_{10}(OH)_2$) and kaolinite ($Al_2Si_2O_5(OH)_4$). Analysis of minor components by SEM-EDX showed the presence of iron sulfides and gypsum. The composition of the solutions resulting from the leaching experiments with 10 mg L^{-1} HA solution and simulated RW is given in Table 2. As expected, the solutions become acidic (pH 2.6–2.7) and rich in sulfate in both leachates. These values remained more or less independent of the solid/liquid ratio of the experiment. The same pH values and sulfate concentrations were observed in column leaching experiments (not described here) with the identical solid material and solutions. Beside high Ca, Fe, Mn, Mg, Al and Na concentrations, transition metal ions as Co, Cu, Ni and Zn were present up to 3 mg L^{-1}. The final composition of the leachates is primarily determined by dissolution of acidic components from the tailings. The initial solution composition and notably the presence or absence of humic acid does not play a significant role. Weak complexing characteristics of the fully protonated HA functional groups and the potential sorption to the tailings material under the acidic conditions may explain why the HA solution does not mobilize more metal ions than the simulated RW. The composition of the leachates obtained in the laboratory experiments is quite similar to that found in some water samples collected at the mining areas (see also Table 2). Those samples were taken from a pond at the bottom of the mining site which is fed by drainage water from the mine in September (summer time in Thailand, sample BP-S and LN-S) and in October (raining season, BP-O and LN-O). The pH-values of the BP-S and LN-S samples are considerably lower than those of the BP-O and LN-O solutions likely due to the dilution by RW. In general, the

Table 1 – Composition of the tailings sample as analyzed by XRF, XRD, SEM-EDX, TOC and ICP-MS (grain fraction: <1 mm)

Element	Content	Method
Si	40.5% (w/w)	XRF
Al	20.5% (w/w)	XRF
Fe	12.7% (w/w)	XRF
As	137.5 μg g^{-1}	ICP-MS
TOC	6.2% (w/w)	TOC-analyzer
Minerals		
Quartz, Jarosite, Gypsum, Muscovite, Kaolinite	N/Q	XRD
Gypsum, FeS_2	N/Q	SEM-EDX

N/Q: Not quantified.

Table 2 – Composition of leachate solution (10 mg L^{-1} HA, 1×10^{-3} mol L^{-1} $NaClO_4$) and water samples collected from a pond on site. BP-S/LN-S are taken in September (summer season), BP-O/LN-O in October (rainy season). (Analytical uncertainties are < 10%.)

	Tailings leachate		BP-S	LN-S	BP-O	LN-O
	HA-solution	sim. rain-water solution				
pH	2.6	2.7	2.43	2.41	5.88	5.22
DOC (mg L^{-1})	N/A	N/A	29.7	28.8	3.8	4.6
Trace elements (mg L^{-1})						
Fe	84.7	119.4	331 (80% Fe(II))	339 (75% Fe(II))	1.4 (86% Fe(II))	2.2 (59% Fe(II))
Al	15.9	21.5	28.4	31.1	0.7	2.2
Mn	23.0	26.9	23.8	24.2	3.0	3.6
Ca	133	164	99.6	104.6	30.4	33.0
Mg	17.3	20.4	12.4	13.3	7.2	7.3
Na	14.9	0.1	5.5	5.9	36.8	35.2
Trace elements (μg L^{-1})						
Co	500	517	349	373	27	28
Ni	1200	1467	1900	900	100	100
Cu	900	1069	182	172	23	16
Zn	2900	3377	1600	1700	N/A	N/A
Cd	11	14	N/A	N/A	N/A	N/A
Pb	0.74	0.5	37	34	1.3	1.3
Ce	267	320	137	148	0.5	1.3
Eu	8.5	8.6	N/A	N/A	N/A	N/A
La	101	107	N/A	N/A	N/A	N/A
Th	41	42	10	11	0.5	0.1
U	23	25	18	19	0.6	0.9
Anions (mg L^{-1})						
SO_4^{2-}	1182	1152	1487	1524	166	173
Cl^-	3.8	2.7	47	57	40	37
NO_3^-	< 0.1	3.6	< 0.1	< 0.1	4.3	1.3
PO_4^{3-}	< 0.1	<0.1	< 0.1	< 0.1	< 0.1	< 0.1

N/A: not analysed.

concentrations of inorganic and organic components in the water samples collected during the rainy season are lower (1) due to the dilution effect and (2) due to oxidation of Fe(II) with subsequent formation of Fe(III)OOH precipitates scavenging the trace elements. The compositional similarity of natural AMD taken from the pond at the site and the leachate obtained from the tailing material in the laboratory demonstrates that the leachate composition is typical for AMD in the investigated system. The nature of the relatively high organic carbon content in the pond water samples is not yet clear and no attempt was made within the present study to elucidate the nature of those compounds.

3.2. *Metal ion speciation in AMD leachates*

We performed simulation experiments in order to estimate the formation of colloidal and precipitating metal species upon dilution of the AMD in presence of humic acid. The acidic solution extracted from the tailing soil was subsequently mixed with humic acid containing solutions with initial pH values of 6.7 (experiment 1) and 9 (experiment 2), respectively. The leachate was diluted by factors of 100, 200, 300 and 500. Resulting Fe and Al concentrations and the pH values of the diluted solutions are given in Tables 3 and 4 and respective data are plotted in Figs. 1 and 2 for both dilution experiments. The pH values established in the final solutions cover a range relevant to natural conditions. Diluted solutions were aged for 1 week in order to reach steady-state conditions and to avoid reaction kinetics overlaying the results. Aim of the experiments was to provide an estimate of the conditions where metal ions in AMD could be mobilized due to colloid formation or could be rather retained by precipitation or co-precipitation.

In a first step we consulted existing thermodynamic data bases in order to estimate the speciation of metal ions in our diluted leachate solutions under oxidizing conditions. We used the speciation code ECOSAT (Keizer and van Riemsdijk, 1994) for all calculations. If not specified explicitly in the text, we took the thermodynamic data summarized by Lindsay (1979), which are implemented in the ECOSAT data base. Solubility of Fe(III) and Al(III) is calculated as a function of pH taking the solution composition of the 1:100 diluted leachate (Table 3) in absence of HA as a basis. The final pH values, Fe and Al concentrations of the diluted leachates obtained in experiments 1 and 2 are compared with calculated solubility curves in Fig. 1. As a result, over-saturation for Fe(III) with

Table 3 – Fe concentration in the leachate solutions diluted with humic acid solution (10 mg L^{-1}) with an initial pH 6.7 (exp. 1) and pH 9 (exp. 2)

Dilution factor for the leachate solution	Fe-conc. after dilution ($mol\,L^{-1}$)	$HA\text{-}COO^-$ concentration ($mol\,L^{-1}$)	Molar ratio Fe(III)/$HA\text{-}COO^-$	Exp. 1		Exp. 2	
				Final pH (initial HA solution pH 6.7)	Fe fraction >450 nm(%)	Final pH (initial HA solution pH 9)	Fe fraction >450 nm (%)
1 : 500	3.94×10^{-6}	5.3×10^{-5}	1 : 13.4	6.1	17.7	7.6	0.2
1 : 300	6.57×10^{-6}	5.3×10^{-5}	1 : 8.1	5.6	17.9	7.2	7.2
1 : 200	9.85×10^{-6}	5.3×10^{-5}	1 : 5.4	5.2	18.7	6.9	17.9
1 : 100	1.97×10^{-5}	5.3×10^{-5}	1 : 2.7	4.6	40.0	6.0	53.4

Initial concentration of Fe in the leachate is 110 mg L^{-1} (1.97×10^{-3} mol L^{-1}); the concentration of carboxylate groups in the HA is taken as 5.3×10^{-3} mol g^{-1} (Rabung et al., 1996).

regard to ferrihydrite (log (K_{sol}): -38.46, Lindsay, 1979) in the pH range of interest ($pH \geqslant 4$) is expected for both dilution experiments. In case of Al(III), the solubility limit with regard to amorphous $Al(OH)_3$ (log (K_{sol}): -32.34, Lindsay, 1979) is expected to be exceeded slightly in a pH range 6.5–7.5. However, oversaturation occurs at $pH \geqslant 5$ when assuming gibbsite as solubility determining solid phase (log (K_{sol}): -33.96, Lindsay, 1979). The presence of humic acid is anticipated to prevent precipitation due to formation of humate complexes. Using the generic parameters for humic acid and its complex formation constants with Al(III) and Fe(III) as published by Milne et al. (2003) and applying the Nica Donnan model (Kinniburgh et al., 1999), results in a speciation plot as given in Fig. 2. According to this calculation, a concentration of 10 mg L^{-1} HA appears to be insufficient to suppress ferrihydrite precipitation completely. According to the calculations, precipitation of ferrihydrite is prevented by humic acid in the higher diluted leachates. The same is true for Al(III) if we consider gibbsite precipitating. If we, however, assume that rather amorphous than crystalline phases are generated under given conditions, Al(III) species should exist as dissolved species in presence of humic acid for all dilutions. The solution speciation of Fe(III)/Al(III) is clearly dominated by humic acid complexes. The calculations predict that humic acid is able to keep considerable amounts of both metal ions via complexation in solution and thus to enhance their mobility.

Experimental data reveal that significant fractions of Fe and Al can be separated from all diluted solutions by filtration through a 450 nm membrane filter (see Tables 3 and 4). This is somewhat in contradiction to the calculations saying that even $Fe(OH)_3$ phases should not precipitate in the higher diluted samples. The presence of relatively high particulate Al fractions ($>450\,nm$)-similar to what is found for Fe—is at first glance also not compatible with the speciation calculations. The Al behavior might be explained by formation of amorphous Fe/Al co-precipitates in the concentrated solutions (1:100 diluted leachate). Another more plausible explanation is considerable flocculation of humic acid by interaction with Fe/Al ions. A number of spectroscopic studies verified that hard Lewis acids like Al(III) as well as Tb(III) and Th(IV) mainly interact with humic acid carboxylate groups (Lee and Ryan, 2004; Monsallier et al., 2003; Denecke et al., 1999). Assuming three carboxylate ligand groups interacting with one trivalent cation and taking the potentiometrically determined carboxylate concentration of the Aldrich HA (5.3×10^{-3} mol g^{-1}; Rabung et al., 1998) leads to the molar metal ion/HA ratios given in Tables 3 and 4. Note that the experimentally determined concentration of carboxylate groups (taken from Rabung et al., 1998) is quite consistent with the generic value for functional HA-groups assumed by Milne et al. (2003) (5.7×10^{-3} mol g^{-1}). The concentration of those metal ions which are strongly interacting with humic acid is dominated by Fe(III) in the leachate. The carboxylate ligand to Fe(III) ion ratio is close to 3:1 in the 1:100 diluted solution, so that HA functional groups are completely occupied with Fe(III), if we consider three carboxylate groups interacting with one trivalent Fe(III) ion. Deprotonated carboxylate groups are mainly responsible for the overall negative net charge of the humic acid macromolecule

Table 4 – Al concentration in the leachate solutions diluted with humic acid solution (10 mg L^{-1}) with an initial pH 6.7 (exp. 1) and pH 9 (exp. 2)

Dilution factor for the leachate solution	Al-conc. after dilution (mol L^{-1})	$HA\text{-}COO^-$ concentration (mol L^{-1})	Molar ratio Al(III)/$HA\text{-}COO^-$	Exp. 1		Exp. 2	
				Final pH (initial HA solution pH 6.7)	Al-fraction >450 nm (%)	Final pH (initial HA solution pH 9)	Al-fraction >450 nm (%)
1 : 500	1.48×10^{-6}	5.3×10^{-5}	1: 35.8	6.1	27.1	7.6	9.1
1 : 300	2.47×10^{-6}	5.3×10^{-5}	1: 21.6	5.6	34.6	7.2	31.9
1 : 200	3.71×10^{-6}	5.3×10^{-5}	1: 14.2	5.2	33.8	6.9	31.7
1 : 100	7.41×10^{-6}	5.3×10^{-5}	1: 7.2	4.6	43.3	6.0	53.8

Initial concentration of Al in the leachate is 20 mg L^{-1} (7.4×10^{-4} mol L^{-1}); the concentration of carboxylate groups in the HA is taken as 5.3×10^{-3} mol g^{-1} (Rabung et al., 1996).

preventing agglomeration and precipitation. Charge neutralization of the HA by the interacting cations will certainly lead to extensive HA flocculation. Flocculation in addition to ferrihydrite precipitation explains the presence not only of Fe(III) but also of Al(III) in the $>450\,nm$ fraction of the 1:100 diluted solution. The existence of Fe and Al in the size fraction $>450\,nm$ in the higher diluted sample solutions, where ferrihydrite precipitation becomes unlikely, must then mainly be due to HA flocculation. The Fe or Al fraction larger than 450 nm decreases at higher dilutions and this particulate fraction is obviously lower for Fe in experiment 2 where the pH is higher. This pH effect may be the consequence of the higher dissociation degree of the humic carboxylic acid groups impeding aggregation. We should also mention that the assumption of three carboxylate groups interacting with one trivalent cation must not necessarily be true. Ternary complex formation has been found for the trivalent actinide ion Cm(III) where e.g. significant fractions of hydroxy humate complexes may easily exist at near neutral pH (Panak et al., 1996). More metal ions can interact with the humic acid until full charge neutralization will be achieved in case of ternary humate carbonate or hydroxy complex formation.

Ca(II) is also known to induce HA flocculation (Schimpf and Petteys, 1997; Benincasa et al., 2002; Bryan et al., 2001). Wall and Choppin (2003) found in their experiments critical coagulation concentrations for Ca(II) of around 10^{-3} mol L^{-1} before significant HA flocculation ([HA] $\sim$ 100 mg L^{-1}, pH 8.3) is observed. Ca(II) concentrations of up to 3.3×10^{-5} mol L^{-1} (in the 1:100 diluted leachate) are two orders of magnitude lower than this threshold. According to our calculations, considerable Ca(II) complexation with HA is only expected at pH > 6.2 so that due to the higher charge and the stronger interaction with HA, the influence of the Fe(III)/Al(III) cations has to be assessed as more relevant for charge neutralization and the experimentally observed HA flocculation.

3.3. *Colloid characterization*

We studied the colloidal fraction (size < 450 nm) in the sequentially diluted leachates by AsFlFFF combined with UV/Vis and ICP-MS detection. The photometric detection allows monitoring of the HA in the FFF effluent while ICP-MS detects colloid-bound metal ions.

The fractograms (Figs. 3 and 4) clearly visualize the existence of an agglomeration process depending on metal ion concentration in the leachate. A clear increase of the average HA colloid size is observed by UV/Vis absorbance with increasing Fe or Al to HA ratio. The peak maximum of the HA size distribution under given conditions lies at $\leqslant 2\,nm$ related to the calibration with polystyrene particles. The average HA size increases considerably by increasing the Fe(III) to HA(carboxylate functional group) ratio. In the fractograms of the solution prepared in experiment.1 containing the highest metal ion concentration (dilution: 1:100), we could hardly find any peak for HA. Only at very large retention times (corresponding to a size of ~200 nm) a small peak could be observed at the same position as for Al and Fe. The major part of the Fe/Al/HA species, however, is located in the >450 nm fraction as has been mentioned already earlier (see Tables 3 and 4). In experiment 2, i.e. at higher pH, the observation is

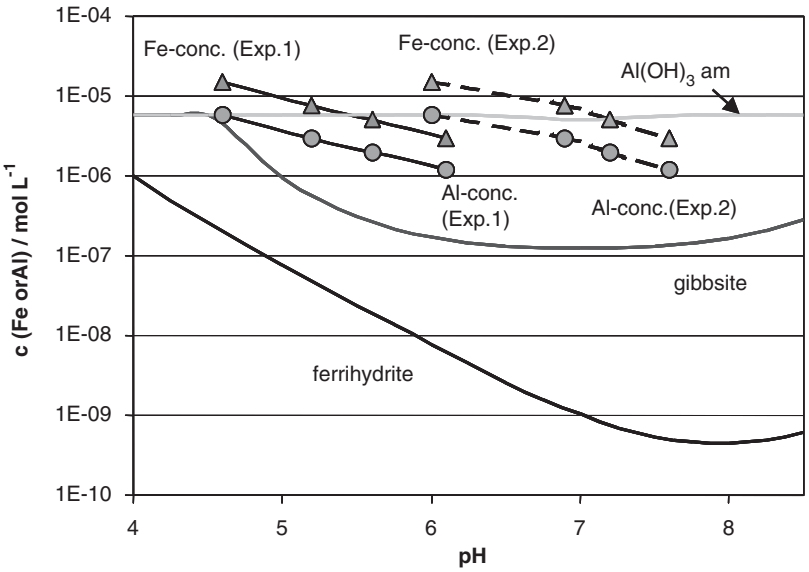

Fig. 1 – Solubility of Fe(III) and Al(III) in absence of humic acid as a function of pH in the diluted (1:100) leachate from coal mining tailings.

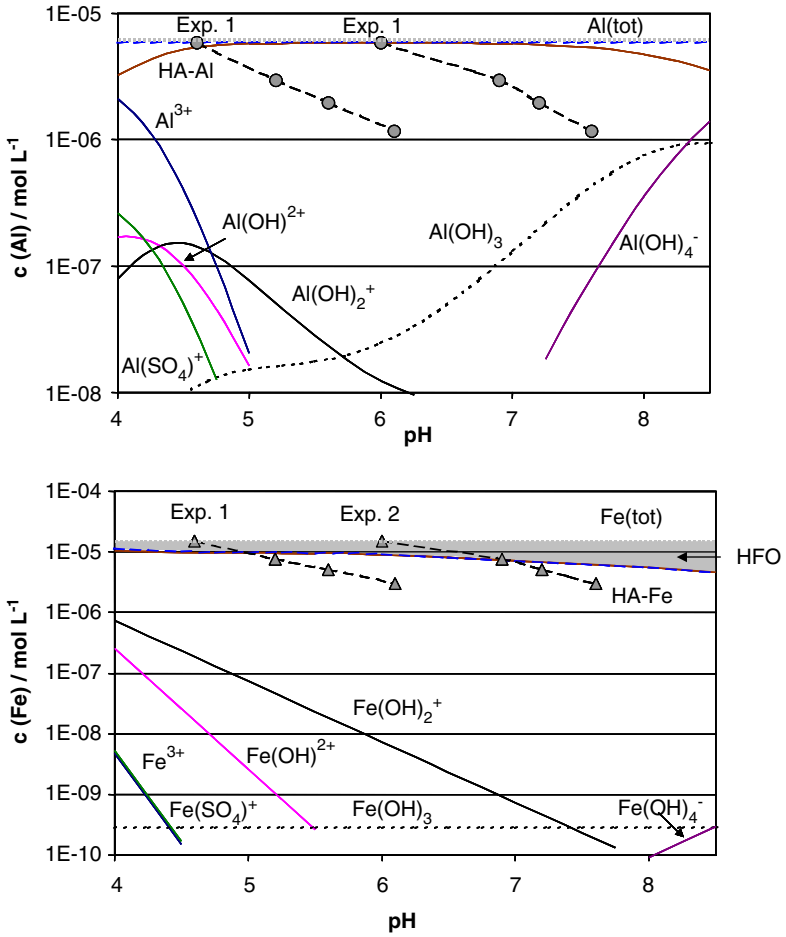

Fig. 2 – Speciation of Fe(III) and Al(III) in presence of humic acid as a function of pH in the diluted (1:100) leachate from coal mining tailings (HFO: hydrous ferric oxide).

somewhat different. The colloid fraction passing the 450 nm filter is not such strongly agglomerated as observed at the lower pH values of experiment 1. The average colloid size at a Fe(III) to HA (carboxylate functional group) ratio of ~1:3 is ~7 nm, where the size distribution ranges from 3 to 20 nm. It appears that there are still functional groups not coordinated

to metal ions which at the higher pH induce a sufficiently high negative surface charge, thus leading to a stronger stabilization of a relatively small colloid fraction in solution. One explanation for this observation could be the formation of hydroxy or carbonate humate ternary complexes at the higher pH with less coordination of HA carboxylate groups to the metal ion.

The combination of FFF with UV/Vis and ICP-MS detection allows not only to observe the evolution of the HA size but also of the HA-bound metal size distribution. Fractograms as given in Figs. 3,4,5 reveal a marked feature: at low metal loading, HA and the metal humate complexes exhibit different size distributions with significantly different peak maxima. Those differences are perceptible in both dilution experiments. It is also striking that the size of colloid borne divalent metal ions such as Cu(II) is always closer to that of HA than that of the trivalent cations (Fe(III) and Al(III)). Colloidal metal ion species are larger than the average HA entities, whereby the higher metal charge seems to increase the observed colloid size. Such behavior was already observed in earlier studies (Hassellöv et al., 1999; Geckeis et al., 2002, 2003; Bouby et al., 2002; Lyven et al., 2003). One possible explanation is the occurrence of metal induced agglomeration of HA macromolecules. Our studies show that this effect appears at even low metal loading. This finding points to the interaction of polyvalent metal ions with more than one HA entity thus acting as bridging unit. A second possibility is that complexed metal ions effectively screen the HA surface charge and thus favor agglomeration of those units. Such processes are in line with the observation that for lower charged metal ions (e.g. Cu(II)) the size increasing effect is smaller than for metals with higher charge (e.g. Fe(III)/Al(III)). This effect is illustrated exemplary in Fig. 5 for U, Ce, Th. measured by ICP-MS additionally after injection of the 1:500 diluted leachate solution (experiment 2) where those metal ions are present at trace concentrations $<1\,\mu g\,L^{-1}$ in the investigated HA solution. The shifts in the observed size distribution pattern are significant and reproducible. Under given conditions uranium exists in the hexavalent state as humate complex of the divalent UO_2^{2+} ion where cerium as a representative of the lanthanides is trivalent and thorium tetravalent. The observations that (1) the average size of the metal bearing colloids is larger than the average size of the HA entities and (2) the dependence of average metal-humate size on the metal ion charge both suggest the existence of metal induced agglomeration processes influenced by the individual metal ion charge.

With increasing metal loading, HA and metal–HA entities progressively grow in size and finally the fractograms for both species approach to almost coincidence. The difference between the peaks of HA (detected by UV–VIS) and the metal–HA fractograms (detected by ICP-MS) obviously can be

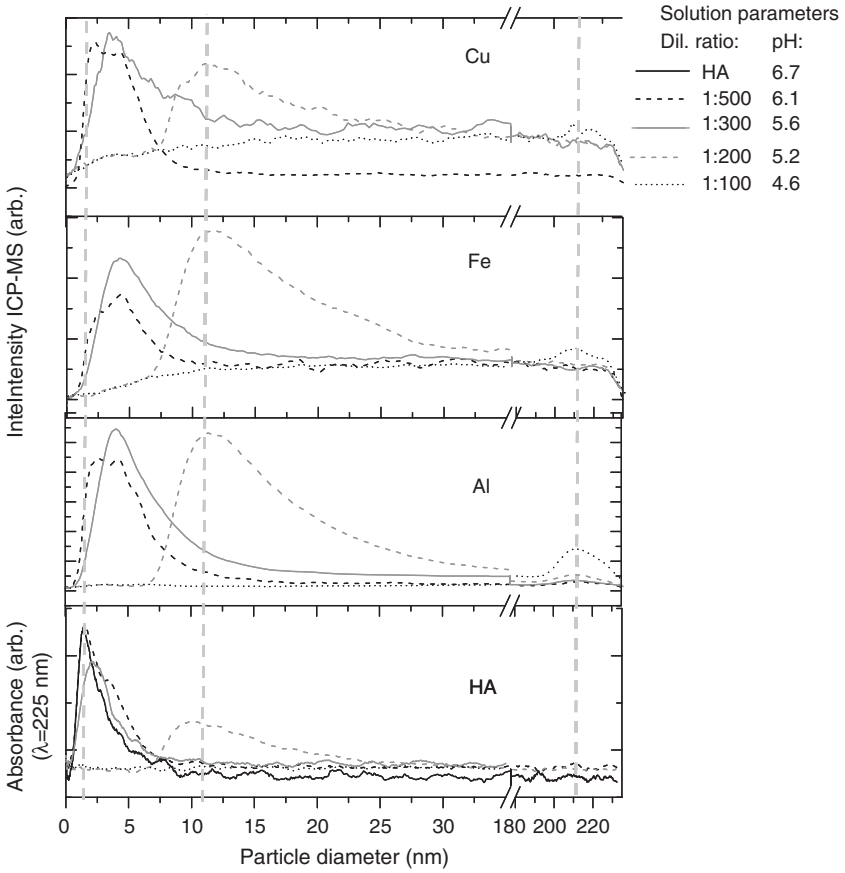

Fig. 3 – AsFlFFF-ICP-MS fractograms for solutions of experiment 1; dilution of the leachate with HA (10 mg L^{-1} in 0.1 mol L^{-1} $NaClO_4$; initial pH: 6.7). A fractogram of the HA solution are included for comparison.

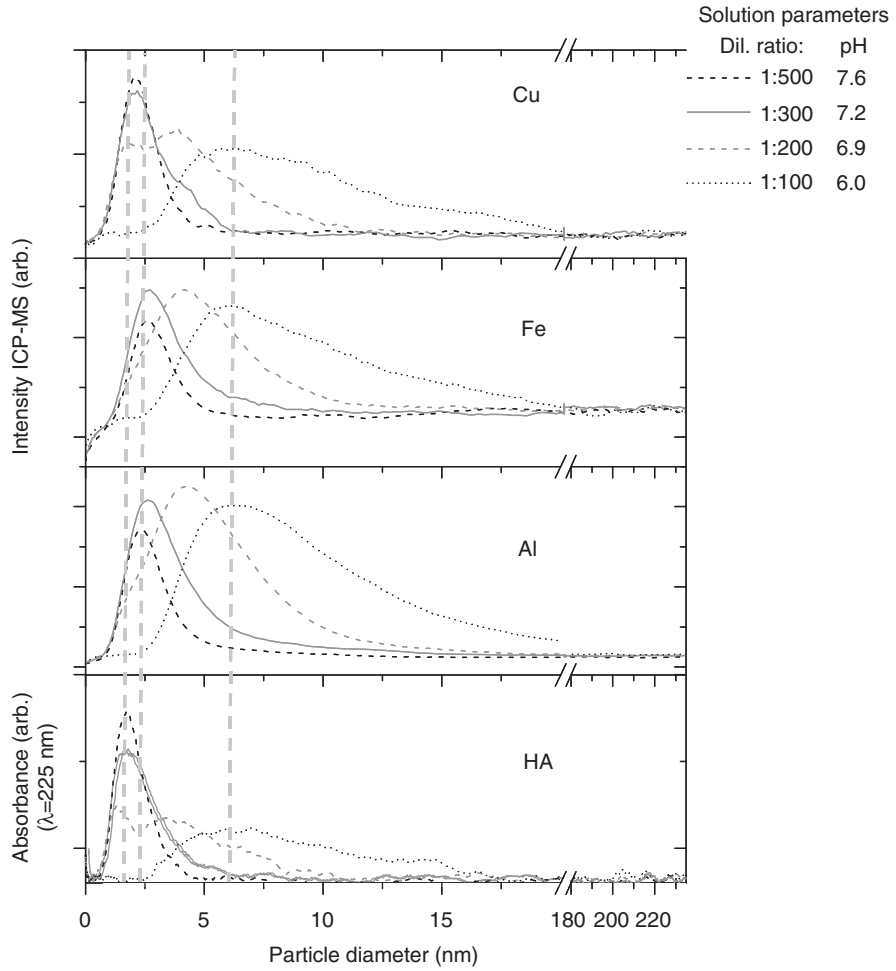

Fig. 4 – AsFlFFF-ICP-MS fractograms for solutions of experiment 2; dilution of the leachate with HA (10 mg L^{-1} in 0.1 mol L^{-1} $NaClO_4$; initial pH: 9).

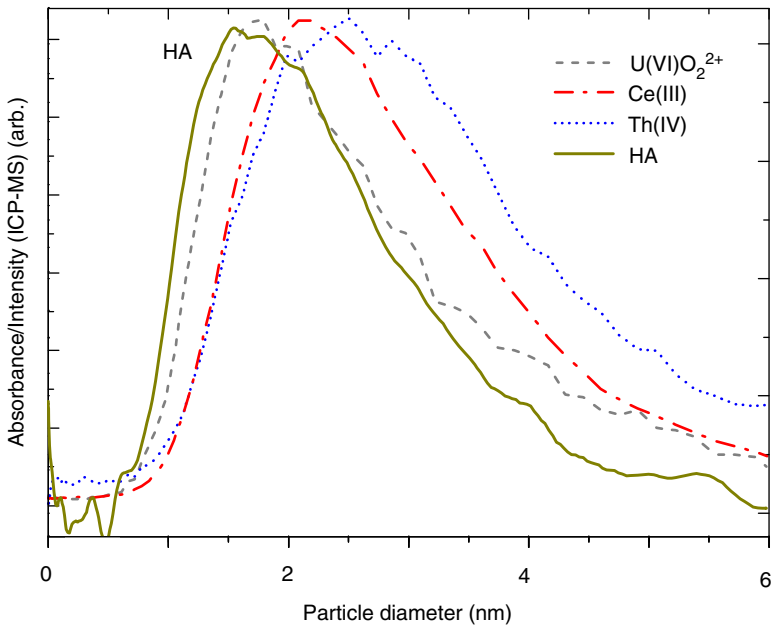

Fig. 5 – AsFlFFF-UV/Vis and ICP-MS fractograms for a diluted leachate (experiment 2; 1:300 dilution; pH 7.2).

taken as a measure for the degree of metal-loading: The larger the difference between the peak maxima, the lower the overall HA loading. In our experiments, the complete HA loading with Fe(III) seems to correspond closely to the complete occupation of three carboxylate groups with one trivalent Fe(III) ion at pH ~ 6 (experiment. 2) while at pH ~ 5 (experiment. 1) loading is already complete if only ~60% of the functional HA groups are occupied (again assuming one Fe ion interacting with three HA carboxylate groups). Under those conditions about half of Fe and Al already form agglomerates with a size >450 nm.

Size evolution of HA upon interaction with another trivalent metal ion (Eu(III)) has been also studied earlier at very low HA concentration (0.26 mg L^{-1}) by using the laser-induced breakdown detection (LIBD) at pH 6.0 (Bouby et al., 2002). A clear HA agglomeration could be established in this experiment only at metal loading ⩾60% (assumption: Eu(III) interaction with three HA carboxylate groups) quite consistent with our present results. Various other investigations by using e.g. using atomic force microscopy (AFM) (Plaschke et al., 2000) or in the frame of spectroscopic studies on actinide complexation with HA (e.g. Czerwinski et al., 1996) show qualitatively the same HA behavior. Precipitation of significant HA fractions has been already stated at M(III)/HA ratios as low as 0.05 – 0.1 if pH decreases below 4 at an ionic strength of $I = 0.1$ mol L^{-1} (M(III): trivalent metal ion, Eu(III) or Am(III)) (Czerwinski et al., 1996). The Fe(III) induced coagulation of natural organic matter was investigated in a recent study by using transmission electron spectroscopy (TEM) and electron energy loss spectroscopy (EELS) (Jung et al., 2005). Fe ions were mainly found to be associated by carboxylate groups in coagulates and, therefore, a charge neutralization/complexation mechanism was suggested to be responsible for the aggregate formation.

4. Conclusions

The experiments indicate that metal ions dissolved in AMD may experience either retention or mobilization when released from the source. When diluted in near neutral natural water, metal ions can be kept to a certain degree in solution by humic substances through complexation. Agglomeration to larger HA aggregates and thus precipitation, sedimentation or attachment to surfaces can predominate under conditions where polyvalent metal ions as Fe(III) and Al(III) saturate the complexing functional HA groups. At very high metal ion concentrations, co-precipitation of Fe-oxyhydroxide/humic acid may also become relevant. Such behavior is in agreement with the outcome of earlier investigations: Transformation of marine dissolved organic matter into agglomerated polymer gels is known to have a shorter oceanic residence time due to enhanced sedimentation (Chin et al., 1998). Flocculation through interaction with polyvalent metal ions as Ca(II), Al(III) (Römkens and Dolfing, 1998) and Fe(III) (Jung et al., 2005) is reported to control the DOC concentration in soil pore water and during drinking water treatment processes. The complexation reaction is responsible for charge neutralization of HA entities thus reducing HA colloid stability (see also Jung et al., 2005). Our studies show that even at lower loading of HA with polyvalent metal ions a size increase is found for the metal–HA complexes as compared with the average HA colloid size. We interpret this result as an indication for polyvalent metal induced humic agglomeration taking place at even low metal ion concentration. Those species nevertheless remain suspended in solution, thus being mobile, and may act as carriers for metal ions.

Acknowledgements

The authors acknowledge the German Academic Exchange Service-Royal Golden Jubilee (DAAD-RGJ) Ph.D. Scholarship to S. S.. The Postgraduate Education and Research in Chemistry (PERCH) scholarship and the Thailand Research Fund (TRF) are grateful for partial financial support. S. S. would like to thank all the co-workers at Forschungszentrum Karlsruhe, Institut für Nukleare Entsorgung, for their help during performing the research in Germany notably assistance with analytical methods. The sample from the mine tailing was kindly provided by Dr. Ponlayuth Sooksamiti, the Office of Mineral Resources (Region III), Chiang Mai, Thailand. We thank Dr. Ron Beckett, Water Studies Centre, Monash University, Melbourne, Australia, for valuable discussions on the FFF results.

REFERENCES

American Water Works Association and Water Pollution Control Federation. 1989. Standard Methods for the Examination of Water and Waste Water. seventh Ed., American Public Health Association, American Water Works Association and Water Pollution Control Federation, Washington DC, pp. 3–102.

Arbhabhirama, A., Phantumvanit, D., Elkington, J., Ingkasuwan, P., 1987. Thailand natural resources profile: is the resource base for Thailand's development sustainable? Thailand Development Research Institute, Bangkok.

Badulis, G.C., 1998. Risk assessment from potential weathering characteristics of Mae Moh lignite mine and power plant wastes Mae Moh distric Lampang province. Graduate School, Chiang Mai University, Chiang Mai.

Benincasa, M.A., Caroni, G., Imperia, N., 2002. Effect of ionic strength and electrolyte composition on the aggregation of fractionated humic substances studied by flow field-flow fractionation. J. Sep. Sci. 25, 405–415.

Bouby, M., Ngo Manh, T., Geckeis, H., Scherbaum, F., Kim, J.I., 2002. Characterization of aquatic colloids by a combination of LIBD and ICP-MS following the size fractionation. Radiochim. Acta 90, 727–732.

Bryan, N.D., Jones, M.N., Birkett, J., Livens, F.R., 2001. Aggregation of humic substances by metal ions measured by ultracentrifugation. Anal. Chim. Acta 437, 291–308.

Bunce, N.J., Chartrand, M., Keech, P., 2001. Electrochemical treatment of acidic aqueous ferrous sulfate and copper sulfate as models for acid mine drainage. Water Res 35, 4410–4416.

Chin, W.-C., Oranella, M.V., Verdugo, P., 1998. Spontaneous assembly of marine dissolved organic matter into polymer gels. Nature 39, 568–572.

Czerwinski, K.R., Kim, J.I., Rhee, D.S., Buckau, G., 1996. Complexation of trivalent actinide Ions (Am^{3+}, Cm^{3+}) with humic acid: the effect of ionic strength. Radiochim. Acta 72, 179–187.

Dang, Z., Liu, Z., Haigh, M.J., 2002. Mobility of heavy metals associated with the natural weathering of coal mine spoils. Environ. Pollut. 118 (3), 419–426.
Denecke, M.A., Bublitz, D., Kim, J.I., Moll, H., Farkes, I., 1999. EXAFS investigation of the interaction of hafnium and thorium with humic acid and Bio-Rex70. J. Synchrotron Radiat. 6, 394–396.
Dinelli, E., Lucchini, F., Fabbri, M., Cortecci, G., 2001. Metal distribution and environmental problems related to sulfide oxidation in the Libiola copper mine area (Ligurian Apennines, Italy). J. Geochem. Explor. 74, 141–152.
Featherstone, A.M., O'Grady, B.V., 1997. Removal of dissolved copper and iron at the freshwater-saltwater interface of an acid mine stream. Mar. Pollut. 34, 332–337.
Frimmel, F.H., 1998. Characterization of natural organic matter as major constituents in aquatic systems. J. Cont. Hydrol. 35, 201–216.
Geckeis, H., Rabung, Th., Ngo Manh, T., Kim, J.I., Beck, H.P., 2002. Humic colloid-borne natural polyvalent metal ions: dissociation experiment. Environ. Sci. Technol. 36, 2946–2952.
Geckeis, H., Ngo Manh, Th., Bouby, M., Kim, J.I., 2003. Aquatic colloids relevant to radionuclide migration: characterization by size fractionation and ICP-mass spectrometric detection. Colloid Surface 217, 101–108.
Gundersen, P., Steinnes, E., 2003. Inuence of pH and TOC concentration on Cu,Zn,Cd, and Al speciation in rivers. Water Res. 37, 307–318.
Guo, L., Wen, L.-S., Tang, D., Santshi, P.H., 2000. Re-examination of cross-flow ultrafiltration for sampling aquatic colloids: evidence from molecular probes. Mar. Chem. 69, 75–90.
Hassellöv, M., Lyven, B., Haraldsson, C., Sirinawin, W., 1999. Determination of continuous size and trace element distribution of colloidal material in natural water by on-line coupling of flow field-flow fractionation with ICPMS. Anal. Chem. 71, 3497–3502.
Hochella, M.F., Moore, J.N., Golla, U., Putnis, A., 1999. A TEM study of samples from acid mine drainage systems: metal-mineral association with implications for transport. Geochim. Cosmochim. Acta 63, 3395–3406.
Jung, A.-V., Chanudet, V., Ghanbajo, J., Lartiges, B.S., Bersillon, J.-L., 2005. Coagulation of humic substances and dissolved organic matter with ferric salt: an electron energy loss spectroscopy investigation. Water Res. 39, 3849–3862.
Keizer, M.G., van Riemsdijk, W.H., 1994. ECOSAT (V. 4.7): A Computer Program for the Calculation of Speciation and Transport in Soil-Water Systems. Department of Soil Science and Plant Nutrition, Wageningen Agricultural University, Wageningen, The Netherlands.
Kimball, B.A., Callender, E., Axtmann, E.V., 1995. Effects of colloids on metal transport in a river receiving acid mine drainage, upper Arkansas River, Colorado, USA. Appl. Geochem. 10, 285–306.
Kinniburgh, D.G., van Riemsdijk, W.H., Koopal, L.K., Borkovec, M., Benedetti, M.F., Avena, M.J., 1999. Ion binding to natural organic matter: competition, heterogeneity, stoichiometry and thermodynamic consistency. Colloid. Surface. A, 151, 147–166.
Kretzschmar, R., Holthoff, H., Sticher, H., 1998. Influence of pH and humic acid on coagulation kinetics of kaolinite: a dynamic light scattering study. J. Coll. Interface Sci. 202, 95–103.
Kucukonder, A., Cam, H., Kucukonder, E., Sogut, O., 2003. Qualititative and quantitative analysis of lignite coal and its ash samples taken from Soma-Darkale region. J. Quant. Spectrosc Radiat. 77, 329–333.
Lee, N.C.Y., Ryan, D.K., 2004. Study of fulvic-aluminum(III) ion complexes by ^{27}Al solution NMR. In: Ghabbour, E., Davies, G. (Eds.), Humic Substances — Nature's most Versatile Materials. Taylor and Francis, Inc., New York, pp. 219–228.
Lee, G., Bigham, J.M., Faure, G., 2002. Removal of trace metals by coprecipitation with Fe, Al, and Mn from natural waters contaminated with acid mine drainage in the Ducktaown Mining District, Tennessee. Appl. Geochem. 17 (5), 569–581.
Lindsay, W.L., 1979. Chemical Equilibria in Soils. Wiley, New York, pp. 449.
Lyven, B., Hassellöv, M., Turner, D.R., Haraldsson, C., Andersson, K., 2003. Competition between iron- and carbon-based colloidal carriers for trace metals in a freshwater assessed using flow field-flow fractionation coupled to ICPMS. Geochim. Cosmochim. Acta 67, 3791–3802.
Matlock, M.M., Howerton, B.S., Atwood, D.A., 2002. Chemical precipitation of heavy metals from acid mine drainage. Water Res 36 (19), 4757–4764.
Milne, C.J., Kinniburgh, D.G., van Riemsdijk, W.H., Tipping, E., 2003. Generic NICA-Donnan model parameters for metal-ion binding by humic substances. Environ. Sci. Technol. 37, 958–971.
Monsallier, J.M., Artinger, R., Denecke, M.A., Scherbaum, F.J., Buckau, G., Kim, J.I., 2003. Spectroscopic study (TRLFS and EXAFS) of the kinetics of An(III)/Ln(III) humate interaction. Radiochim. Acta 91, 567–574.
Munka, L.A., Faure, G., Pridea, D.E., Bigham, J.M., 2002. Sorption of trace metals to an aluminum precipitate in a stream receiving acid rock-drainage; Snake River, Summit County, Colorado. Appl. Geochem. 17, 421–430.
Ngo Manh, T., Geckeis, H., Kim, J.I., Beck, H.P., 2001. Application of the flow field flow fractionation (FFFF) to the characterization of aquatic humic colloids: evaluation and optimization of the method. Colloid. Surface. 181, 289–301.
Panak, P., Klenze, R., Kim, J.I., 1996. A study of ternary complexes of Cm(III) with humic acid and hydroxide or carbonate in neutral ph range by time-resolved laser fluorescence spectroscopy. Radiochim. Acta 74, 141–146.
Plaschke, M., Römer, J., Klenze, R., Kim, J.I., 2000. Influence of europium(III) on the adsorption of humic acid onto mica studied by AFM. Surf. Interface Anal. 30, 297–300.
Rabung, Th., Geckeis, H., Kim, J.I., Beck, H.P., 1998. The influence of anionic ligands on the sorption behaviour of Eu(III) on natural hematite. Radiochim. Acta 82, 243–248.
Römkens, P.F.A.M., Dolfing, J., 1998. Effect of Ca on the solubility and molecular size distribution of DOC in soil solution samples. Environ. Sci. Technol. 32, 363–369.
Sahuquillo, A., Rigol, A., Rauret, G., 2002. Comparison of leaching tests for the study of trace metals remobilization in soils and sediments. J. Environ. Monit. 4 (6), 1003–1009.
Schemel, L.E., Kimball, B.A., Bencala, K.E., 2000. Colloid formation and metal transport through two mixing zones affected by acid mine drainage near Silverton. Appl. Geochem. 15, 1003–1018.
Schimpf, M.E., Petteys, M.P., 1997. Characterization of humic materials by field-flow fractionation. Colloid Surface 120, 87–100.
Sigg, L., Stumm, W., 1989. Aquatische Chemie. VDF Zürich, pp. 76.
Stevenson, F.J., 1994. Humus Chemistry — Genesis, Composition, Reactions. Wiley, New York.
Sun, B., Zhao, F.J., Lombi, E., McGrath, S.P., 2001. Leaching of heavy metals from contaminated soils using EDTA. Environ. Pollut. 113, 111–120.
Vigneault, B., Campbell, P.G.C., Tessier, A., De Vitre, R., 2001. Geochemical changes in sulfidic mine tailings under a shallow water cover. Water Res 35, 1066–1076.
Wall, N.A., Choppin, G.R., 2003. Humic acids coagulation: influence of divalent cations. Appl. Geochem. 18, 1573–1582.
Yukselen, M.A., Alpaslan, B., 2001. Leaching of metals from soil contaminated by mining activities. J. Hazard. Mater. 87, 289–300.
Zänker, H., Moll, H., Richter, W., Brendler, V., Hennig, C., Reich, T., Kluge, A., Hüttig, G., 2002. The colloid chemistry of acid rock drainage solution from an abandoned Zn–Pb–Ag mine. Appl. Geochem. 17, 633–648.

Available online at www.sciencedirect.com
SCIENCE DIRECT
Talanta 68 (2006) 1726–1731
Talanta
www.elsevier.com/locate/talanta

Electroanalysis of sulfonamides by flow injection system/high-performance liquid chromatography coupled with amperometric detection using boron-doped diamond electrode☆

Anchana Preechaworapun[a], Suchada Chuanuwatanakul[a], Yasuaki Einaga[b], Kate Grudpan[c], Shoji Motomizu[d], Orawon Chailapakul[a,*]

[a] *Materials Chemistry and Catalysis Research Unit, Department of Chemistry, Faculty of Science, Chulalongkorn University, Patumwan, Bangkok 10330, Thailand*
[b] *Department of Chemistry, Faculty of Science and Technology, Keio University, 3-1014-1 Hiyoshi, Yokohama, Kanagawa 223-8522, Japan*
[c] *Department of Chemistry, Faculty of Science, Chiang Mai University, Chiang Mai 50200, Thailand*
[d] *Department of Chemistry, Okayama University, Okayama 700-8530, Japan*

Received 23 May 2005; received in revised form 15 August 2005; accepted 15 August 2005
Available online 23 September 2005

Abstract

Sulfonamides (SAs) were electrochemically investigated using cyclic voltammetry at a boron-doped diamond (BDD) electrode. Comparison experiments were carried out using a glassy carbon electrode. The BDD electrode provided well-resolved oxidation, irreversible cyclic voltammograms and higher current signals when compared to the glassy carbon electrode. Results obtained from using the BDD electrode in a flow injection system coupled with amperometric detection were illustrated. The optimum potential from a hydrodynamic voltammogram was found to be 1100 mV versus Ag/AgCl, which was chosen for the HPLC-amperometric system. Excellent results of linear range and detection limit were obtained. This method was also used for determination of sulfonamides in egg samples. The standard solutions of 5, 10, and 15 ppm were spiked in a real sample, and percentage of recoveries was found to be between 90.0 and 107.7.

Keywords: Sulfonamides; Boron-doped diamond thin film electrode; Cyclic voltammetry; Flow injection system; HPLC; Amperometric detection

1. Introduction

Sulfonamides (SAs) have been used as antibacterial agents for over 60 years. They are often used for prevention or treatment of poultry leucocytozoonosis and coccidiosis, and are generally co-administered in feed. The European Union (EU) has set a maximum residue limit (MRL, 100 ng g^{-1}) for SAs in foods of animal origin such as meat, milk and eggs [1]. Therefore, the determination of such residues in meat and other animal by-products (milk and egg) used for human consumption has become an important task.

Owing to concern over sulfonamide residues in food products of animal origin, a number of techniques have been proposed for their detection, including, immunoassay [2,3], thin layer chromatography (TLC), gas chromatography (GC) and gas chromatography–mass spectrometry (GC-MS) [4], capillary electrophoresis [5], and high performance liquid chromatography (HPLC) [6–17] and high performance liquid chromatography–mass spectrometry (HPLC-MS) [18–20]. HPLC with UV and a fluorometry detector were common methods for determining these drugs [6–9]. The alternative for determination of these SAs was HPLC with an electrochemical detector (HPLC-EC) using the amperometric technique [14]. HPLC-EC has been proved to be quite sensitive and inexpensive.

The diamond is one of nature's best insulators, but when doped with boron, the material can possess either semiconducting or semimetallic electronic properties depending on the doping level [21]. Therefore, the boron-doped diamond thin film electrode has shown unique characteristics that make it partic-

☆ Presented at the 13th International Conference on Flow Injection Analysis, April 24–29, 2005, Las Vegas, Nevada, and erroneously omitted from Talanta 68(2) 2005.

* Corresponding author. Tel.: +66 2 2187615; fax: +66 2 541309.
E-mail address: corawon@chula.ac.th (O. Chailapakul).

0039-9140/$ – see front matter © 2005 Elsevier B.V. All rights reserved.
doi:10.1016/j.talanta.2005.08.040

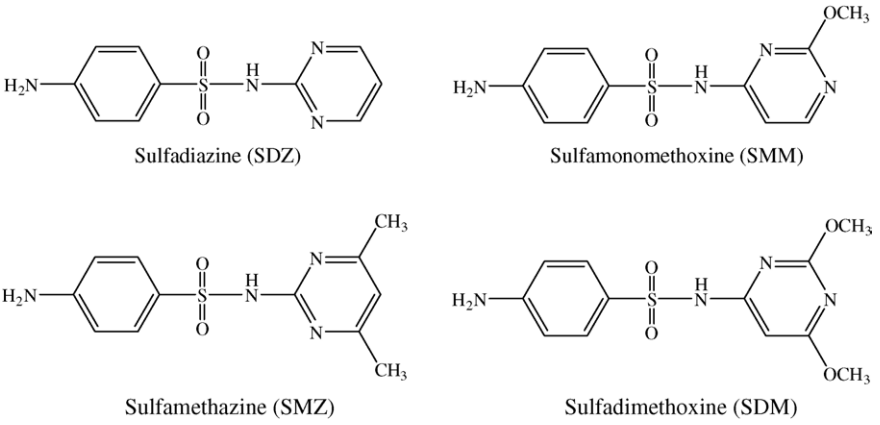

Fig. 1. Chemical structures of four SAs analyzed in this study.

ularly attractive for electrochemical applications, such as: (i) very low and stable voltammetric background current, which results in the improvement of signal-to-background [22,23]; (ii) long-term response stability as well as excellent activity towards any redox species without any pre-treatment [24–27]; (iii) low sensitivity to dissolved oxygen [28]; (iv) a wide working potential window in aqueous solution [29,30]; (v) slight adsorption of polar organic molecules [25]; and (vi) high resistance to deactivation. These material properties are the impetus for our interest in studying and developing diamond electrodes for electrochemical applications. With respect to the outstanding properties of BDD film, quite a number of applications, based on the use of this new material for electrochemical quantitation, have been reported [14,27,31–47]. This synthetic type of diamond film has already been applied as an amperometric detector in flow-injection (FI) analysis [27,31–37,40,42–46] and liquid chromatography [14,37–41,47]. Furthermore, the BDD electrode has been used for the treatment of wastewater [48,49].

This paper reported the use of the BDD electrode to detect four SAs: sulfadiazine, SDZ; sulfamethazine, SMZ; sulfamonomethoxine, SMM; and sulfadimethoxine, SDM. The structures of these four compounds are shown in Fig. 1. Cyclic voltammetry, flow injection analysis and HPLC with an amperometric detector were used in this study. The applicability of the method to analyze hen egg laying samples was demonstrated.

2. Experiment

2.1. Apparatus

The FIA and HPLC system used in this study consisted of a Water Model 510 solvent delivery system (Water Associates Inc, Milford, MA, USA), an injector system (Rheodyne no. 7125) with a 20-μL loop, Inertsil C4 column (GL Science, 150 mm × 4.6 mm i.d.; particle size, 5 μm), a thin layer flow-cell (GL Science Inc.), and an amperometric detector (Autolab Potentiostat 30; Metrohm, Switzerland). The following apparatus used in the sample preparation comprised a mini centrifuge (Cole Parmer, USA); an ultrasonic-homogenizer (Ney Dental, USA); Mixer (National, Matsushita Electric industrial Co. Ltd., Japan); and a micro-centrifugal ultrafilter unit (Ultrafree-MC/PL, regenerated cellulose ultra-filtration membrane, nominal molecular mass limit = 5000, capacity ≤0.5 mL, Millipore, Bedford, MA, USA).

2.2. Reagents

HPLC grade acetonitrile and ortho-phosphoric acid were purchased from Merck (Darmstad, Germany). Deionized water was from a Milli-Q-gradient system (Millipore, $R \geq 18.2\,M\Omega$ cm). Sodium dihydrogen orthophosphate 1-hydrate and disodium hydrogen phosphate were purchased from BDH (VWR international Ltd., England). SMM, SDM, SMZ and SDZ standards were obtained from Sigma (St. Louis, MO, USA). Stock standard solution (500 ppm) of each SA was prepared in acetonitrile:deionized water (50:50, v/v). The stock standards were stored at 4 °C. Working mixed standard solutions of these four SAs were prepared by diluting the stock solutions with 0.1 M phosphate solution.

2.3. Electrode

The BDD electrode grown on conductive Si (1 0 0) substrate using the microwave plasma-assisted chemical vapor deposition (MPCVD) system was obtained from Associate Professor Yasuaki Einaga's laboratory [23]. A mixture of acetone and methanol at a ratio of 9:1 (v/v) was used as the carbon source. B_2O_3, used as the boron source, was dissolved in the acetone–methanol solution at a B/C atomic ratio of 1:100. The BDD electrode was rinsed with isopropanol and then deionized water prior to use.

The glassy carbon (GC) electrode was purchased from Bioanalytical System Inc. (area 0.07 cm^2). It was pre-treated by sequential polishing with 1 and 0.3 μm of alumina/water slurries on felt pads, followed by rinsing with deionized water prior to use.

2.4. Electrochemical measurements

2.4.1. Cyclic voltammetry

Electrochemical measurements were carried out in a single compartment three-electrode glass cell, with a volume of

50 mL. The BDD electrode was pressed against a smooth ground joint at the bottom of the cell, and isolated by an O-ring (area 0.07 cm^2). Ohmic contact was made by placing the backside of the Si substrate onto a brass plate. The GC electrode was also used as a working electrode in a comparison study with the BDD electrode. A platinum wire and Ag/AgCl with a salt bridge were used as the counter and reference electrodes, respectively. Cyclic voltammetry was performed with an Autolab Potentiostat 30. The electrochemical equipment was housed in a faradaic cage to reduce electronic noise.

2.4.2. Flow injection and HPLC analysis with amperometric detection

The measurements (FIA) using the BDD electrode as an amperometric sensor were carried out in a 0.1 M phosphate solution (pH 3.0) at an applied potential of 1100 mV versus Ag/AgCl. The FIA and HPLC system used in this study consisted of a Water Model 510 solvent delivery system, with a flow rate of 1.0 mL min^{-1}; the length of the tubing connecting the injector and the detector in the flow injection system was 20 cm, an injector system, with a 20-μL loop; a thin layer flow-cell; and an amperometric detector. The potential of the electrochemical detector was set using a computer-controlled potentiostat. The thin layer flow-cell consisted of the Ag/AgCl reference electrode and a stainless steel counter electrode. A 1-mm thick silicon rubber gasket was used as a spacer in the cell. The geometric area of the electrode in the cell was estimated at 0.6 cm^2. During the measurements, the flow cell was maintained at room temperature (25 ± 1 °C). An Intertsil C4 column was used for the separation of the SAs. The 0.1 M sodium dihydrogen phosphate (pH 3.0), acetonitrile (80:20; v/v), was used as the mobile phase for FIA experiments, and eluent in the liquid chromatographic experiments.

2.5. The preparation of egg samples

This method used less organic solvent [16]. An accurate 0.2 g of the sample was taken into a 1.5 mL micro-centrifuge tube and homogenized in 0.4 mL of 10% (v/v) perchloric acid solution (in water) with an ultrasonic-homogenizer for 1 min. Next, this micro-centrifuge tube was centrifuged at 6000 rpm for 3 min. A 0.3 mL portion of supernatant liquid was put into an Ultrafree-MC/PL and centrifuged at 6000 rpm for 5 min. The 20 μL of solution in ultra-filtrate was injected into the HPLC system.

2.6. Recovery test

The recoveries of SAs were determined from three egg blank samples, accurately weighed at 1.0 g, and each spiked with mix standards for a concentration of 5, 10, and 15 ppm, respectively. Then an accurate 0.2 g homogenate was transferred into a 1.5 mL micro-centrifuge tube and homogenized in 0.4 mL of 10% (v/v) perchloric acid solution (in water) with an ultrasonic-homogenizer for 1 min. Preparation steps for the egg samples followed.

3. Results and discussion

3.1. pH dependence study

In initial experiments, the electrochemical behavior of four SAs was investigated at the BDD electrode in 0.1 M phosphate solution from pH 2.0 to 7.0. Cyclic voltammograms of SAs at various pH phosphate solutions were obtained. It was found that changing pH phosphate solution effected the oxidation peak current. The best-resolved and highest anodic signals of SAs were obtained at pH 3. Therefore, pH 3 was chosen as the optimal pH.

3.2. Cyclic voltammetry

Fig. 2A and B show the cyclic voltammograms for 50 μM SDM together with the corresponding background voltammogram in 0.1 M phosphate solution (pH 3.0) at the BDD and GC electrodes. The background current for the GC electrode was ∼10 times higher than that obtained from the BDD electrode. The BDD exhibited a well-defined irreversible oxidation peak at ∼1100 mV versus Ag/AgCl, whereas the GC electrode provided an ill-defined irreversible oxidation peak. No cathodic peak was

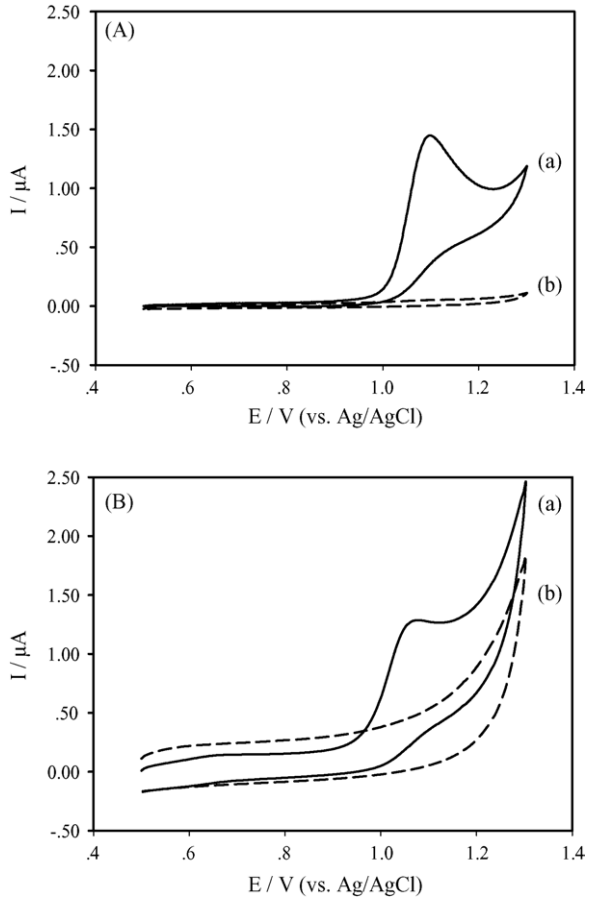

Fig. 2. Cyclic voltammograms for (A) BDD and (B) GC electrodes vs. Ag/AgCl in 50 μM SDM in 0.1 M phosphate solution pH 3.0 (a) and 0.1 M phosphate solution pH 3.0 (b). The sweep rate was 50 mV s^{-1}. The area of electrodes was 0.07 cm^2.

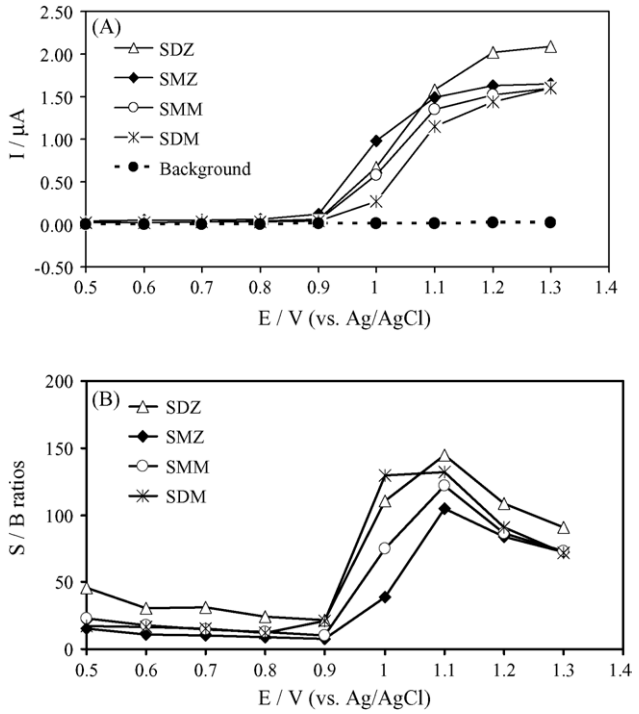

Fig. 3. Hydrodynamic voltammetric results for 10 ppm of each SA. The average peak current obtained from injections ($n = 4$) of (A) background (0.1 M sodium dihydrogen phosphate (pH 3.0):ACN (80:20; v/v), SDZ, SMZ, SMM and SDM in 0.1 M sodium dihydrogen phosphate (pH 3.0):ACN (80:20; v/v). Phosphate solution was used as a carrier stream. The flow rate was 1 mL min^{-1}. (B) Hydrodynamic voltammogram of signal-to-background ratios.

observed at either electrode on the reverse scan within the investigated potential range (+500 to +1300 mV).

3.3. Flow injection analysis with amperometric detection

To obtain the optimal potential for amperometric detection in flow injection analysis, the hydrodynamic behavior of SAs was studied. Fig. 3 shows a hydrodynamic voltammetric *I–E* curve obtained at the BDD electrode for 20 μL injections of 10 ppm to each SA in 0.1 M sodium dihydrogen phosphate (pH 3.0):ACN (80:20; v/v) as the carrier solution. Each datum represents the average of four injections. The absolute magnitude of the background current at each potential is also shown for comparison. The S/B ratios were calculated from Fig. 3A at each potential to obtain the maximum potential point. The hydrodynamic voltammetric S/B ratios versus potential curve are shown in Fig. 3B, with the maximum S/B ratio at 1100 V. Hence, this potential was set for quantitative amperometric potential detection in HPLC analysis experiments.

3.4. HPLC analysis with amperometric detection

In previous papers [7–10] on reversed-phase HPLC analysis of SAs, the C18 or C8, non-polar sorbent columns were used the most frequently. The C18 and C8 sorbents required a large volume of strong elution solvents as the mobile phase. The separation in this experiment was performed using a C4 column, which remarkably reduced the volume of elution solvents required and provided a high signal and clear separation, as described previously [15–17].

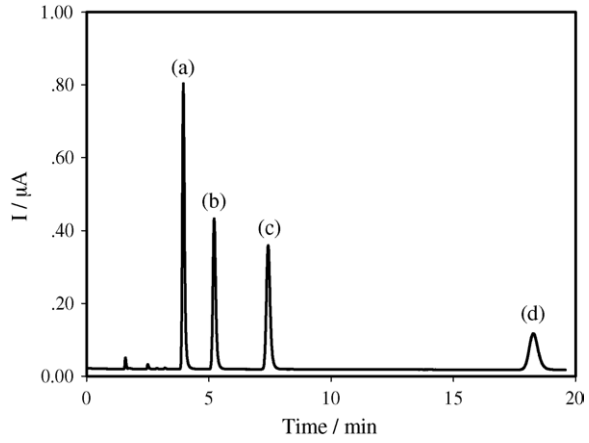

Fig. 4. HPLC-EC chromatogram of a standard mixture containing 10 ppm concentration of (a) SDZ; (b) SMZ; (c) SMM; and (d) SDM at the BDD electrode. The mobile phase was 0.1 M sodium dihydrogen phosphate (pH 3.0):ACN (80:20; v/v). The injection volume was 20 μL, and the flow rate 1 mL min^{-1}.

The results were analyzed by a chromatographic technique (HPLC), coupled with amperometric detection on the BDD electrode. The pH of the mobile phase was selected at 3.0 in order to reduce the above information. The chromatogram of standard solution of the four SAs in 0.1 M sodium dihydrogen phosphate (pH 3.0):ACN (80:20; v/v) solution, as the mobile phase, is presented in Fig. 4. The retention times of the four SAs; SDZ, SMZ, SMM, and SDM, at a concentration of 10 μg mL^{-1}, were 4.0, 5.2, 7.5, and 18.0 min, respectively. Twenty minutes were required to complete separation of the four SAs.

3.5. Method characteristics

The calibration characteristics of the SAs at the BDD electrode are shown in Table 1. The detection limit (DL) and quantitative limit (QL) for the four SAs under these experimental conditions were obtained from $DL = 3S_B/b$ and $QL = 10S_B/b$, when S_B was the standard deviation of the mean value for 10 signals of the blank and b was the slope of the straight line in the analytical curve [50].

From the standard deviation (S_B), the straight line slope of the analytical curve (b), the calculated value of DL and the QL is shown in Table 1. The current responses of SAs var-

Table 1
Linear range (LR), detection limit (DL), slope (b), and quantitative limit (QL) of SDZ, SMZ, SMM, and SDM

SAs	LR (ppm)	Equation $y = bx + a$	R^2	DL (ppm)	QL (ppm)
SDZ	0.050–100	$y = 0.2922x + 0.6232$	0.9905	0.011	0.037
SMZ	0.050–100	$y = 0.2915x + 0.1610$	0.9974	0.012	0.040
SMM	0.050–100	$y = 0.2939x + 0.3084$	0.9959	0.011	0.037
SDM	0.100–300	$y = 0.2898x + 0.6433$	0.9910	0.032	0.107

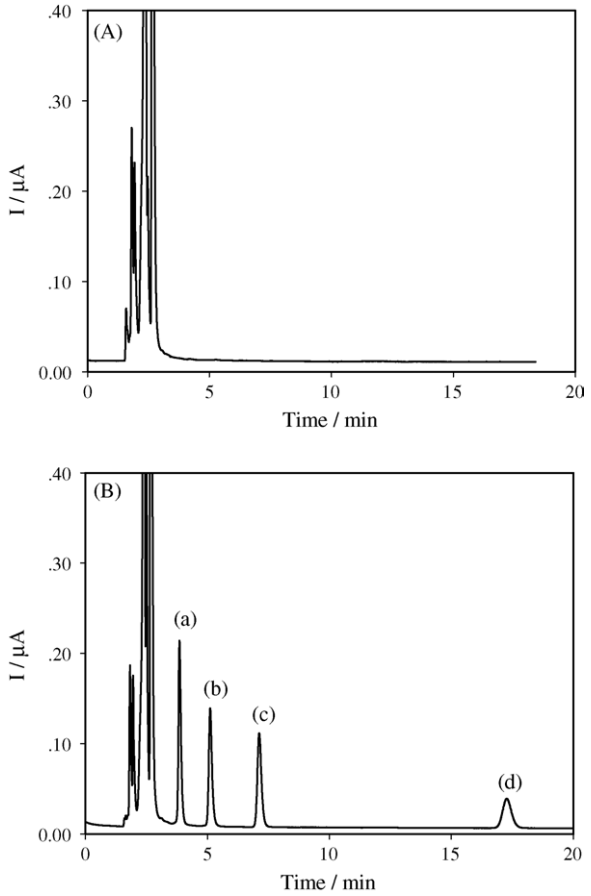

Fig. 5. HPLC-EC chromatograms obtained from egg samples: (A) blank egg sample and (B) egg sample spiked to a 10 ppm concentration of (a) SDZ; (b) SMZ; (c) SMM; and (d) SDM at the BDD electrode. The mobile phase was 0.1 M sodium dihydrogen phosphate (pH 3.0):ACN (80:20; v/v). The injection volume was 20 μL, and the flow rate 1 mL min^{-1}.

ied linearly with the standard concentrations, covering a range of 0.05–100 ppm for SDZ, SMZ and SMM, and 0.1–300 ppm for SDM. The results indicated that this proposed method can be applied for the determination of four SAs in egg samples.

3.6. Application

Egg samples were analysis by the HPLC/EC system. Fig. 5 shows clearly the chromatograms, with clear/sharp peaks and short retention times by using a C4 column and an isocratic mobile phase of 0.1 M sodium dihydrogen phosphate (pH 3.0):ACN (80:20; v/v). The experiment was repeated three times in order to assess the reproducibility in real sample. The recoveries of four SAs were determined by injecting a blank egg sample, spiked together with the standard samples. The recoveries and %R.S.D. of SDZ, SMZ, SMM, and SDM at three different spiked levels are summarized in Table 2. This procedure allowed rapid and efficient purification of SAs and resulted in high recovery (Mean of percentage of recoveries was found to be between 90.0 and 107.7) and reproducibility (%R.S.D. < 4.9% and S.D. < ± 4.7).

Table 2
Analysis four SAs in egg samples ($n = 3$)

SAs	Mean of percentage recovery ($x \pm$ S.D.)			%R.S.D.		
	5 ppm	10 ppm	15 ppm	5 ppm	10 ppm	15 ppm
SDZ	103.0 ± 4.7	96.9 ± 1.9	93.3 ± 1.6	4.5	2.0	1.7
SMZ	107.7 ± 3.8	98.8 ± 2.3	95.3 ± 2.1	3.5	2.3	2.2
SMM	103.2 ± 2.9	94.9 ± 2.3	91.3 ± 1.9	2.8	2.4	2.1
SDM	94.7 ± 1.2	90.0 ± 2.5	95.0 ± 4.7	1.3	2.8	4.9

4. Conclusions

BDD electrodes exhibit excellent performance for the electrochemical detection of SAs (SDZ, SMZ, SMM, and SDM) in egg samples. The optimum potential from the hydrodynamic voltammogram was found to be 1100 mV versus Ag/AgCl, which was chosen for the HPLC-amperometric system. An excellent linearity, and detection and quantitation limit were obtained. This proposed method was used for determination of SAs in egg samples. Percentage recoveries were found to be acceptable.

Acknowledgements

We would like to acknowledge support from the Thailand Research Fund (TRF) for Research Senior Scholars, The Enhancement on the Country's Performance and Competitiveness Program, and the Ratchadaphisek Somphot Grant, Chulalongkorn University.

References

[1] Commission of the European Community, The rules governing medical products in the European Community IV, Brussels, 1991.
[2] W. Heering, E. Usleber, R. Dietrich, E. Martlbauer, Analyst 123 (1998) 2759.
[3] S.R.H. Crooks, G.A. Baxter, M.C. O'Connor, C.T. Elliot, Analyst 123 (1998) 2755.
[4] V.B. Reeves, J. Chromatogr. B. 723 (1999) 127.
[5] M.-R.S. Fuh, S.-Y. Chu, Anal. Chim. Acta 499 (2003) 215.
[6] I. Garcia, L. Sarabia, M.C. Ortiz, J.M. Aldama, Analyst 129 (2004) 766.
[7] J.-F. Jen, H.-L. Lee, B.-N. Lee, J. Chromatogr. A. 793 (1998) 378.
[8] S. Baskaran, D.R. Lauren, P.T. Holland, J. Chromatogr. A 746 (1996) 25.
[9] F.D. Zayas-Blanco, M.S. Garcia-Falcon, J. Simal-Gandara, Food Control 15 (2004) 375–378.
[10] M. Noa, N. Perez, R. Gutierez, I. Escobar, G. Diaz, S. Vega, G. Prado, G. Urban, J. AOAC Int. 85 (2002) 1415.
[11] K. Albert, K.L. Riter, R.L. Smallidge, J. AOAC Int. 86 (2003) 623.
[12] C.D.C. Salisbury, J.C. Sweet, R. Munro, J. AOAC Int. 87 (2004) 1264.
[13] M.I. Saleh, F.W. Pok, J. Chromatogr A. 763 (1997) 173.
[14] T.N. Rao, B.V. Sarada, D.A. Tryk, A. Fujishima, J. Electroanal. Chem. 461 (2000) 175.
[15] N. Furasawa, J. AOAC Int. 85 (2002) 848.
[16] N. Furusawa, Anal. Chim. Acta 481 (2003) 255.
[17] K. Kishida, N. Furusawa, Talanta 67 (2005) 54.
[18] M.T. Combs, M. Ashraf-Khorassani, L.T. Taylor, J. Pharm. Biomed. Anal. 25 (1999) 301.
[19] K. Heinig, J. Henion, J. Chromatogr. B. 732 (1999) 445.
[20] J. Abian, M.I. Churchwell, W.A. Korfmacher, J. AOAC Int. 629 (1993) 267.
[21] J. Xu, M.C. Granger, Q. Chen, J.W. Strojek, T.E. Lister, G.M. Swain, Anal. Chem. 69 (1997) 591A.

[22] S. Jolley, M. Koppang, T. Jakson, G.M. Swain, Anal. Chem. 69 (1997) 4099.
[23] T. Yano, D.A. Tryk, K. Hashimoto, A. Fujishima, J. Electrochem. Soc. 145 (1998) 1870.
[24] E. Popa, H. Notsu, T. Miwa, D.A. Tryk, A. Fujishima, Electrochem. Solid-State Lett. 2 (1999) 49.
[25] J. Xu, Q. Chen, G.M. Swain, Anal. Chem. 70 (1998) 3146.
[26] B.V. Sarada, T.N. Rao, D.A. Tryk, A. Fujishima, Anal. Chem. 72 (2000) 1632.
[27] W. Siangproh, P. Ngamkot, O. Chailapakul, Sens. Actuators B 91 (2003) 60.
[28] T.N. Rao, I. Yagi, T. Miwa, D.A. Tryk, A. Fujishima, Anal. Chem. 71 (1999) 2506.
[29] J.W. Strojek, M.C. Granger, T. Dallas, M.V. Holtz, G.M. Swain, Anal. Chem. 68 (1996) 2031.
[30] G.M. Swain, R. Ramesham, Anal. Chem. 65 (1993) 345.
[31] O. Chailapakul, E. Popa, H. Tai, B.V. Sarada, D.A. Tryk, A. Fujishima, Electrochem. Commun. 2 (2000) 422.
[32] M.A. Witek, G.M. Swain, Anal. Chim. Acta 440 (2001) 119.
[33] H. Notsu, T. Tatsuma, A. Fujishima, J. Electroanal. Chem. 523 (2002) 86.
[34] N. Wangfuengkanagul, O. Chailapakul, J. Pharm. Biomed. Anal. 28 (2002) 841.
[35] N. Wangfuengkanagul, O. Chailapakul, Talanta 58 (2002) 1213.
[36] W. Siangproh, N. Wangfuengkanagul, O. Chailapakul, Anal. Chim. Acta 499 (2003) 183.
[37] O. Chailapakul, W. Siangproh, B.V. Sarada, C. Terashima, T.N. Rao, D.A. Tryk, A. Fujishima, Analyst 127 (2002) 1164.
[38] T.A. Ivandini, B.V. Sarada, C. Terashima, T.N. Rao, D.A. Tryk, H. Ishiguro, Y. Kubota, A. Fujishima, J. Electroanal. Chem. 521 (2002) 117.
[39] C. Terashima, T.N. Rao, B.V. Sarada, D.A. Tryk, A. Fujishima, Anal. Chem. 74 (2002) 895.
[40] M.C. Granger, J. Xu, J.W. Strojek, G.M. Swain, Anal. Chim. Acta 397 (1999) 145.
[41] C. Terashima, T.N. Rao, B.V. Sarada, Y. Kubota, A. Fujishima, Anal. Chem. 75 (2003) 1564.
[42] S. Palaharn, T. Charoenraks, N. Wangfuengkanagul, K. Grudpan, O. Chailapakul, Anal. Chim. Acta 499 (2003) 191.
[43] T. Charoenraks, S. Palaharn, K. Grudpan, W. Siangproh, O. Chailapakul, Talanta 64 (2004) 1247.
[44] K. Boonsong, S. Chuanuwatanakul, N. Wangfuengkanagul, O. Chailapakul, Sens. Actuators B 108 (2005) 627.
[45] O. Chailapakul, M. Amatatongchai, P. Wilairat, K. Grudpan, D. Nacapricha, Talanta 64 (2004) 1253.
[46] J. Xu, G.M. Swain, Anal. Chem. 70 (1998) 1502.
[47] T. Charoenraks, S. Chuanuwatanakul, K. Honda, Y. Yamaguchi, O. Chailapakul, Anal. Sci. 21 (2005) 241.
[48] J. Inieata, P.A. Michaud, M. Panizza, C. Comninellis, Electrochem. Commun. 3 (2001) 346.
[49] P. Canizares, C. Saez, J. Lobato, M.A. Rodrigo, Electrochim. Acta 49 (2004) 4641.
[50] D.A. Skoog, F.J. Holler, T.A. Nieman, Principle of Instrumental Analysis, Saunders College Publishing, Philadelphia, 1998.

Available online at www.sciencedirect.com
SCIENCE DIRECT®
Talanta 68 (2006) 1720–1725
Talanta
www.elsevier.com/locate/talanta

Flow-injection in-line complexation for ion-pair reversed phase high performance liquid chromatography of some metal-4-(2-pyridylazo) resorcinol chelates

Supalax Srijaranai [a,*], Saiphon Chanpaka [a], Chutima Kukusamude [a], Kate Grudpan [b]

[a] *Department of Chemistry, Faculty of Science, Khon Kaen University, Khon Kaen 40002, Thailand*
[b] *Department of Chemistry, Faculty of Science, Chaing Mai University, Chaing Mai 50200, Thailand*

Received 22 December 2004; accepted 9 March 2005
Available online 21 September 2005

Abstract

Flow injection (FI) was coupled to ion-pair reversed phase high performance liquid chromatography (IP-RPHPLC) for the simultaneous analysis of some metal-4-(2-pyridylazo) resorcinol (PAR) chelates. A simple reverse flow injection (rFI) set-up was used for in-line complexation of metal-PAR chelates prior to their separation by IP-RPHPLC. The rFI conditions were: injection volume of PAR 85 μL, flow rate of metal stream 4.5 mL min^{-1}, concentration of PAR 1.8×10^{-4} mol L^{-1} and the mixing coil length of 150 cm. IP-RPHPLC was carried out using a C_{18} μBondapak column with the mobile phase containing 37% acetonitrile, 3.0 mmol L^{-1} acetate buffer pH 6.0 and 6.2 mmol L^{-1} tetrabutylammonium bromide (TBABr) at a flow rate of 1.0 mL min^{-1} and visible detection at 530 and 440 nm. The analysis cycle including in-line complexation and separation by IP-RPHPLC was 16 min, which able to separate Cr(VI) and the PAR chelates of Co(II), Ni(II) and Cu(II).

Keywords: Flow injection; In-line complexation; Ion pair reversed phase high performance liquid chromatography; Metal-PAR chelates

1. Introduction

Liquid chromatography has been widely recognized as one of the methods for multi-element and sensitive analysis of metal ions. Various modes of liquid chromatography have been used, including normal phase [1–3], reversed phase and ion exchange chromatography (IEC) [4–10]. Since the introduction of ion-pair reversed phase high performance liquid chromatography (IP-RPHPLC) [11,12] for the separation of charged solutes, IP-RPHPLC has gained wide acceptance as an alternative method to IEC for charged analytes, including metal ions. IP-RPHPLC offers multi-element detection capacity, selectivity and sensitivity of analysis. Moreover, the reversed-phase stationary phase has the benefit of lower cost compared to the IEC stationary phase.

Most of the reports on IP-RPHPLC for metal analysis [13–16] are based on the separation as their chelates. Pre-complexation of metal ions with appropriate ligands has many advantages such as increasing selectivity between metal ions, the ability to determine speciation and increasing sensitivity for chelates with high absorptivity. Among the many ligands successfully used for IP-RPHPLC separation of metal ions, 4-(2-pyridylazo) resorcinol (PAR) is one of the most widely used ligands. PAR is an azo dye has been used for the spectrometric determination of over 40 different metals [17]. PAR forms ionic complexes with large absorptivity ($\sim 10^4$ L cm^{-1} mol^{-1}) [18] at about 500 nm. It has been shown to be an effective reagent for the determination of metals using HPLC with either pre-column [19] or post column complexation techniques [20,21].

Typically, complexation of metal ions is performed by batch or external to the chromatographic system before injection. External complexation is time consuming and the large amounts of chemicals used mean more waste to discharge. It is prone to contamination, especially for trace level determinations. Nowadays, the main consideration includes automation of the method, low operating costs, less waste as well as high sample throughput.

Flow injection (FI) has been known with features of a simple operational basis, using inexpensive hardware, straightforward thus leading to convenient operation, high sample throughput, cost effective performance and versatility. FI has been widely

* Corresponding author. Tel.: +66 43 202222/41x2243; fax: +66 43 202373.
E-mail address: supalax@kku.ac.th (S. Srijaranai).

0039-9140/$ – see front matter © 2005 Elsevier B.V. All rights reserved.
doi:10.1016/j.talanta.2005.03.043

used as an analytical tool and also combined with the other analytical techniques [22].

Flow injection coupled with HPLC systems is usually intended to improve general features of the analytical process such as sensitivity, precision, rapidity, cost, etc. [23]. FI coupled with HPLC is used in two different modes, i.e., pre- or post-column arrangements. For the pre-column arrangement, as in the present study, the FI port is placed before the HPLC. The specific objectives of pre-column coupling are automation of sample clean-up and/or preconcentration steps, automatic implementation of derivatization reactions and saving reagents. Two methods have been used to couple FI as precolumn of HPLC. The first method, the sample plug is injected through the FI valve and then passed through HPLC loop. In the second method, the sample from the FI system is retained in a precolumn placed in HPLC loop.

Previous work in this laboratory has involved metal analysis by IP-RPHPLC via batch complexation with PAR [24]. In the work described here, a simple FI system was developed as the in-line precolumn for complexation of some metal-PAR chelates before being analysed by IP-RPHPLC. The FI part (rFI) is operated by injecting a PAR reagent solution into a metal ion solution flowing stream. A portion of the PAR-metal mixture zone is then sampled with the HPLC injection valve for subsequent separation and further detection.

2. Experimental

2.1. Chemicals and reagents

All the reagents used were of analytical reagent (AR) grade, 4-(2-pyridylazo) resorcinol and tetrabutylammonium bromide (TBABr) were purchased from Fluka (Switzerland). 2-Diethylaminoethanol was obtained from Merck (Germany). Methanol and acetonitrile were of HPLC grade from Lab-Scan (Thailand). The atomic absorption standard solutions (1000 mg L^{-1}) of Cu(II), Cd(II), Co(II), Hg(II), Zn(II), Fe(III) and Pb(II) were obtained from Ajax Finechem (Australia) whereas Ni(II) was purchased from BDH (England). Cr(VI) oxide was obtained from Merck (Germany). Aqueous solutions were prepared with deionized water obtained from RiOs^{TM} type I simplicity 185 (Millipore Waters, USA) throughout the experiment. Standard solutions of metal ions were prepared daily by stepwise dilution of 1000 mg L^{-1} stock solution with water. Stock PAR solution (0.001 mol L^{-1}) was prepared by dissolving an accurately weighed amount of 4-(2-pyridylazo)resorcinol in water and stored in a dark bottle. Working solution was prepared daily with water and appropriate volume of 2-diethylaminoethanol was added to make the concentration of 2.5×10^{-4} mol L^{-1} in such a PAR solution.

2.2. Instruments

A schematic representation of the rFI coupled with the HPLC system is shown in Fig. 1.

The rFI system used a 505s 505LA peristaltic pump (Watson Marlow, England). PFA Teflon tubes (1.5 mm i.d.) were employed for the reaction coils and were connected to a six-port low-pressure injection valve, four way switching valve (Upchurch, USA) was used to allow the metal-chelates flow to HPLC system. A manual operation using a stopwatch was for time control.

The chromatographic set-up consisted of a Waters 6000A Dual Pump, a Rheodyne injector with 20 μL sample loop and a Waters 484 Tunable Absorbance Detector (Waters, USA) equipped with Waters 740 Data Module Integrator (Waters, USA), and the Millinium 32 Software data acquisition system was used. A 996 photodiode array (Waters, USA) was also used for the study of interferences. A C_{18}-μBondapak (3.9 mm i.d. × 300 mm) coupled to a guard column (Waters, USA) was used as the stationary phase.

The spectra of the metal chelates in batchwise experiments were obtained with a Agilent 8453 (USA) UV–vis spectrophotometer equipped with a 1 cm quartz cell.

2.3. Procedure

Once the baseline of the HPLC was steady, a complete cycle (4 steps) of the rFI-HPLC manifold was started. The 4 steps include prefill, complexation, separation and washing. In the first (prefill) step, the aqueous solution containing metal ions was pumped through the rFI manifold for 30 s, this period was long enough to fill the transmission line with metal solution. The HPLC was in the load mode throughout this step to maintain a steady baseline of mobile phase.

During the prefill step, an aliquot of PAR was filled into the loop connected to V2 (at LOAD position).

Step 2, the complexation step, was started by switching V2 to INJECT position. The metal ions merged with PAR and complexation occurred during their passage through the reaction coil (RC). To avoid a dilution edges of the zone and to allow only the middle zone of the PAR chelates to pass into the HPLC-loop, the valve V3 was switched after 8 s of injection of PAR. The subsequent time period of 2 s, was enough to rinse and fill the HPLC-loop (20 μL).

Then, step 3 (separation step), was initiated via HPLC-valve (V4). The PAR-chelates were introduced and then separated in the HPLC system.

Finally, step 4 (washing step), was to wash the rFI and HPLC-loop for the next analysis, while separation was taking place on the HPLC column.

3. Results and discussion

3.1. Coupling of rFI to IP-RPHPLC

The rFI was chosen instead of normal FI because of its low background noise for HPLC baseline as well as lower PAR consumption. The rFI was coupled to the HPLC by switching valve (V3) shown in the diagram (Fig. 1).

Factorial design was used to investigate the influence of parameters of the rFI system on the peak height (absorbance). The four variables studied were: flow rate of metal ions stream, injection volume of PAR, length of the mixing coils and concen-

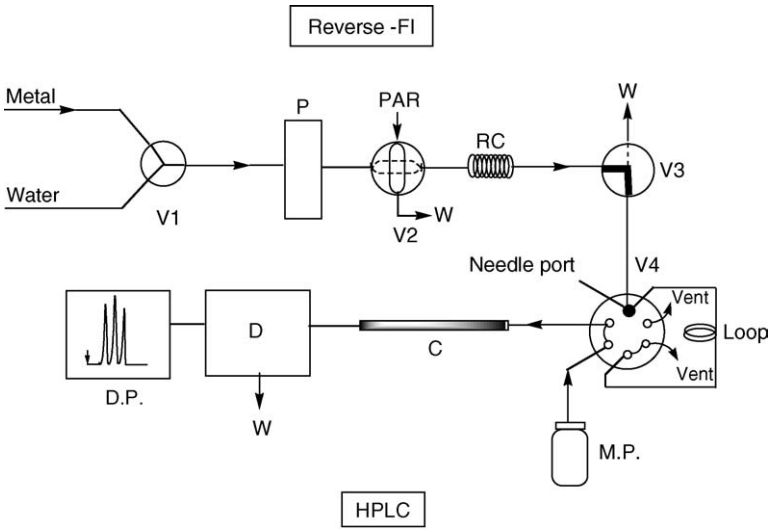

Fig. 1. Diagram of FI-HPLC in-line derivatization system: P, peristaltic pump; RC, reaction coil; V1, three way valve; V2, low pressure injection valve; V3, switching valve; V4, high pressure injection valve; C, analytical column; M.P., mobile phase; D, UV–vis detector/photodiode array detector; D.P., data processor; W, waste.

tration of PAR. A factorial design for four variables at two levels (2^4 resolution, 16 experiments) was performed. According to the results obtained from the factorial design, the chosen parameters to be optimized were the concentration of PAR, injection volume of PAR solution and flow rate of metal stream. The variable size simplex was then employed for optimization. The mixing coil length of 150 cm was used throughout the experiment.

In-line complexation of metal-PAR chelates was performed using the rFI which the optimum conditions were: mixing coil length of 150 cm, injection volume of PAR 85 μL, flow rate of metal stream 4.5 mL min^{-1} and concentration of PAR 1.8×10^{-4} mol L^{-1}. The PAR chelates were then separated via IP-RPHPLC.

Synchronization of the FI manifold and the HPLC is very important to achieve good performance of the coupling system. The time intervals and valve positions of the rFI-HPLC were investigated using the results obtained from the study of the optimization of the rFI. Manual operation of the rFI-HPLC system was found to provide satisfied precision.

The complete cycle of rFI coupling to IP-RPHPLC was 120 s, where as the analysis time of the HPLC was 14 min. Operating periods and valve position for rFI-IPRPHPLC are summarized in Table 1 and Fig. 2.

3.2. IP-RPHPLC of metal-PAR chelates

In IP-RPHPLC, the metal chelates, which are successfully separated, have to be stable and kinetically inert [25]. It is known that the retention behavior of chelates in IP-RPHPLC depends strongly on complex composition (metal:ligand), which is governed by the nature of the central metal ion. The mobile phase composition is also govern the separation. The principal parameters of interest in the mobile phase are pH, buffer (type and concentration), organic modifier and ion pairing agent (long-chain alkyl ions with a charge opposite that of analytes). There are several mechanisms [26–28] explaining the retention behavior of IP-RPHPLC, such as the ion-exchange mechanism, the solvophobic theory and dynamic equilibrium.

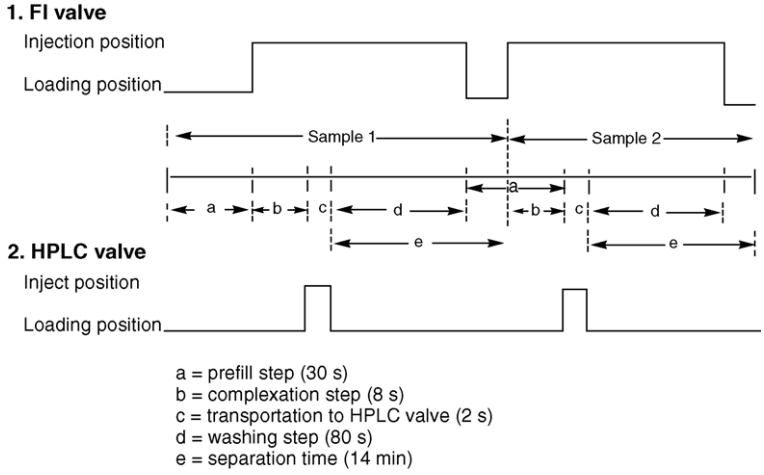

Fig. 2. Diagram of timing control for operation of valves in the FI-HPLC system.

Table 1
Valves positions and operating times for rFI-HPLC

Step	Time (s)	Valve position				In-line complexation operation	
		V1	V2	V3	V4	Medium pump	Stage of operation
Sample 1							
1	30	To V2	Load	To waste	Load	Metals	Prefill
2	38	To V2	Inject	To V4	Load	Metals	Complexation
3	40	To V2	Inject	To V4	Inject	Metals	Separation
4	120	To V2	Load	To V4	Load	Water	Washing
Sample 2							

Typically, PAR forms anionic chelates with metals at the metal to ligand ratio of 1:2 [29]. Thus, cationic ion pairing agent, tetrabutyl ammonium bromide was used. The optimum mobile phase was obtained by slightly adjusting the one obtained in our previous work [24]. The mobile phase composition was 37% acetonitrile, 6.2 mmol L^{-1} TBABr and 3.0 mmol L^{-1} acetate buffer pH 6.0.

Baseline separation of three metal-PAR chelates was achieved within 14 min, with the elution order of Co(II)-PAR, Ni(II)-PAR and Cu(II)-PAR. The excess PAR was detected at the retention time of 9.6 min. The chromatogram is shown in Fig. 3.

Using the optimum mobile phase and the detection at 440 nm, Cr(VI) was retained shortly (4.9 min) after unretained peak (at 3.3 min), as shown in Fig. 4. The spectrochromatogram corresponding to Fig. 4 is shown in Fig. 5. For the condition used, Cr(VI) might present as its oxyanion ($HCrO_4^-$) [30]. Thus, it could interact with ion pairing agent in the same manner to the anionic chelates. The peak at 4.9 min which was identified as Cr(VI) gives the absorption spectrum (as shown in Fig. 6) identical to the spectrum of Cr(VI) detected by UV–vis spectrometer. The resolutions between pairs were as follow: 1.4 for Cr(VI) and Co(II)-PAR, 1.0 for Co(II)-PAR and Ni(II)-PAR, 2.4 for Ni(II)-PAR and excess PAR, and 1.3 for excess PAR and Cu(II)-PAR.

3.3. Performance of rFI-IP-RPHPLC

Quantitative features including linearity and reproducibility for retention time and peak area were studied using the optimum condition. Calibration graphs were prepared by plotting the concentration of each metal ion (μg mL^{-1}) against the peak area. The limit of detection (LOD) was deduced based on three times of baseline signal. The calibration equation, coefficient of correlation (r^2), recovery, reproducibility and LOD are summarized in Table 2.

3.4. Interferences

The effect of interferences on the chromatography of metal-PAR chelates was investigated. The chosen ions are the ions able to form chelate with PAR including Cd(II), Cr(III), Hg(II), Mn(II), Fe(III), Pb(II) and Zn(II). These metal ions were individually injected into the rFI-HPLC. All of the studied ions could not form chelates with PAR under the condition used. Only peak, which was identified as PAR (9.6 min) was observed.

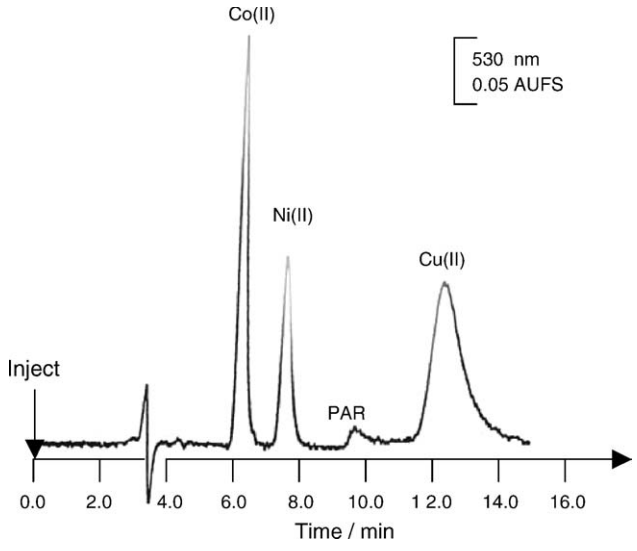

Fig. 3. Chromatogram of metal-PAR chelates; condition: C_{18} column, mobile phase 37% acetonitrile, 6.2 mmol L^{-1} TBABr and 3.0 mmol L^{-1} acetate buffer pH 6.0, flow rate of mobile phase 1.0 mL min^{-1} visible detection at 530 nm; peak: 0.10 μg mL^{-1} Co(II), 0.20 μg mL^{-1} Ni(II), excess PAR and 0.80 μg mL^{-1} Cu(II).

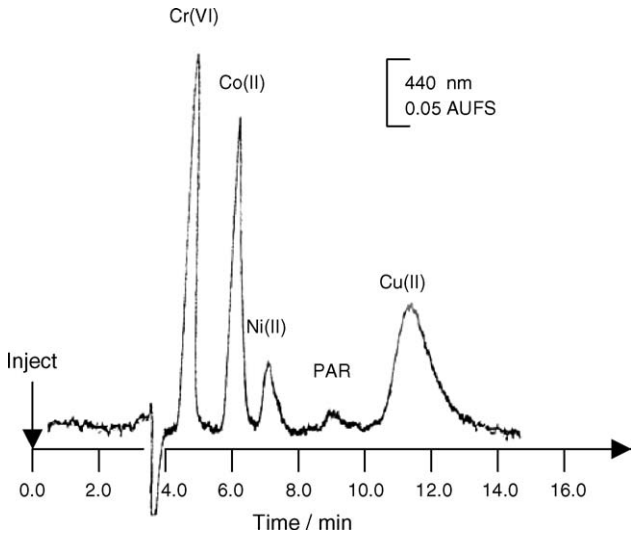

Fig. 4. Chromatogram for Cr(VI) and metal-PAR chelates; peaks: 5.0 μg mL^{-1} Cr(VI), 0.10 μg mL^{-1} Co(II), 0.10 μg mL^{-1} Ni(II), excess PAR and 0.40 μg mL^{-1} Cu(II) (condition as described in Fig. 3, except visible detection at 440 nm).

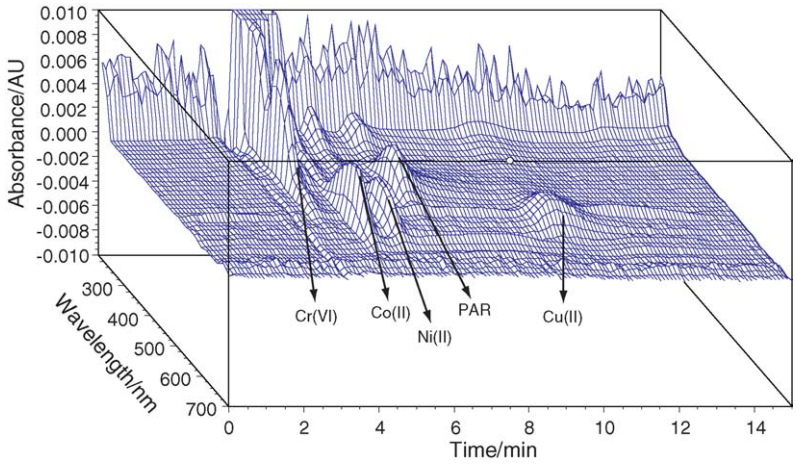

Fig. 5. 3D plot of Cr(VI) and metal-PAR chelates of chromatogram in Fig. 4.

Table 2
The quantitative features of rFIA-HPLC

Chelates	Concentration of metal ion ($\mu g\,mL^{-1}$)	Linear equations $Y = AX + C$	Correlation coefficient (r^2)	R.S.D.[a] (%) ($n = 11$)		LOD (3σ) ($\mu g\,mL^{-1}$)	Percent recovery
				t_R	Area		
Cr(VI)	1.00–6.00	$473.51X - 0.17$	0.9961	2.0	0.94	1.00	113
Ni(II)-PAR	0.01–0.20	$341.66X - 4.73$	0.9983	2.1	0.91	0.02	84
Co(II)-PAR	0.01–0.40	$547.21X - 0.61$	0.9952	0.6	0.97	0.03	96
Cu(II)-PAR	0.05–0.60	$293.80X + 5.49$	0.9986	2.4	0.71	0.15	102

[a] Concentration of each metal was described in Fig. 4.

The study on tolerance level of the metal ions which could not form chelates with PAR was studied by individually spiking the metal ions at difference amounts (ranging from 0.5 to 10.0 $\mu g\,mL^{-1}$) into the mixture of 0.10 $\mu g\,mL^{-1}$ Co(II), 0.20 $\mu g\,mL^{-1}$ Ni(II), 0.40 $\mu g\,mL^{-1}$ Cu(II) and 5.0 $\mu g\,mL^{-1}$ Cr(VI). It was found that the presence of the foreign ions did not affect the retention time of the PAR chelates of Co(II), Ni(II) and Cu(II). However, the quantitative signals (both peak height and peak area) were affected by the addition of the foreign ions. Cu(II)-PAR was strongly influenced when the concentrations

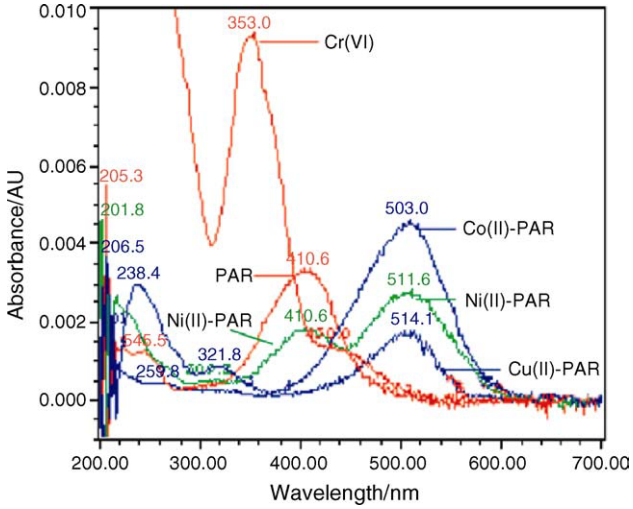

Fig. 6. The absorption spectra of chromatogram in Fig. 4.

of the foreign ions increase to 2.5 times resulted in decreased of peak height and peak area. The effect on Ni(II)-PAR was observed when the foreign ions increase to five times greater than Ni(II), resulted in the decreasing of peak height and peak area. This effect was also observed for Co(II) when the concentration of the foreign ion was 10 times to Co(II). The peak area of Cr(VI) was not affected by the addition of the foreign ion. However, the obtained spectra and the 3D plots (results not shown) revealed that neither PAR chelates of the foreign ions nor the ternary complexes were formed. According to the obtained results indicating that in such a condition, quantity of PAR was enough for all of metal ions. Furthermore, to ensure the excess amount of PAR, 10 times higher concentration of PAR, i.e., 1.0×10^{-3} mol L^{-1} was used. Similar results were obtained and large peak of excess PAR overlapped the analyte peaks. The effect of interference on the present method was obviously seen when compared to the previous work [24] on precomplexation of metal-PAR chelates by batch method prior to the analysis by IP-RPHPLC. This may attribute to the nature of the flow system, which a short time that stream of reagents are reacted. Neither physical equilibrium nor chemical equilibrium (i.e., the completeness of reaction) has been attained by the time it was detected.

3.5. Analysis of real sample

According to the study, it is possible to analyse Cr(VI) simultaneously with Ni(II). The present method was applied to the analysis of chrome plating waste water. The samples were collected from chrome plating plant in Khon Kaen and were

Table 3
Results of analysis of chrome plating waste water

Metal	Concentration ($\mu g\,mL^{-1}$)			
	Sample 1		Sample 2	
	FI-HPLC	AAS	FI-HPLC	AAS
Cr(VI)	984.5 ± 6.4[a]	980.8 ± 7.9[a]	69.3 ± 10.7[a]	72.6 ± 9.3[a]
Co(II)	N.D.[b]	N.D.[b]	N.D.[b]	N.D.[b]
Ni(II)	1574.6 ± 10.2[a]	1580.9 ± 12.0[a]	121.4 ± 7.4[a]	126.8 ± 8.2[a]
Cu(II)	N.D.[b]	N.D.[b]	N.D.[b]	N.D.[b]

[a] S.D. ($n = 3$).
[b] Not detected.

analysed after dilution, pH adjustment and filtration through 0.45 μm membrane. The results obtained are listed in Table 3, which were in good agreement with that of AAS.

4. Conclusion

In the present study, a simple combination of rFI and HPLC resulted in a powerful technique for simultaneous analysis of metal ion as their PAR chelates. The rFI was coupled to HPLC with simple operation. Using the developed rFI for in-line complexation gives benefit of less PAR consumption, less analysis time and less waste disposed comparison to the batch derivatization. The analysis cycle consists of in-line complexation (ca. 2 min) and separation by IP-RPHPLC (14 min). The method was successfully applied for the separation of Co(II), Ni(II) and Cu(II) as their PAR chelates.

Acknowledgements

The authors are grateful for the financial support from the Thailand Research Fund (TRF) and the Postgraduate Education and Research Program in Chemistry (PERCH).

References

[1] J.F.K. Huber, J.C. Kraak, H. Veening, Anal. Chem. 44 (1972) 1554.
[2] E. Gaetani, C.F. Laureri, A. Mangia, G. Parolari, Anal. Chem. 48 (1976) 1725.
[3] D.F. Gasparrini, M.N. Galli, J. Chromatogr. 161 (1978) 356.
[4] Y. Nagaosu, H. Kawabi, Anal. Chem. 63 (1991) 28.
[5] S.J. Tsai, H.T. Yan, Analyst 118 (1993) 521.
[6] T. Yasui, A. Yochi, H. Yamada, H. Wada, J. Chromatogr. A 659 (1994) 359.
[7] L. Qiping, W. Yuanchao, L. Jinchum, C. Jieke, Talanta 42 (1995) 901.
[8] R.M. Cassidy, S. Elchuk, Anal. Chem. 54 (1982) 1558.
[9] N. Cardillicchio, J. Chromatogr. 640 (1993) 207.
[10] W. Shotyk, J.J. Potthast, J. Chromatogr. A 706 (1995) 163.
[11] D.P. Wittmer, N.O. Nuessle, Haney, Anal. Chem. 44 (1975) 743.
[12] S.P. Sood, L.E. Sartori, D.P. Wittmer, W.G. Haney, Anal. Chem. 48 (1976) 1422.
[13] E. Kaneko, H. Hoshino, T. Yotsuyanagi, Anal. Chem. 63 (1991) 2219.
[14] J.J. Lucena, P. Barak, L.H. Apaolaza, J. Chromatogr. A 727 (1996) 253.
[15] Z.L. Ma, Y.P. Wang, C.X. Wang, F.Z. Miao, W.X. Ma, Talanta 44 (1997) 743.
[16] N. Vachirapatama, G.W. Dicinoski, A.T. Townsend, P.R. Haddad, J. Chromatogr. A 956 (2002) 221.
[17] S.J. Tsai, Y. Lee, Analyst 116 (1991) 615.
[18] J.R. Jezorek, H. Freiser, Anal. Chem. 51 (1979) 373.
[19] H.L. Sun, H.M. Lui, S.J. Tsai, Analyst 115 (1990) 133.
[20] M.D.H. Amey, D.A. Bridle, J. Chromatogr. 640 (1993) 323.
[21] N. Cardellicchio, P. Rogone, S. Cavalli, J. Riviello, J. Chromatogr. A 770 (1997) 185.
[22] K. Grudpan, Talanta 64 (2004) 1084.
[23] M.D. Luque de Castro, M. Valcarcel, J. Chromatogr. 600 (1992) 183.
[24] S. Srijaranai, R. Burakham, R.L. Deming, T. Khammeng, Talanta 56 (2002) 655.
[25] P. Janos, Anal. Chim. Acta 414 (2000) 113.
[26] J.C. Kraak, K.M. Jonker, J.F.K. Huber, J. Chromatogr. 142 (1977) 671.
[27] C. Horváth, W. Melander, I. Molnár, J. Chromatogr. 125 (1976) 129.
[28] B.A. Bidlingmeyer, J. Chromatogr. 186 (1979) 418.
[29] A.C. Co, A.A. Ko, L. Ye, C.A. Lucy, J. Chromatogr. A 770 (1997) 69.
[30] N.S. Chamberlain, R.V. Day, in: The 11th Purdue Industrial Waste Conference, 1956, p.129.

Down scaling: From operation on lab bench space to manipulation at a valve

Kate Grudpan[1, 2*], Supada Khonyoung[1], Supaporn Kradtap Hartwell[1, 2], Somchai Lapanantnoppakhun[1, 2] and Jaroon Jakmunee[1, 2]

[1] Department of Chemistry, Faculty of Science Faculty of Science, Chiang Mai University, Chiang Mai 50200 Thailand
[2] Institute for Science and Technology Research and Development, Chiang Mai University, Chiang Mai 50200 Thailand

Abstract

Down scaling for chemical analysis with flow-based techniques with the emphasis on sequential injection systems is reviewed. Sequential Injection (SI) systems with Lab-on-Valve (LOV) offer various advantages. SI with Lab-at-Valve (LAV) approach serves as an alternative cost effective means for automation and miniaturization in chemical analysis. Development of the techniques and their features are discussed.

Keywords miniaturization, flow based techniques, sequential injection analysis, lab-on-valve (LOV), lab-at-valve (LAV), cost effective analysis

1. Introduction

Research and development have favored the direction of "zero emission" and "greener" chemistry. This has also led to various approaches for cost effective chemical analysis. Flow-based techniques offer not only advantages gained in term of automation but also to down scaling in chemical analysis such as reduction in chemicals/ volumes used and waste, and in sample consumption; much less analysis time (leading to high sample through-puts), and less activities involving glassware cleaning. All concern cost effectiveness [1].

Flow injection analysis (FIA) may be known as an analytical technique based on microfluidic manipulation of samples and reagents. Usually, a sample is injected into a carrier/reagent solution which transports the sample zone into a detector to monitor changes due to the desired (bio)chemical reactions which have been taken place. Chemical information will be obtained from the detector response (absorbance, conductance, current, fluorescence, radioactivity, mass spectra, etc.), such as concentration from a calibration graph (signal value vs. concentration) [2, 3, 4].

Microfluidics have been employed for flow analytical techniques either in continuous flow modes, such as FIA and chromatography with constant unidirection (forward) flow of carrier to transport a sample from an injector to a detector, or programmable flow modes such as sequential injection analysis (SIA) with flow reversal to mix sample with reagent(s) or to stop flow to accommodate reaction time [2, 3, 5].

FIA was introduced by Ruzicka and Hansen as an approach for downscaling from batch analysis to flow analysis-from a beaker to microfluidics [3, 6, 7]. As the second generation, SIA was developed for more degrees in automation by having a bi-directional pump for programmable flow.

2. Lab-on-Valve (LOV) Approaches

Ruzicka [8] proposed a SI with "Lab-on-Valve" (LOV) system, as the third generation, to perform micro- or nanoanalysis by integrating all the necessary laboratory facilities for a variety of analytical schemes, including sampling, chemical reaction, and detection in a conduit at a multiposition valve. The conduit is a very precisely positioned engraved Plexiglas using computer-aided-design (CAD). This is mounted to replace the headpiece of a selection valve (see Figure 1 [3]). As SI-LOV is a system/device for analytical processes taking place, it could serve then as a type of micro-total analysis system (μ-TAS). SI-LOV has proven to have more tolerance than that of chip based approaches for real applications to dirty samples or samples with complicate matrices.

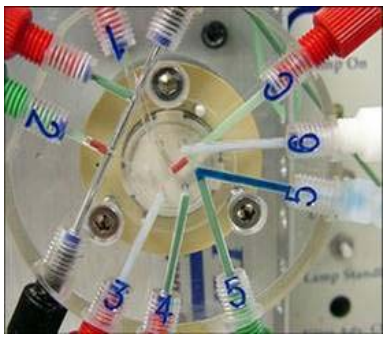

Fig. 1 SIA -Lab-On-Valve®
(more detail in www.flowinjection.com)

SI-LOV has become a platform for microSI manipulation using microliter volumes of sample and reagents per analysis. SI-LOV has been cooperated well with various techniques apart from UV-VIS such as bead injection, sequential injection affinity chromatography, mass spectrometry, capillary electrophoresis, atomic spectroscopy (AAS, ICP-AES and ICP-MS) and potentiometry.

Ruzicka has demonstrated the usefulness of SI-LOV systems to various applications [7, 9, 10, 11], including environmental analysis, pharmaceutical and bioanalytical assays.

Hansen, Wang and Miró have extensively reviewed the applications of the microSI-LOV systems with various sample

*Corresponding author.
E-mail: kate@chiangmai.ac.th

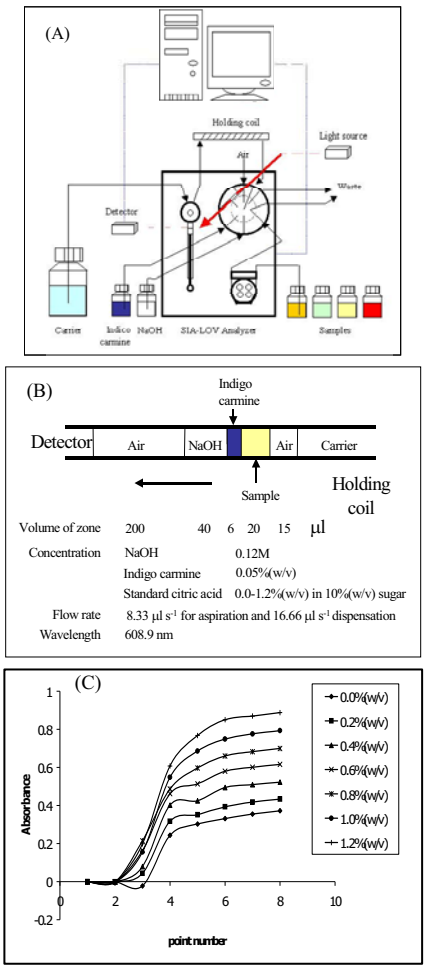

Fig. 2 Mono-segmented flow using SI-LOV for microtitration (adapted from ref 27): (A) the SI-LOV system, (B) the conditions and (C) the signal profiles.

pretreatment methods for determination of trace levels of elements using ETAAS and ICPMS. These sample pretreatments include sample dilution, dialysis, derivatization, hydride generation, liquid-liquid and solid phase extraction, chromatographic separation and preconcentration with beads and packed column [12, 13, 14, 15, 16, 17, 18, 19, 20, 21, 22, 23].

Coupling of the SI-LOV system with other detection systems such as AAS, FT-IR, electrochemistry has also been reviewed [24, 25].

Some previous reviews may be sources for information (Table 1). Table 2 summarizes some SIA-LOV developments.

Employing SI-LOV, micro-segmented microflow analysis [27] can be performed. Air segments are introduced to sandwich the sample-reagent plug to eliminate dispersion between the sample-reagent zone and the carrier stream. This enables promotion of mixing of analyte and reagent(s), with longer residence time and better sensitivity with low reagent consumption being possible. This was demonstrated by microtitration. By flow reversal, three solutions can be mixed together well in a mono-segmented zone. The air bubbles are to be discarded prior to absorbance measurement to obtain a smooth response. It should be noted that the signal profiles are not in the shape of peaks, which are different from normal SI-grams. (see Fig. 2). The concentration of a sample analyte can be obtained via a calibration graph. By the mono-segmented SI-LOV approach, the determination of copper using 2-carboxy-2'-hydroxy-5'-sulfoformazyl benzene (Zincon) has been reported [32].

3. Lab-at-Valve (LAV) Approaches

As an alternative cost effective micro-total analysis system, the Lab-at-Valve (LAV) approach has been investigated. A LAV unit can be fabricated using an ordinary and less precise machine tool by designing for suitable function for the chemistry of interest, and for easy attachment at a port of a conventional selection valve in a simple usual way. There is no need to take out any part of a usually available selection valve [1, 47].

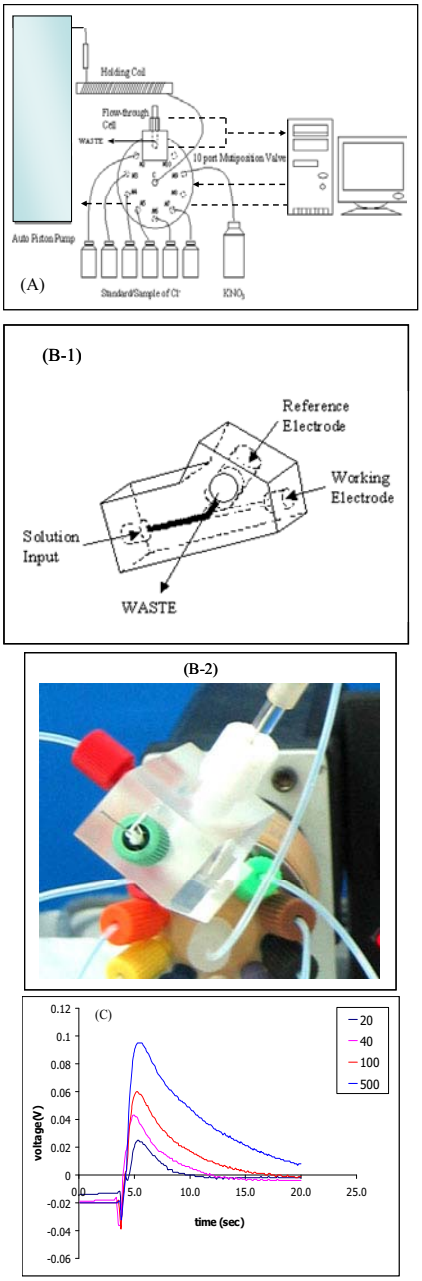

Fig. 3 SI-LAV for the potentiometric determination of chloride (adapted from ref 1, 47): (A) the SI-LAV system (B) the LAV flow cell and (C) the signal profiles

Table 1: LOV reviews and related articles

Analyte/sample/application field(s)	**Features (detection)**	**ref**
affinity separation, fermentation monitoring and functional cellular assay	µSI-LOV with various possible detectors for bionalytical assays	10
trace level metals	implementation of FI/SI-sample separation/preconcentration, mentioned LOV *(ETASS/ ICPMS)*	22
pharmaceutical samples	SI-LOV for chromatography and BI	9
trace level metals	progress in implementing miniaturized FI/SI systems for online separation and preconcentration, mention LOV *(ICPMS)*	19
ultra-trace level heavy metals	SI-BI-LOV for online solid phase extraction and preconc. *(ETASS/ ICPMS)*	20
trace level metals	SI-LOV with BI microcolumn for preconcentration *(ETASS/ ICPMS)*	21
	SI-LOV with other cost effective flow-based technique development	1
	impact of FI in modern chemistry including BI-LOV	17
	3 generations of FIA (FI, SI, BI-LOV)	18
	SIA for complicated online sampling manipulation (dilution, dialysis, gas diffusion, enzymatic and immunoassay) mentioned LOV *(ETAAS and ICPMS)*	25
trace level metals in complex matrices	FI/SI LOV for liquid-liquid extraction, precipitation, hydride generation, ion exchange/chelating packed column	14
	LOV mesofluidic system	15
	progress in implementing miniaturized FI/SI systems for online separation and preconcentration, mentioned LOV *(ETAAS)*	16
	programmable ufluidics to replace batch wet chem. *(various)*	7
nutrient (phosphorus) in fresh water and environmental solids	µSI-LOV microcolumn for dynamic fractionation *(spectrophotometry/ fiber optic)*	12
environmental field	SI with solid reactors, packed column for chem. derivatization, chrom. sep. and preconcentration including SI-BI with jet ring or LOV to accommodate dynamic fractionation of trace elements *(many)*	13
pharmaceutical samples	SIA (mentioned LOV) *(spectro, fluorescence, chemiluminescence, electrochem.)*	24
trace level metals	impact of FIA and SIA, LOV	23

Table 2: LOV with various detection techniques and applications

Detection	Analyte/sample	Features	ref
spectrophotometry	phosphate	molybdenum blue chemistry	8
	protease	enzymatic activity assay	
	immunoglobulin G	bioligand interaction assay protein G immobilized on Sepharose beads	
	ammonia, glucose, glycerol, free iron	μSI-LOV for offline and online monitoring of small scale fermentation	25
	nitrate, nitrite and orthophosphate	μSI-LOV with Cd foil filled microcolumn utilizing stopped flow	26
	acidity in fruit juice	mono-segmented flow micro-titration with SI-LOV	27
	DNA assay	crystal violet solution was de-colored inside the flow cell of the LOV at the presence of 5 l - DNA/HindIII within a certain pH range	28
	ketoprofen, naproxen, bezafibrate, diclofenac, ibuprofen and salicylic acid in surface water, urban wastewater, and urine	lab-on-valve (LOV) with bead injection (BI) for on-line solid-phase extraction (SPE) as a front end to highperformance liquid chromatography (HPLC)	29
	enzyme AChE and ACE	SI-LOV micro-reactor for enzyme kinetic and inhibition studies	30
	Cu (II) and Fe (II)	SI-LOV using reaction of 5-Br-PSAA) with Cu (II) and/or Fe (II)	31
	Cu (II)	SI-LOV with air segment using reaction of Cu(II) and Zincon	32
spectrofluorometry	nucleic acid sequences	SIA-LOV for sandwich hybridization of specific DNA probes to the target sequence	33
chemiluminescence	Tetracycline	LOV with bismuthate immobilized microcolumnfor in situ oxidation of KBr and generation of bromine as oxidant for the bromine-hydrogen peroxide-tetracycline (TC) chemiluminescent reaction	34
ICPMS	Ni (II) and Bi (II) in reference materials and spiked urine	SI-LOV with renewable ion exchange micro-column	35
UV-Vis and electrospray ionization MS	biotin containing conjugates and lysosomal-b-galactosidase in human cell homogenates	LOV-BI system for biotin conjuates using immobilized streptavidin	36
mass spectrometry	peptide mixture	affinity chromatographic-LOV system using multiple ligand affinities to proteins immobilized on beads.	37

Table 2 (con)

Detection	Analyte/sample	Features	ref
ETAAS	Pb (II)	SI-BI-LOV using Sephadex G-25 impregnated by dithizone	38
	Cd (II)	PTFE material for use as a means for separation and preconcentration of trace levels of metal ions with SI and SI-LOV	39
	Cd (II)	Octadecyl Immobilized Surface for Precipitate Collection with a Renewable Microcolumn in LOV	40
	Cr (VI) and Cr (III)	bead injection (BI) with renewable reversed-phase surfaces in a sequential injection-lab-on-valve (SI-LOV) mode - C18 sorption of Cr(VI) - DPC	41
	Cd (II), Pb (II) and Ni (II)	SI-LOV system using chelating Sepharose beads as sorbent material	42
	Ni (II) in saline matrices	Lab-On-Valve (μSI-LOV) for bead injection separation/pre-concentration of Ni-dimethylglyoxime (DMG) chelate	43
CVAAS	Hg (II)	SI-LOV for hydride generation	44
potentiometry	Ca (II)	SIA-LOV with solid contact ion selective electrode and pH electrode based on polyaniline	45
capillary electrophoresis	10 anions including chloride and sulfate	μSI-CE interfaced with LOV and demonstrated various injections such as electrokinetic, hydrodynamic and head column field amplification sample stacking injections	46

Table 3 Comparison of SI-LAV features to those of ion-selective electrode (ISE), ion chromatography (IC) and conventional titration with silver nitrate solution.

	LAV	ISE	IC	Titration with Ag^+solution	
Sample throughput	++++	+(+)	++	++	
Consumption:					
• sample	+	+++	+	+++	
• reagent	+	+	+++	+++	
Glassware	-	++	++	+++	
Cleaning activities	-	++	++	+++	
Automation	+++	++	+++	+	(conventional)
				+++	(auto-titrator)
Cost					
• system/ apparatus	++	++	+++	+	(conventional)
				+++	(auto-titrator)
• per sample	+	+	++	+++	

"+" refers to more scale

SI-LAV for chloride determination was proposed (Fig. 3) [47]. For potentiometry, a simple LAV flow through electrode system can be assembled. Both are Ag/AgCl electrodes, one a reference electrode (silver chloride activated surface-silver wire soaked in a constant chloride concentration in a small tube covered with a membrane), another as a working electrode situated in a flow channel. The potential difference due to the concentration cell effect is recorded as a peak. The SI-LAV provides a very simple, fast, precise, accurate, automatic and economical procedure for chloride determination and was applied to some water samples. Comparisons of features of SI-LAV to that of the conventional titration using silver nitrate solution, ISE, and ion-chromatography may be considered as illustrated in Table 3.

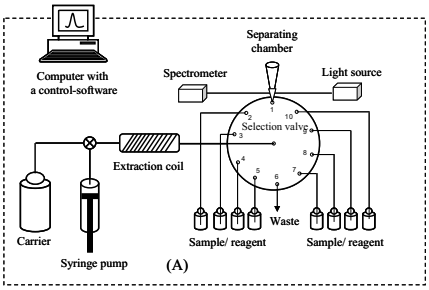

Fig. 4 SIA-LAV on-line micro solvent extraction (adapted from ref 48): (A) the SI-LAV system and (B) the LAV unit

The SI-LAV approach has been proposed for a novel alternative for simple on-line automated liquid-liquid microextraction [48, 49]. Sample, reagent and organic solvent are sequentially aspirated into an extraction coil connected to a central port of a conventional selection valve. Flow reversal enables good efficient extraction.

The aqueous and organic phases can be separated in a conical separating chamber, situated with a fiber-optic spectrophotometer to monitor the absorbance change in either the organic or aqueous layer. The unit (Fig. 4) is attached to one port of the valve. Applications have been made to the assays of anionic surfactant in water samples and diphenhydramine hydrochloride in pharmaceutical preparations by forming ion-association compounds with methylene blue and bromocresol green, respectively. Table 4 demonstrates some features of solvent extraction in comparison with conventional batch, FIA and SI-LAV formats.

Table 4 Features of solvent extraction performed in conventional batch, FIA and SI-LAV formats

	Conventional batch	FIA	SI-LAV
Consumption:			
reagents	+++	++	+
sample	+++	++	+
solvent	+++	++	+
Sample through-put	+	+++	++
Less hazardous (safety)	+	+++	+++
Cost			
• apparatus/ instrument	+	++	++
• per sample	+++	++	+

"+" refers to more scale

The SI-LAV setup for the previously described on-line solvent extraction may also be used for some applications employing stopped flow [51] (see Fig. 5(A)), such as the kinetic study of the persulfate-iodide reaction:

$$S_2O_8^{2-} + 2I^- \longrightarrow 2SO_4^{2-} + I_2$$

Employing a constant concentration of persulfate but varying the iodide concentration, signal profiles for a stopped flow mode can be obtained, as shown in Fig. 5(B). Rates for each reaction condition can be obtained from the slope of the peak profile. The order of reaction in a rate law can then be deducted from the graph (log [iodide] vs. log [rate], as illustrated in Fig. 5(C)).

Exploiting SI-LAV with air-segmented flow for automated on-line bead-based immunoassay has been made. The system provides precise delivery of micro-volumes of reagent and precise time of incubation and washing steps via manipulation of the syringe pump. Based on competitive enzyme linked immuno sorbent assay (ELISA), hyaluronan (HA), a biomarker, can be assayed by the competition of HA immobilized on beads and HA in the solution, to bind with a fixed amount of biotinylated HA-binding proteins (b-HABPs). After separation, anti-biotin conjugated with enzyme and a suitable substrate are introduced to follow the binding reaction of the immobilized HA and b-HABPs, whose degree of binding is indirectly proportional to the

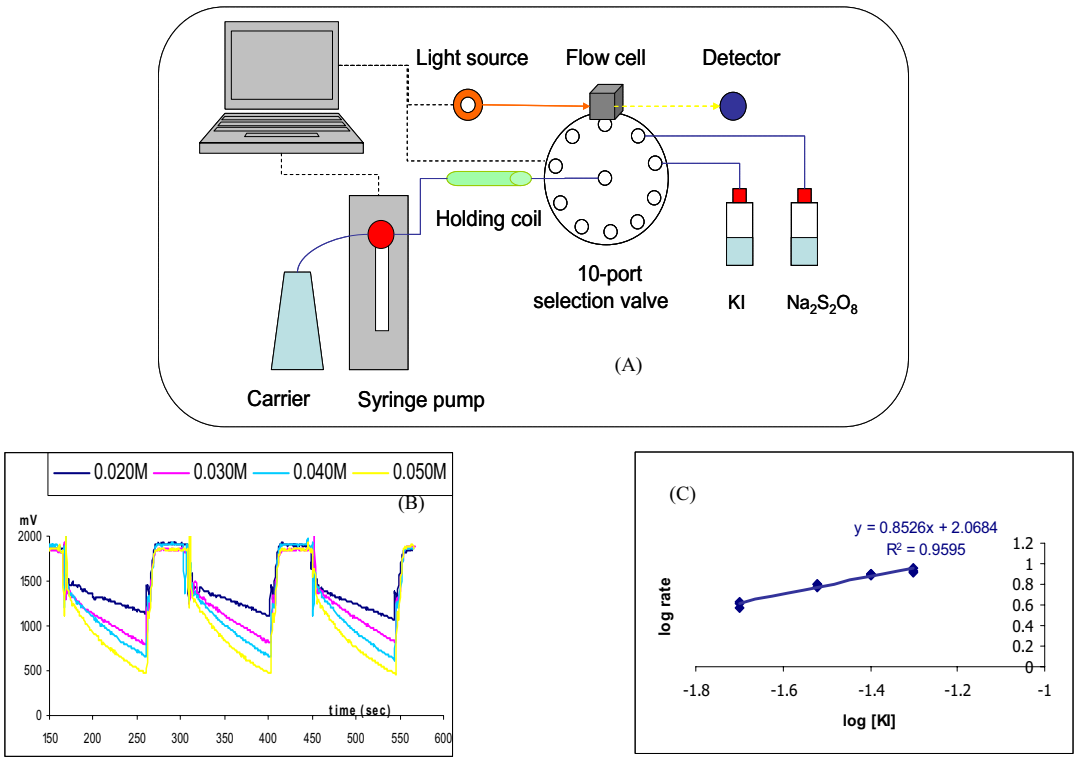

Fig. 5 SI-LAV for kinetic study of perfulfate-iodide reaction: (A) the SI-LAV system, (B) the signal profiles and (C) relation of log [Iodide] vs. log [Rate]

amount of HA in solution. Total analysis time for this automation is 30 min, comparing to 5-8 h for the conventional batch well ELISA. The system has been applied to human serum [52].

Investigation in progress is another SI-LAV system with bead injection for application to clinical analysis for the immunoassay for chondroitin 6-sulfate (C6S) as a biomarker for cartilage disease [53].

4. Conclusion

Flow based techniques provide advantages in automation and miniaturization, favoring "zero emission" and "greener" chemistry approaches. Sequential Injection (SI) with Lab-on-Valve (LOV) features give benefit in down scaling for chemical analysis. SI with Lab-at-Valve (LAV) approach may serve as a cost effective alternative. This enables down scaling chemical analyses, from operation on lab bench space to the manipulation at a valve.

Acknowledgements

The authors thank The Thailand Research Fund (TRF) (for support), Postgraduate Education and Research Program in Chemistry (PERCH) (for partial support), Professor Shoji Motomizu (for collaborative work), Professor Tadao Sakai (for collaborative work under the Frontier Research Project: Materials for 21st Century- Materials Development for Environment, Energy and Information) and Professor Gary Christian (for valuable comments).

References

[1] K. Grudpan, *Talanta*, **64**, 1084(2004).
[2] J. Ruzicka, e-book, Flow Injection Analysis, 3rd ed., 2005.
[3] www.flowinjection.com., (25 October 2006).
[4] G. D. Christian, Anal. Chim. Acta, **499**, 5(2003).
[5] G. D. Christian, Chiang Mai J. Sci., **32**, 81(2005).
[6] J. Ruzicka, E. H. Hansen, Anal. Chem., **72**, 212A(2000).
[7] J. Ruzicka, Collect. Czech. Chem. Commun., **70**, 1737(2005).
[8] J. Ruzicka, *Analyst*, **125**, 1053(2000).
[9] P. Solich, M. Polasek, J. Klimundova, J. Ruzicka, *Trend. Anal. Chem.*, **23**, 116(2004).
[10] L. D. Scampavia, J. Ruzika, *Anal. Sci.*, **17**, i429(2001).
[11] J. Ruzicka, e-book, Sequential Injectionfor Biomolecular Assays, 2004.
[12] M. Miro, E. H. Hansen, D. Buanuam, *Environ. Chem.*, **3**, 26(2006).
[13] M. Miro, E. H. Hansen, *Trend. Anal. Chem.*, **25**, 267(2006).
[14] E. H. Hansen, *J. Environ. Sci. Heal. A*, **40**, 1507(2005).
[15] J. H. Wang, *Anal. Bioanal. Chem.*, **381**, 809(2005).
[16] J. H. Wang, E. H, Hansen, *Trend. Anal. Chem.*, **2**, 1(2005).
[17] E. H. Hansen, *Talanta*, **64**, 1076(2004).
[18] E. H. Hansen, J. H. Wang, *Anal. Lett.*, **37**, 345(2004).
[19] J. H. Wang, E. H. Hansen, *Trend. Anal. Chem.*, **22**, 836(2003).
[20] J. H. Wang, E. H. Hansen, M. Miro, *Anal. Chim. Acta*, **499**, 139(2003).
[21]J. H. Wang, E. H. Hansen, *Trend. Anal. Chem.*, **22**, 225(2003).
[22] E. H. Hansen, J. H. Wang, *Anal. Chim. Acta*, **467**, 3(2002).
[23] E. H. Hansen, M. Miró, *Trends Anal. Chem.*, In press, Online: DOI; 10.1016/j.trac.2006.07.010.
[24] A. M. Pimenta, M. C. B. S. M. Montenegro, AN. Araujo, J. M. Calatayud, *J. Pharmaceut. Biomed.*, **40**, 16(2006).
[25] C. H. Wu, L. Scampavia, J. Ruzicka, B. Zamost, *Analyst*, **126**,291(2001).
[26] C. H. Wu, J. Ruzicka, *Analyst*, **126**, 1947(2001).

[27] J. Jakmunee, L. Pathimapornlert, S. K. Hartwell, K. Grudpan, *Analyst*, **130**, 299(2005).
[28] X. W. Chen, J. H. Wang, Z. L. Fang, *Talanta*, **67**, 227(2005).
[29] J. B. Quintana, M. Miro, J. M. Estela, V. Cerda, *Anal. Chem*., **78**, 2832(2006).
[30] Y. Chen, A. D. Carroll, L. Scampavia, J. Ruzicka, *Anal. Sci*., **22**, 9(2006).
[31] S. Ohno, N. Teshima, T. Sakai, K. Grudpan, M. Polasek, *Talanta*, **68**, 527(2006).
[32] T. Leelasattarathkul. S. Liawruangrath, M. Rayanakon, W. Oungpipat, B. Liawruangrath, *Talanta*, **70**, 656(2006).
[33] K. A. Edwards, A. J. Baeumner, *Anal. Chem*., **78**, 1958(2006).
[34] M. Yang, Y. Xu, J. H. Wang, Anal. Chem., **78**, 5900(2006).
[35] J. Wang, E. H. Hansen, *J. Anal. At. Spectrom*., **16**,1349(2001).
[36] Y. Ogata, L. Scampavia, J. Ruzicka, C. R. Scott, M. H. Gelb, F. Turecek, *Anal. Chem*., **74**, 4702(2002).
[37] Y. Ogata, L. Scampavia, T. L. Carter, E. Fan, F. Turecek, *Anal. Biochem*., **331**, 161(2004).
[38] P. Ampan, J. Ruzicka, R. Atallah, G. D. Christian, J. Jakmunee, k. Grudpan, *Anal. Chim. Acta*, **499**, 167(2003).
[39] X. B. Long, R. Chomchoei, P. Gala, E. H. Hansen, *Anal. Chim. Acta*, **523**, 279(2004).
[40] Y. Wang, J. H. Wang, Z. L. Fang, *Anal. Chem*., **77**, 5396(2005).
[41] X. B. Long, M. Miro, M, E. H. Hansen, *Anal. Chem*., **77**, 6032(2005).
[42] X. B. Long, E. H. Hansen, M. Miro, *Talanta*, **66**, 1326(2005).
[43] X. B. Long, M. Miro, R. Jensen, E. H. Hansen, *Anal. Bional. Chem*., **386**, 739(2006).
[44] H. Erxleben, J. Ruzicka, *Anal. Chem*., **77**, 5124(2005).
[45] T. Kikas, A. Ivaska, *Talanta*, In press, Online: DOI; 10.1016/j.talanta. 2006.03.049. [46] C. H. Wu, L. Scampavia, J. Ruzicka, *Analyst*, **127**, 898(2002).
[47] J. Jakmuneea, L. Patimapornlert, S. Suteerapataranon, N. Lenghor, K. Grudpan ,*Talanta*, **65**, 789(2005).
[48] R. Burakham, J. Jakmunee, K. Grudpan, *Anal. Sci*, **22**, 137(2006).
[49] R. Burakham, S. Lapanantnoppakhun, J. Jakmunee, K. Grudpan., *Talanta* ,**68**, 416(2005).
[50] K. Grudpan, K. Watlaiad, T. Suekane, N. Lenghor, S. Lapanantnoppakhun, J. Jakmunee, T. Sakai, S. Motomizu, Abstracts of Papers, The 10th International Conference on Flow Analysis, Porto, Abstract 159.
[51] K. Grudpan, J. Jakmunee, S. K. Hartwell, S. Lapanantnoppakhun, R. Burakham, Abstracts of Papers, The 10th International Conference on Flow Analysis, Porto, Abstract 296.
[52] S. K. Hartwell, B. Srisawang, P. Kongtawelert, J. Jakmunee, K. Grudpan,*Talanta*, **66**, 521(2005).
[53] R. Chantiwas, P. Kongtawelert, S. Kradtap, K. Grudpan, Abstracts of Papers, The 13th International Conference on Flow Injection Analysis, Las Vegas, Abstract 118.

(Received October 29, 2006)

Available online at www.sciencedirect.com
SCIENCE DIRECT
Analytica Chimica Acta 575 (2006) 151–158
ANALYTICA CHIMICA ACTA
www.elsevier.com/locate/aca

An absorbance-based micro-fluidic sensor for diffusion coefficient and molar mass determinations

Adam D. McBrady [a], Rattikan Chantiwas [b], Ana Kristine Torgerson [a], Kate Grudpan [b,c], Robert E. Synovec [a,*]

[a] *Department of Chemistry, Box 351700, University of Washington, Seattle, WA 98195, United States*
[b] *Institute for Science and Technology Research and Development, Chiang Mai University, Chiang Mai 50200, Thailand*
[c] *Department of Chemistry, Faculty of Science, Chiang Mai University, Chiang Mai 50200, Thailand*

Received 4 April 2006; received in revised form 19 May 2006; accepted 24 May 2006
Available online 3 June 2006

Abstract

The H-Sensor reported herein is a micro-fluidic device compatible with flow injection analysis (FIA) and high performance liquid chromatography (HPLC). The device detects analytes at two separate off-chip absorbance flow cells, providing two simultaneous absorbance measurements. The ratio of these two absorbance signals contains analyte diffusion coefficient information. A theoretical model for the sensing mechanism is presented. The model relates the signal Ratio to analyte diffusion coefficient. The model is qualitatively evaluated by comparing theoretical and experimental signal Ratio values. Experimental signal Ratios were collected via FIA for a variety of analytes, including sodium azide, benzoic acid, amino acids, peptides, and proteins. Measuring absorbance at multiple wavelengths provides higher order data allowing the analyte signals from mixtures to be deconvolved via classical least squares (CLS). As a result of the H-Sensor providing two simultaneous signals as a function of time for each sample injection, two simulated second-order HPLC chromatograms were generated using experimental H-Sensor data. The chemometric deconvolution method referred to as the generalized rank annihilation method (GRAM) was used to demonstrate chromatographic and spectroscopic deconvolution. GRAM also provides the signal Ratio value, therefore simultaneously obtaining the analyte diffusion coefficient information during deconvolution. The two chromatograms successfully serve as the standard and unknown for the GRAM deconvolution. GRAM was evaluated on chromatograms at various chromatographic resolutions. GRAM was found to function to a chromatographic resolution at and above 0.25 with a percent quantitative error of less then 10%.

Keywords: Absorbance; Chemometrics; Flow injection; Liquid chromatography; Sensor; Molar mass; Diffusion coefficient

1. Introduction

The power of hyphenated chromatographic techniques and their subsequent higher order data sets has been known for some time [1,2]. Hyphenation within separation science falls within two categories. The first category generally refers to coupled-column separation techniques such as two-dimensional separations (i.e., LC × GC, GC × GC). The second category concerns a separation combined with a multi-channel detector (i.e., LC–MS, GC-FTIR) and is referred to as a hyphenated system [3]. This report concerns the development and initial proof-of-principle evaluation of such a multi-channel detector, termed the H-Sensor.

Based upon the concept of the previously developed microfabricated T-Sensor [4–9], and H-Filter [10], the H-Sensor selectivity is diffusion coefficient dependent. The name of the detector arises from its characteristic H-shaped flow channel. The H-shape allows two flow streams to merge under laminar flow conditions. The two streams are termed the sample stream and the receiving stream. The only difference between the two streams is that the sample stream initially contains analyte(s) within a host solvent while the receiving stream initially contains only the host solvent. Both enter the microfabricated flow channel at the left hand branches of the H, as depicted in Fig. 1. After merging, the two streams travel down the central channel. While in the central channel, the analytes within the sample stream are allowed

* Corresponding author. Tel.: +1 206 685 2328; fax: +1 206 685 8665.
E-mail address: synovec@chem.washington.edu (R.E. Synovec).

0003-2670/$ – see front matter © 2006 Elsevier B.V. All rights reserved.
doi:10.1016/j.aca.2006.05.083

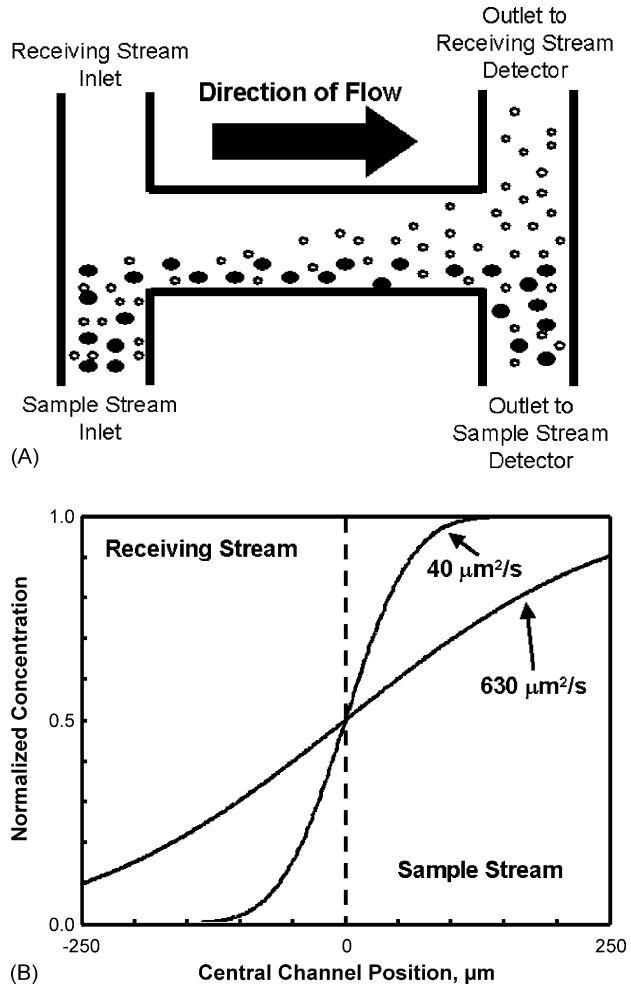

Fig. 1. (A) A schematic diagram of H-Sensor flow cell. The sample stream enters from the lower left hand side of flow channel. The sample stream merges with the receiving stream and flows from left to right down central channel. In the central channel, the smaller analytes (illustrated by small open symbols) within the sample stream diffuse into the receiving stream. The larger analytes (illustrated by larger black symbols) pre-dominantly remain in the sample stream. Upon reaching the end of the central channel, the two streams diverge and exit to their respective absorbance detector. (B) Theoretical diffusion profiles of two analytes having diffusion coefficients of 630 and 40 $\mu m^2/s$. Generated by Crank's solution (Eq. (2)) for the H-Sensor dimensions used in these studies: 500 μm wide × 200 μm deep × 2 cm long at a total flow rate of 4 μL/min (residence time of 30 s). The Ratio of the analyte having a diffusion coefficient of 630 $\mu m^2/s$ was predicted to be 0.38 while the Ratio of the analyte having a diffusion coefficient of 40 $\mu m^2/s$ was predicted to be 0.09.

to diffuse into the receiving stream. Smaller analytes, having larger diffusion coefficients, diffuse more rapidly from the sample stream into the receiving stream than larger analytes with smaller diffusion coefficients, as illustrated graphically in Fig. 1. Upon reaching the end of the central channel, the two streams diverge and exit the channel at the right-hand branches of the H. Each stream then flows into a separate off-chip absorbance flow cell. Both the sample and receiving stream fluidic paths and detectors should be identical. The detectors are capable of monitoring the absorbance at one wavelength or over a wavelength spectrum.

This report begins with the development of a quantitative theoretical description of the H-Sensor's detection principles. The theory relates an experimental signal Ratio to analyte diffusion coefficient. The signal Ratio is defined as the absorbance of the receiving stream over the absorbance of the sample stream. The experimental signal Ratios obtained via flow injection analysis (FIA) are reported and compared to theoretical predictions. The report also outlines the potential that the H-Sensor holds in sample mixture deconvolution. Absorbance recorded at multiple wavelengths creates a three-dimensional data set (time, absorbance, and wavelength). This multi-dimensionality allows for data deconvolution. We report successful application of classical least squares (CLS) deconvolution to H-Sensor data of a binary mixture. Lastly, using a simulated chromatographic time axis, we examine the future applicability of the H-Sensor for high performance liquid chromatography (HPLC) by performing the chemometric deconvolution and quantification method referred to as the generalized rank annihilation method (GRAM) [11,12] on co-eluting chromatographic peaks.

2. Theory

To provide a better understanding of the proof-of-principle experiments discussed in this report, a theoretical description of the H-Sensor is provided. This theory aims to derive a theoretical expression that relates the aforementioned signal Ratio value to analyte diffusion coefficient. The Ratio is defined as the experimentally measured absorbance of the receiving stream, A_R, divided by the experimentally measured absorbance of the sample stream, A_S, as presented in Eq. (1).

$$\text{Ratio} = \frac{A_R}{A_S} \tag{1}$$

A larger Ratio value indicates a larger diffusion coefficient. To theoretically determine the Ratio value one must first determine the theoretical absorbance values of each stream at the time of detection. As absorbance is proportional to concentration, it is apparent that the theoretical analyte concentration in each stream as the stream exits the H-Sensor chip needs to be determined. Towards that goal, a more thorough understanding of the on-chip fluid dynamics is needed.

The H-Sensor's dimensions are such that laminar flow dominates. Therefore, mixing between the sample and receiving streams occurs primarily via diffusion. Crank's solution for one-dimensional diffusion, from an initial step profile at x equal to zero, when the diffusion is not influenced by the analyte concentration, describes the concentration of an analyte at time t and position x as [13]:

$$C = \int \frac{C_0}{2}[1 + \text{erf}(\xi)] \tag{2}$$

where erf(ξ) is the error function of argument $\xi = x/(4Dt)^{1/2}$, and C_0 is the initial analyte concentration at the time when the streams merge ($t = 0$). Applying Crank's solution to the H-Sensor is straightforward. The zero time point, $t = 0$, is defined as the time at which the sample and receiving streams merge, while maintaining laminar flow [5]. At this instant, the sample concentration profile across the channel is assumed to be a step function. Crank's solution provides analyte concentration across

the width of the channel (the x dimension) at any time, t. Solving Eq. (2) at a given time for a variety of x-positions yields a concentration profile, such as those seen in Fig. 1B. In Fig. 1B, the x-axis is the width of the central flow channel. Fig. 1B presents theoretical concentration profiles for two analytes with different diffusion coefficients: 630 and 40 $\mu m^2/s$. The profiles were generated using a typical residence time of 30 s beyond the instant of stream merging. The analyte with the larger diffusion coefficient diffuses more readily across the channel resulting in a shallower concentration gradient than the analyte with the smaller diffusion coefficient.

This model assumes that the receiving and sample streams split at the center of the chip, $x = 0$, before exiting and heading to the two detectors. Therefore, the theoretical absorbance values of each stream are directly proportional to the total concentration of analyte in each side of the flow channel at a time equal to the residence time. The analyte concentrations can be calculated by taking the integral of the concentration profile (Eq. (2)) over the appropriate limits at time equal to the residence time. Allowing w to equal the channel width, the sample stream's limits are from $x = (w/2)$ to 0. The receiving stream's limits are from $x = 0$ to $-(w/2)$.

$$\text{Sample stream concentration} = \int_0^{w/2} \frac{C_0}{2}[1 + \text{erf}(\xi)] \quad (3)$$

$$\text{Receiving stream concentration} = \int_{-w/2}^{0} \frac{C_0}{2}[1 + \text{erf}(\xi)] \quad (4)$$

Dividing the receiving stream concentration by that of the sample stream yields the theoretical Ratio, R_t, for an analyte with known diffusion coefficient. This Ratio is independent of the initial analyte concentration, as shown in Eq. (5).

$$R_t = \frac{\text{Recieving stream concentration}}{\text{Sample stream concentration}} = \frac{\int_0^{w/2}[1 + \text{erf}(\xi)]}{\int_{-w/2}^{0}[1 + \text{erf}(\xi)]} \quad (5)$$

The initial concentration of the analyte entering the sample stream does not significantly influence the theoretical Ratio as long as the concentration is low enough as to not significantly influence the diffusion coefficient of the analyte.

For ease of visualization and discussion, we have taken the liberty of relating the theoretical and experimental Ratio values to molar mass rather than diffusion coefficient. The following generalized equation was used to find the diffusion coefficient of an analyte with a known molar mass.

$$D = 10^4 \times M^{-0.6} \quad (6)$$

In Eq. (6), M is molar mass and D is diffusion coefficient in $\mu m^2/s$. The values for the coefficient and exponent in Eq. (6) are representative of a large selection of specific values given in the second edition of the polymer handbook [14]. Eq. (6) serves as an adequate tool for determining the trend of the diffusion coefficient to molar mass relationship for a large group of analytes (i.e., random coil linear molecules in a good solvent). This theory is not designed for predicting accurate diffusion coefficients or molar masses for a particular analyte. However, the theory provides an adequate tool for evaluating the Ratio data given by the H-Sensor is terms of molar mass for a large sampling of diverse analytes.

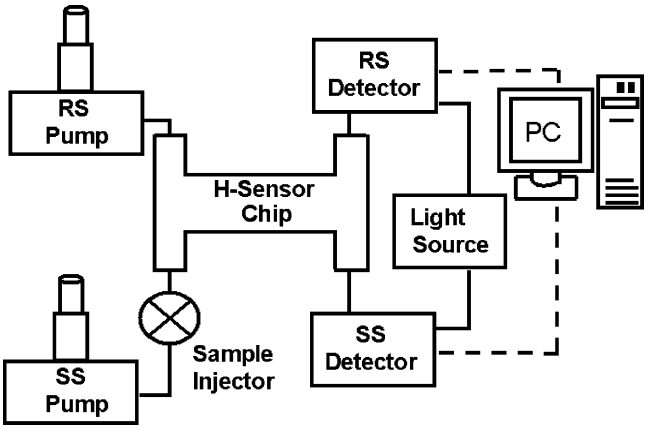

Fig. 2. A schematic diagram of the H-Sensor set up for flow injection analysis (FIA). RS and SS stand for receiving stream and sample stream, respectively.

Theoretical Ratios were calculated using Eq. (5) for the hypothetical analytes shown in Fig. 1B. The analyte with a diffusion coefficient of 630 $\mu m^2/s$ has a theoretical Ratio of 0.38. The second hypothetical analyte, with a diffusion coefficient of 40 $\mu m^2/s$, has a theoretical Ratio value of 0.09. Using Eq. (6) to convert the diffusion coefficients to molar mass, one sees that a $D = 40$ $\mu m^2/s$ is indicative of an analyte with an approximate molar mass of 10,000 g/mol. The much higher 630 $\mu m^2/s$ diffusion coefficient corresponds to a lower molar mass of about 100 g/mol.

3. Experimental

The H-Sensor system was assembled as shown in Fig. 2. The receiving stream and sample stream pumps were microgradient syringe pumps (Microgradient System, Brownlee Labs, Santa Clara, CA). The sample stream pump carried fluid through an injector fitted with a 1.5 μL sample loop (6 port, Rheodyne, Rohnert Park, CA). Detector flows cells, for the RS and SS detectors, respectively, were constructed from PEEK crosses (Upchurch Scientific, Oak Harbor, WA). Fluid entered and exited the flow cells in a straight line. It is essential that the fluid flow in both streams on the chip and off the chip be identical. Great care was taken in ensuring the lengths, and inner diameters of the tubing as well as all fluidic fittings were identical. Specifically, the flow cells should be positioned such that they create an equal backpressure (i.e., identical fluidic path length). Equalizing the backpressure helps maintain an equal on-chip split of the two streams. With great care any H-Sensor induced disturbance of the original analyte peak profile can be minimized. The light source for each flow cell entered perpendicular to the fluid stream and exited in the straight line. A bifurcated fiber optic cable (300UM Aluminum ZFQ-1437, Ocean Optics, Dunedin, FL), modified in house such that it has 1/16 in. outer diameter, was used to carry light to each flow cell from a continuous Xenon lamp (Hamamatsu, Bridgewater, NJ). The light for each flow cell was collected via a second fiber optic cable (FIA-P400-SR